SCHOOL OF CIVIL ENGINEERING

JOINT HIGHWAY RESEARCH PROJECT

FHWA/IN/JHRP-79-3

THE EFFECT OF LABORATORY COMPACTION ON THE COMPRESSIBILITY OF A COMPACTED HIGHLY PLASTIC CLAY

A. DiBernardo

C. W. Lovell

PURDUE UNIVERSITY
INDIANA STATE HIGHWAY COMMISSION

Interim Report

THE EFFECT OF LABORATORY COMPACTION ON THE COMPRESSIBILITY OF A COMPACTED HIGHLY PLASTIC CLAY

TO: H. L. Michael, Director
Joint Highway Research Project

FROM: C. W. Lovell, Research Engineer
Joint Highway Research Project

February 8, 1979

Project: C-36-5M

File: 6-6-13

Attached is an Interim Report on the HPR Part II study titled "Improving Embankment Design and Performance". This is Interim Report No. 5 and is titled "The Effect of Laboratory Compaction on the Compressibility of a Compacted Highly Plastic Clay". It is authored by Albert DiBernardo and C. W. Lovell of our staff.

The report describes the experimental program on the compressibility of laboratory compacted St. Croix clay. The effects of compaction water content and effort level were evaluated for both the as-compacted and saturated conditions of the clay. In addition, compaction prestress and volumetric strain upon soaking were measured, and statistically valid equations to predict these were derived. Research on these quantities for field compacted soil continues.

The Report is submitted as partial fulfillment of the objectives of the study. Copies of the report will also be submitted to ISHC and FHWA for their review, comment and similar acceptance.

Respectfully submitted,

C. W. Lovell /ms

C. W. Lovell
Research Engineer

CWL:ms

cc:
A. G. Altschaeffl
W. L. Dolch
R. L. Eskew
G. D. Gibson
W. H. Goetz
M. J. Gutzwiller
D. K. Hallock
D. E. Hancher
K. R. Hoover
J. F. McLaughlin
R. F. Marsh
R. D. Miles
P. L. Owens
G. T. Satterly
C. F. Scholer
M. B. Scott
K. C. Sinha
C. A. Venable
L. E. Wood
E. J. Yoder
S. R. Yoder

Digitized by the Internet Archive
in 2011 with funding from
LYRASIS members and Sloan Foundation; Indiana Department of Transportation

http://www.archive.org/details/effectoflaborato00dibe

Interim Report

THE EFFECT OF LABORATORY COMPACTION ON THE COMPRESSIBILITY OF A COMPACTED HIGHLY PLASTIC CLAY

by

Albert DiBernardo
Graduate Instructor in Research

and

C. W. Lovell
Professor of Civil Engineering
Joint Highway Research Project

Project No.: C-36-5M

File No.: 6-6-13

Prepared as Part of an Investigation

Conducted by

Joint Highway Research Project
Engineering Experiment Station

Purdue University
in cooperation with the

Indiana State Highway Commission

and the

U.S. Department of Transportation
Federal Highway Administration

The contents of this report reflect the views of the authors who are responsible for the facts and the accuracy of the data presented herein. The contents do not necessarily reflect the official views of policies of the Federal Highway Administration. This report does not constitute a standard, specification, or regulation.

Purdue University
West Lafayette, Indiana
February 8, 1979

TECHNICAL REPORT STANDARD TITLE PAGE

1. Report No. JHRP-79-3	2. Government Accession No.	3. Recipient's Catalog No.

4. Title and Subtitle
THE EFFECT OF LABORATORY COMPACTION ON THE COMPRESSIBILITY OF A COMPACTED HIGHLY PLASTIC CLAY

5. Report Date
February 1979

6. Performing Organization Code

7. Author(s)
Albert DiBernardo and C. W. Lovell

8. Performing Organization Report No.
JHRP-79-3

9. Performing Organization Name and Address
Joint Highway Research Project
Civil Engineering Building
Purdue University
W. Lafayette, Indiana 47907

10. Work Unit No.

11. Contract or Grant No.
HPR-1(16) Part II

12. Sponsoring Agency Name and Address
Indiana State Highway Commission
State Office Building
100 North Senate Avenue
Indianapolis, Indiana 46204

13. Type of Report and Period Covered
Interim Report

14. Sponsoring Agency Code

15. Supplementary Notes
Prepared in cooperation with the U. S. Department of Transportation, Federal Highway Administration. Part of the Study titled "Improving Embankment Design and Performance".

16. Abstract

The compressibility of the plastic St. Croix clay is to be studied for both laboratory and field compaction. This interim report deals with the laboratory-compacted phase. The clay was compacted to three levels of kneading type effort and at water contents dry of optimum, at optimum and wet of optimum. As-compacted compressibilities were assessed in the oedometer, and compaction prestress values were interpreted from the e-log p curves. These values were always less than the compaction pressures previously applied to the soil. A statistically valid prediction equation for prestress was written in terms of the compaction pressure and an interaction between compaction pressure and compaction water content.

Other compacted samples were saturated under confinement, with the aid of vacuum and backpressure. The volume changes incurred depended upon the compaction variables as well as the confinement. It was possible to develop a correlation between this volumetric strain and the compaction pressure and water content. Soaked compressibilities were also measured and compared with the as-compacted values. Comparable studies with samples of field compacted clay are under way, and will be reported in a separate report.

17. Key Words
laboratory compaction, compressibility, compaction prestress, volume change, clay

18. Distribution Statement
No restrictions. This document is available to the public through the National Technical Information Service, Springfield, Virginia 22161

19. Security Classif. (of this report) Unclassified	20. Security Classif. (of this page) Unclassified	21. No. of Pages 187	22. Price

Form DOT F 1700.7 (8-69)

ACKNOWLEDGMENTS

The kind encouragement and helpful suggestions provided by Professor A. G. Altschaeffl is appreciated. Many thanks are extended to Professor W. D. Kovacs; his review of parts of this manuscript was helpful. Sincere thanks are certainly due Dr. R. A. Abeyesekera for his laboratory assistance and valuable suggestions for improvement.

The authors are grateful to the Indiana State Highway Commission and the Federal Highway Administration for the financial sponsorship of this study. The research was administered through the Joint Highway Research Project, Purdue University, West Lafayette, Indiana.

Special thanks are extended to Mr. David Weitzel, Mr. James Johnson, and Mr. Gary Witsman for their cooperative efforts and helpful discussions throughout this study, and to Mr. Alan Lux for his laboratory assistance.

Finally, many thanks are due Mrs. Edith Vanderwerp and Mrs. Janice Bollinger for the secretarial help and particularly Ms. Peg McFarren for the drafting work.

Mrs. Joyce Taylor typed the manuscript.

TABLE OF CONTENTS

Page

LIST OF TABLES.................................. v

LIST OF FIGURES................................. vii

LIST OF ABBREVIATIONS AND SYMBOLS................ x

SPECIAL NOTES AND CONVERSIONS...................xiii

HIGHLIGHT SUMMARY xiv

INTRODUCTION.................................... 1

REVIEW OF THE LITERATURE........................ 4

- Characteristics of Partially Saturated Soils....... 4
  - Pore Fluid Characteristics of a Three Phase System...................................... 4
  - Effective Stress Concepts........................ 16
  - Theoretical Considerations of Unsaturated Compression.................................... 23
- Characteristics of Compacted Fine-Grained Soils.... 35
  - Theories and Structure........................... 35
  - Compressibility Characteristics.................. 43

EXPERIMENTAL APPARATUS AND PROCEDURE............. 57

- Soil Studied...................................... 57
- Sample Preparation................................ 62
- Compaction and Sampling........................... 63
  - Apparatus.. 63
  - Procedure.. 66
  - Discussion....................................... 67
- As-Compacted Compressibility...................... 73
  - Apparatus.. 73
  - Procedure.. 75
  - Discussion....................................... 78
- Soaked Compressibility............................ 81
  - Apparatus.. 81
  - Procedure.. 82
  - Discussion....................................... 85

RESULTS AND DISCUSSION OF RESULTS................ 87

Page

As-Compacted Compressibility........................ 87
  Compaction... 87
  Compression vs. Time Relations..................... 90
  Compressibility Characteristics.................... 97
  Compactive Prestress............................... 104
Soaked Compressibility............................... 111
  Compaction... 111
  Compression and Pore Pressure Measurements......... 114
  Volume Change on Saturation........................ 120
  Compressibility Characteristics.................... 126
Statistical Correlations............................. 135
  Results of Statistical Analysis.................... 139
  Discussion of Prediction Models.................... 150

CONCLUSIONS AND RECOMMENDATIONS...................... 159

Conclusions.. 159
Recommendations for Future Research.................. 162

BIBLIOGRAPHY... 164

APPENDICES... 172

Appendix A: Compaction Data.......................... 172
Appendix B: Compressibility Data..................... 174
Appendix C: Supplementary Figures.................... 183
Appendix D: List of Negative Numbers for Photographs........................... 187

LIST OF TABLES

Table Page

1. Effects of Compaction Process on Residual Pore Water Pressure (After Lambe, 1961)............. 10
2. Proposed Effective Stress Principles for Unsaturated Soils............................... 21
3. Prestress Results Obtained by Woodsum (1951)... 45
4. Compaction Pressure and Prestress (From Abeyesekera, 1978)................................... 50
5. St. Croix Clay Classification.................. 60
6. Initial Compaction Variables for As-Compacted Compressibility Samples....................... 91
7. Values of Compactive Prestress and Prestress Ratio.. 106
8. Initial Compaction Variables for Soaked Compressibility Samples........................... 112
9. Ratios of Maximum Excess Pore Water Pressure to Pressure Increment......................... 115
10. Mishu's (1963) Results for One-Dimensional Volume Change on Wetting...................... 124
11. Summary Table of As-Compacted and Soaked Compressibility Behavior........................... 134
12. Compaction Variables for Compactive Prestress Statistical Analysis........................... 141
13. Compaction Variables for One-Dimensional Percent Volume Change on Saturation Statistical Analysis...................................... 142
14. Statistical Data for Prediction Equations...... 144

Appendix
Table Page

A1. Moisture·Density Data for the Three Impact Compaction Levels.............................. 172

A2. Density and Saturation Data for Mold and Oedometer Samples.............................. 173

B1. As-Compacted Compressibility Test Data......... 174

B2. Soaked Compressibility Test Data............... 179

LIST OF FIGURES

Figure Page

1. Hypothetical Curves for Fine-Grained Soils (From Yoshimi, 1958) 14
2. Mohr's Circle of Stresses on an Unsaturated Soil Element (After Danielson, 1963) 31
3. Results of Prestress Tests on Compacted Shale 48
4. Effect of One-Dimensional Compression on Structure (After Lambe, 1958b) 52
5. Boring Profile and Location 58
6. Illustration of Force Sieving Technique 59
7. Grain Size Distribution 61
8. California Kneading Compactor 64
9. Compaction, Sampling, and Extruding Equipment 65
10. Sampling of Compacted Specimen 68
11. Moisture·Density·Energy Relations for Impact Method 69
12. Dynamic Foot Pressure vs. Gage Pressure 72
13. Karol-Warner Consolidation Apparatus 74
14. Loading Frame 76
15. Compression vs. Time (After Yoshimi, 1958) 80
16. Back Pressure Saturation Device 83
17. Correspondence Between Kneading and Impact Methods 88
18. Compression vs. Time (Dry of Optimum) 93
19. Compression vs. Time (Near Optimum) 94

Figure Page

20. Comparison of Relative Compressions for Dry, Wet, and at Optimum Samples.................... 96

21. Effect of Moisture Content on Compressibility (Low Energy).................................. 98

22. Effect of Moisture Content on Compressibility (Standard Proctor)............................ 100

23. Effect of Compactive Effort on Compressibility (Dry of Optimum)............................. 102

24. Effect of Compactive Effort on Compressibility (Wet of Optimum)............................. 103

25. Prestress Values (kN/m^2) for As-Compacted Compressibility Tests.......................... 107

26. Prestress Ratio vs. Degree of Saturation........ 110

27. Initial Moisture·Density Condition for Soaked Compressibility Test Samples.................. 113

28. Comparison of Methods for Obtaining R_{100} and T_{100}.. 118

29. Typical Pore Pressure Build-Up and Dissipation Curves.. 119

30. Volume Change Under Load on Saturation.......... 122

31. Effect of Confinement on Soaked Compressibility Behavior (Dry of Optimum)...................... 128

32. Comparison of Soaked Compressibility Behavior for Low Energy and Standard Proctor Samples..... 130

33. Effect of Confinement on Soaked Compressibility Behavior (Wet of Optimum)...................... 131

34. Effect of Compaction Pressure on Soaked Compressibility Behavior (Dry of Optimum).......... 132

35. Residual Analysis for Compactive Prestress Prediction Equation............................. 146

36. Residual Analysis for One-Dimensional Percent Volume Change on Wetting........................ 148

Figure Page

37. Prediction of Compactive Prestress.............. 151

38. Prediction of Percent Volume Change on Wetting.. 154

39. Joint Regions of Observations for Prediction Models... 157

Appendix Figure

C1. Effect of Moisture Content on Compressibility (Modified Proctor).............................. 183

C2. Effect of Compactive Effort on Compressibility (Near Optimum).................................. 184

C3. Volume Change During Saturation................. 185

C4. Effect of Compaction Pressure on Soaked Compressibility Behavior (Wet of Optimum).......... 186

LIST OF ABBREVIATIONS AND SYMBOLS

AASHTO - American Association of State Highway and Transportation Officials

BTH - bottom of hole

HRB - Highway Research Board

ISHC - Indiana State Highway Commission

LIR - Load increment ratio

MSE - error mean square

PWP - pore water pressure

SPSS - Statistical Package for the Social Science

S.R. - State Route

U.S. - United States

B_w - pore water pressure coefficient

^{o}C - degrees Celsius

cm - centimeter

e - void ratio

e_o - initial void ratio

ft - feet

in - inch

k_a - pore air permeability

k_w - pore water permeability

kg - kilogram

kN - kilonewton

m - meter

mm - millimeter

P_c - compaction pressure (kN/m^2)

P_o - confining pressure (kN/m^2)

P_s - compactive prestress (kN/m^2)

P_s/P_c - prestress ratio (dimensionless)

pcf - pounds per cubic foot

$\hat{P}_s$ - estimated response value of compactive prestress (kN/m^2)

psi - pounds per square inch

r - radius of meniscus

R^2 - coefficient of multiple determination

R_a^2 - adjusted R^2

R_{100} - compression value at 100% primary consolidation (millimeters)

S_r - initial degree of saturation

t - time

T_s - surface tension

t_{100} - elapsed time for 100% primary consolidation (minutes)

u_w - pore water pressure

u_a - pore air pressure

u_c - capillary pressure

Δu_a - excess pore air pressure

Δu_w - excess pore water pressure

u_a-u_w - matrix suction

$\Delta u/\Delta\sigma$ - excess pore water pressure by applied pressure increment

w - water content (%)

γ_d - dry density (kN/m^3) - see Special Note

γ_w - unit weight of water (kN/m^3)

σ - total applied stress (kN/m^2)

σ' - effective stress (kN/m^2)

τ - viscous resistance

SPECIAL NOTES AND CONVERSIONS

The results of this study are presented in the internationally standardized system of SI units.

If reference is made to the results of others, the units presented therein are maintained in due respect that author.

Unless otherwise noted, the density of the soil refers to the unit weight and is presented in kN/m^3.

U.S. Customary	SI Equivalent
in	0.0254 m
ft	0.3048 m
lbf	4.45 N
tonf	8.90 kN
kgf	9.807 N
lbf/in^2	6.895 kN/m^2
kgf/cm^2	98.07 kN/m^2
lbf/ft^2	47.88 N/m^2
ton/ft^2	95.76 kN/m^2
lbf/ft^3	0.1572 kN/m^3

HIGHLIGHT SUMMARY

Compaction is a means by which material is mechanically densified at constant water content to improve its engineering properties in a given application. An increase in unit weight is the most well-known effect of the compaction process, and specifications are commonly written based on allowable percentages of a maximum value. However, unit weight may have little effect on the compressibility behavior, just as the void ratio of a compacted soil may have little effect on strength, due to the influence of structure. Moreover, with the construction of higher embankments becoming more common, it is increasingly important to specify the placement variables such that compressibility may be controlled in both the short and long term.

Conventional oedometer tests were performed on a kneading compacted highly plastic residual clay to determine the effects of water content, dry density, and compaction pressure on the as-compacted and soaked compressibility behavior. As-compacted specimens were incrementally loaded; of particular interest was the value of compactive prestress induced during the compaction process. Environmental changes due to increased saturation were simulated using a back pressuring technique. Of interest was the one-dimensional percent volume change on wetting under load.

The experimental findings showed that samples compacted dry of optimum had a higher capacity for prestressing than samples compacted wet of optimum. Additionally, the ratio of compactive prestress to compaction pressure was found to be always less than unity for the ranges of partial saturation and compaction pressure considered. The results also indicated that the volume change occurring on saturation may be influenced by the value of compactive prestress. The results further show that the soaked compressibility behavior is related to the sample macrostructure resulting from loading and saturating

Statistical analyses were performed to establish the best predictive models for compactive prestress and one-dimensional percent volume change on wetting, in terms of the important compaction variables. The statistical models show that initial water content and nominal compaction pressure are the principle variables influencing each response. Such equations allow prediction and control of the compressibility of high cohesive embankments for both the as-compacted and soaked conditions.

INTRODUCTION

Compacted soils are used primarily for the construction of earth embankments and earth fills. During design, the engineer must establish suitable placement variables, e.g., water content, dry density, and compaction effort, so as to insure adequate performance of the completed structure in both the short and long term. Typically, the shear strength of the compacted mass is of major concern, and recent studies (Essigmann, 1976; Scott, 1977; Price, 1978) have provided the engineer with the capability of predicting its laboratory and field response value in terms of the important compaction variables. However, the demand for high embankments is increasing, and it is becoming increasingly more important to specify compaction procedures so that embankment compressibility can be adequately predicted and controlled in both the as-compacted and long term conditions.

A compacted soil is a three-phase system consisting of soil grains or aggregations, water, and air. During the compaction process, densification is achieved by air void reduction at constant water content. The influence of this procedure on compressibility behavior depends considerably on: (1) the compaction water content, (2) the amount of compaction, (3) the compaction mode—all of which

affect the compacted clay structure. In service, this structure may be altered with time due to environmental changes, which, in turn, may affect a change in compressibility behavior.

The research reported herein was conducted in an effort to examine the compressibility behavior of a laboratory compacted soil in the as-compacted and soaked condition. The type of soil used was a highly plastic residual clay, and the mode of compaction was of the kneading type. To determine the as-compacted compressibility characteristics, the compacted samples were trimmed to appropriate size and incrementally loaded in the oedometer. Of particular interest was the value of compactive prestress.

In order to simulate the changes in the mass that may occur in-service, compacted specimens were saturated in the oedometer under an equivalent embankment load. A back pressuring technique was employed to achieve full saturation of the oedometer specimens. Of major interest was the percent volume change which occurred during saturation under loading.

The ultimate purpose of this research was to establish models which can be used to accurately predict laboratory compressibility characteristics in terms of the important compaction variables. The models proposed will provide the engineer with a tool for controlling the as-compacted and long term compressibility.

A similar study on the compressibility characteristics of field-compacted samples of the same soil will soon be in

progress. Combined, the results of both studies will allow the engineer to establish suitable compaction specifications for controlling such behavior.

REVIEW OF THE LITERATURE

The intent of this review is two-fold: to review previous findings with respect to compacted clay compressibility, as well as provide the reader with the background information needed for its understanding. The first major section deals with the basic phenomena and theories which have shown to govern the behavior of partially saturated soils in general. The second major section is specifically connected with compaction and compacted clay compressibility. Combined, both sections should provide an understanding of compacted clay from a phenomological and engineering point of view.

Characteristics of Partially Saturated Soils

Pore Fluid Characteristics of a Three Phase System

Much of the initial work dealing with pore fluids in unsaturated soils was performed by agricultural researchers interested in the connection between plant growth and energy to extract water from soil (Briggs (1897), Buckingham (1907), Schofield (1935), Schofield and Da Costa (1938)- as referenced by Croney and Coleman (1960)). Only with the advance of major earth embankments and airfield construction did civil engineers become interested in the pore fluids of unsaturated soils, particularly compacted clays.

As previously mentioned, a compacted clay is a three-phase system consisting of soil grains, water, and air. The solid phase consists of insoluble mineral particles which are considered incompressible, but may, in the form of aggregations, form a compressible mass. It is the intent of this discussion however, to deal only with the nature of the pore fluids; that is, what are the properties of these fluids, how are they affected by different compaction processes, and how do they affect the engineering properties of the mass.

Yoshimi (1958) refers to four possible states of fluid continuity in an unsaturated soil mass. They are as follows:

(1) Continuous water with small air bubbles: This condition represents a high degree of saturation; however, no reliable data are available on the lower limit. The water plus air bubbles flow as a homogeneous fluid provided the size of the pore channel is larger than the air bubbles.

(2) Smaller channels filled with water, and larger channels blocked by air voids: Flow of water through the capillary pore channels is negligible. Air voids can block pore channels and provide considerable resistance to the penetration of air.

(3) Continuous water and continuous air: This flow condition requires the pore space to be large, so that both phases can form continuous channels. This condition is unlikely for fine-grained soils.

(4) Discontinuous water and continuous air: The soil water is continuous only in the smaller capillaries. The air is continuous through voids or channels.

According to Yoshimi, a compacted mass with a degree of saturation less than approximately 95 percent represents condition (4); that is, the pore air forms voids and/or channels and the pore water, continuous only in the smaller capillaries, is under negative pressure and can only be displaced by considerable applied stress.

The air phase of a compacted clay exists in different forms, namely, dissolved air, free air, and air bubbles. The equilibrium concentration of air dissolved in water is a function of the partial pressure of air and temperature, and for the purposes of this study will not be considered. Free air, on the other hand, fills the void spaces and forms continuous channels. Since this air is typically in contact with water, it is saturated with water vapor (Baver, 1956). For soils compacted to low degrees of saturation, the air content is high and the pores are large, thus, the air may flow freely through the clay. As the degree of saturation increases however, thin necks of water between pores tend to close, thereby occluding air in the form of bubbles (Barden, 1965). Barden (1965) cites an investigation on compacted silty clay which determined occlusion at a moisture content 3 percent above standard optimum. Leonards (1975) states occlusion in compacted clays depends on the type of clay and the method of achieving the desired molded water content, and

can occur at degrees of saturation ranging between 80 and 92 percent. Air bubbles of small dimensions may also be found directly on the surface of the soil particles. According to Aitchison (1956), these bubbles are within the layer of adsorbed water, but separated from the particle surface by a fine film of water. Within the zone of strongly adsorbed water, the pressure conditions in the water—and hence in individual air bubbles—are determined principally by the attractive forces on the particle surface.

The water phase of a compacted soil is commonly under negative (less than atmospheric) pressure. In the literature this phenomenon has been referred to by many names, such as, suction, capillary pressure or tension, pressure deficiency, and negative pore water pressure. Croney and Coleman (1960) defined negative pore water pressure as a pressure deficiency (below atmospheric) measured in situ or in the laboratory with the soil subject to the stress regime associated with the particular loading conditions under consideration.

Hilf (1956) investigated negative pore water pressures in a compacted clay and concluded they were the algebraic sum of two components—air pressure and capillary pressure. In its simplest, yet adequate form, Hilf's formulation for the overall pore pressure in an unsaturated soil is:

$$u = u_a + u_c \tag{1}$$

where u = pressure in the water at the meniscus

u_a = pressure in the air

u_c = capillary pressure

In compacted soils the value of u_c is typically negative, thereby representing a state of tension in the pore water. The magnitude is governed by the radius of the meniscus and can be obtained from

$$u_c = - \left[\frac{T_s}{r_1} + \frac{T_s}{r_2} \right] \qquad (2a)$$

or

$$u_c = - \frac{2\ T_s}{R_s} \qquad (2b)$$

where T_s is surface tension and r_1 and r_2 are radii of curvature of the two sections formed by passing two planes through the point and at right angles to each other. In a mixture of water and air, the air bubbles do not necessarily have the same shape and size, and Equation (2b) is commonly assumed, where R_s is the average radius for the mixture. From these equations it follows that the smaller the meniscus radius, the more negative is the pore water pressure; consequently, for soils compacted at high degrees of saturation, the effect of u_c is small.

Aitchison (1960) suggests that the capillary model should not be used to explain fundamental soil-water interactions, since the true configuration in a soil-water-air system may differ markedly from that in any form of capillary model. Aitchison, however, does state that experimental evidence shows such a model may be used if the capillary stress range is less that 220 atmospheres.

Hilf verified the validity of the u_a term in his formulation from laboratory tests. He found that when an ambient

air pressure was applied to a cylindrical capillary tube, the pressure at every point in the column was equally changed, even though the height of capillary rise and the curvature of the meniscus remained the same. It was this finding that allowed Hilf to measure pore water pressures in a compacted soil by increasing the boundary air pressure. This procedure may be applicable for low degrees of saturation, but for higher degrees, in which the air is occluded, the pore air pressure will not equal the applied boundary air pressure, and the test results may be misleading (Leonards, 1975).

Values of negative pore water pressure for compacted cohesive soils have been reported by Hilf (1956), Bishop, et al. (1960), Blight (1963), and Gibbs and Coffey (1963). In soil mechanics, the value of the pore water pressure, whether it be positive or negative, is of major concern, since it has a direct effect on effective stress, thereby influencing soil behavior.

Lambe (1961) was instrumental in showing the effects of different compaction processes on laboratory measured residual pore pressures for a Vicksburg silty clay and a kaolinite soil. Lambe's results are summarized in Table 1. As indicated, the higher the molding water content, the less is the negative pore water pressure. Lambe attributes this trend to an increasing amount of dispersion; consequently, the soil mass is more compressible (in the low pressure range) and has less capacity for prestressing. This contention is also attributed to increasing compactive effort.

TABLE I EFFECTS OF COMPACTION PROCESS ON RESIDUAL PORE WATER PRESSURE (AFTER LAMBE, 1961)

COMPACTION VARIABLE	EFFECT*
MOLDING WATER CONTENT	PWP increases with increasing water content
EFFORT	PWP increases with increasing effort
COMPACTION METHOD	Kneading gives less negative PWPs than static
TEMPERATURE	Samples compacted cool (40°F) have less negative PWPs than sample compacted warm (75°)
CONFINEMENT	Removing sample from mold may cause a reduction in PWP
METHOD OF MOISTURE ATTAINMENT	Samples once wetter than the molding water content have less negative PWP

PWP = pore water pressure

*None of the negative pwp's reported were less than -1 atmosphere

Olson and Langfelder (1965) measured negative pore water pressures on a compacted clay and found them to be more negative, i.e., less than -1 atmosphere, than any previously reported in the engineering literature. In their approach they used the axis translation technique and high air entry porous stones to measure negative pore water pressure. They related surface area with negative pore water pressure and found that the larger the surface area, the more negative the pressure. Other findings presented show trends that are in agreement with those presented in Table 1.

Many researchers have attached considerable importance to the capillary model (Kelvin (1871), Gardner (1920), Schofield (1935), Keen (1924)—as referenced by Sridharan (1968)), but few have investigated the value of R_s (Equation (2b)), and how it affects the value of negative pore water pressure.

In an attempt to determine negative pore water pressure in compacted and artificially sedimented clays, Sridharan (1968), using the simple capillary model, obtained pore size distributions to better approximate R_s. Based on his findings, Sridharan concluded that for partially saturated soils there is an optimum degree of saturation at which the effective negative pore water pressure is a maximum; the optimum degree was found to be primarily dependent on the soil type and soil structure.

The movement of liquid through an unsaturated soil is brought about by the action of gravity, capillarity, or externally applied pressure, either alone or in combination

thereof. In the as-compacted state, the movement of moisture occurs primarily through the action of capillarity, however, when subjected to compression, it is believed that all actions occur simultaneously. In the following, soil moisture movement will be discussed briefly, i.e., only to explain the relationship between air and water permeability in an unsaturated soil. For a more indepth review of this phenomenon, the reader is referred to: Muskat (1946), Croney (1952), Croney and Coleman (1953), and Baver (1956).

Carman (1953), in considering the redistribution of capillary held moisture within an unsaturated porous medium, concluded that two mechanisms can be attributed to moisture redistribution, namely, vapor distillation through the air-filled voids and the flow of liquid through the water-filled voids—both mechanisms occuring simultaneously until the curvature of the capillary meniscus is uniform at all points. Additionally, he stated that the flow of capillary held moisture can only occur through the moisture filled pores and that the suction force, or the difference in capillary tensions, creates movement from areas of lower to higher tension. In a compacted clay this force will be greater in the smaller capillaries than in the larger ones, due to the smaller radius of curvature. As a result, water will flow from the larger to the smaller capillaries, and once an equilibrium condition is reached, all the water will be in the smaller capillaries (Yoshimi, 1958). Therefore, since pore size can be related to permeability (Garcia-Bengochea,

1978), the water permeability of an unsaturated soil would be less than a saturated soil, where both large and small pores are filled with water. Of course, this can only be concluded if such factors as soil composition, characteristics of the permeant, structure, void ratio, and degree of saturation remain constant (Lambe, 1958b).

Baver (1956) cited the works of several authors concerned with air permeability (k_a) and the physical characteristics of unsaturated soils. All of the investigations referred to were performed on relatively granular material, i.e., fine sand and powdered loam, and indicated that k_a increased and decreased, respectively, with increasing porosity and increasing water content. In other words, the presence of additional liquid in the pores restricts the flow of air through the soil, as does also, a decrease in porosity. It is believed that these same findings also apply to the liquid permeability of unsaturated fine-grained soils. (Since the air and liquid must share the pores, a retardation of liquid movement occurs due to the presence of air).

Yoshimi (1958) presented a set of hypothetical curves which illustrates the air-water permeability phenomena previously discussed. These curves are shown in Figure 1 and are applicable for fine-grained soils. The ordinate is labelled the "percent relative permeability" and is considered the permeability of an unsaturated porous body to that of a saturated porous body. As shown, at degrees of saturation ranging from 0 to 50 percent, the air permeability is 100

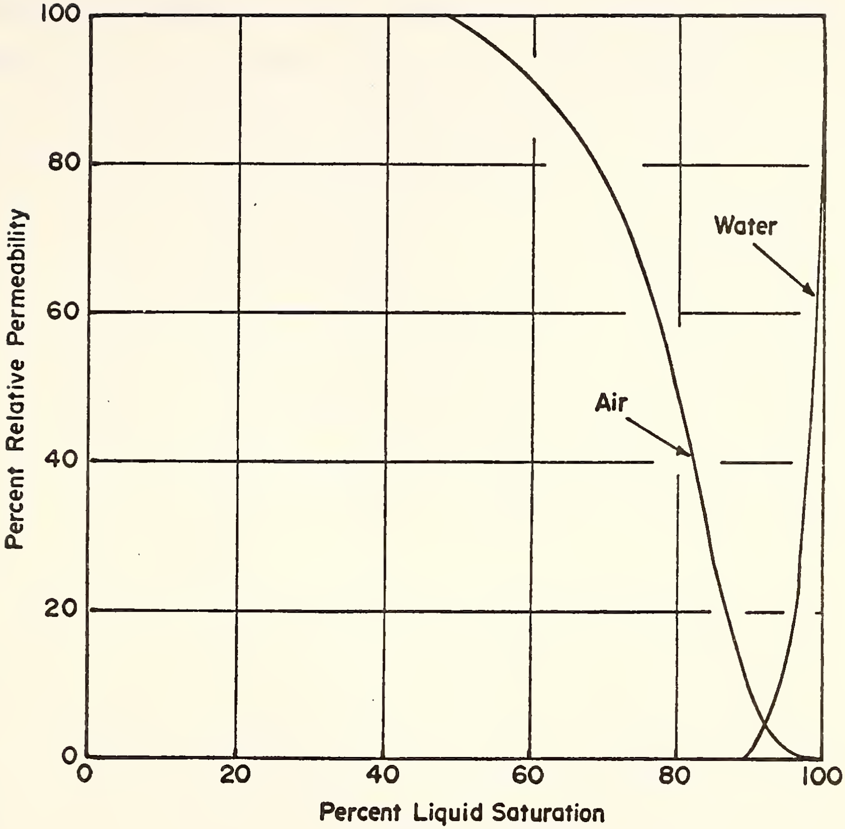

FIGURE 1 HYPOTHETICAL CURVES FOR FINE-GRAINED SOILS (FROM YOSHIMI, 1958)

percent, i.e., the water phase is in the smaller capillaries and does not affect the flow of gas. As the degree of saturation increases, the air permeability decreases sharply, however, the water remains immobile. In fact, the water permeability remains zero to approximately 85 percent saturation, and at 95 percent, rises sharply.

Teerawong (1962), as cited by Danielson (1963), experimentally obtained curves similar to those shown in Figure 1 using oil or brine as the wetting agent in a clay media. He observed that as the relative air permeability decreases, the liquid saturation approaches a critical value—the saturation at which the resistance to outflow of pore fluids is maximum. For the clay used in his study, this critical value was found to be at 89.5 percent.

Olson (1963), Langfelder et al. (1968), and Barden and Sides (1970) determined that air permeability is virtually zero when clays are compacted near their optimum moisture content. This is in agreement with Figure 1 and the critical value concept proposed by Teerawong. Clearly, this indicates that the pore air network is no longer continuous.

It is hopeful that the foregoing has thrown some light onto the complex nature of air-water interactions within an unsaturated soil. In this study no attempt was made to determine the initial negative pore water pressure or the changes under one dimensional applied stress, therefore the qualitative results presented will be useful in understanding the volume change characteristics of compacted St. Croix clay.

Effective Stress Concepts

The concept of effective stress is well established in soil mechanics, and for water saturated soils can be expressed as (Skempton, 1960):

$$\sigma' = \sigma - (1-a)\ u_w \qquad (3)$$

where σ' = effective normal stress

σ = total normal stress

a = area of contact between the particles, per unit gross area of material

u_w = pressure in the pore water

Few doubt that "a" is very small for soils, and Equation (3) reduces to the commonly used Terzaghi (1936) effective stress principle, namely, $\sigma' = \sigma - u_w$. It is this concept which has proven to govern soil behavior.

Skempton (1960) has shown however, that the Terzaghi equation does not give the true effective stress, and proposed the following formulations:

(a) for shear stress

$$\sigma' = \sigma - (1 - \frac{a \tan \psi}{\tan \phi'})\ u_w \qquad (4a)$$

where ψ = angle of internal friction

ϕ' = the effective angle of shearing resistance

and (b) for volume change

$$\sigma' = \sigma - (1 - C_s/C)\ u_w \qquad (4b)$$

where C_s = the compressibility of the solid substance comprising the particles

C = compressibility of the porous material

According to Abeyesekera (1978), the validity of Skempton's equations have never been proved or disproved. However, for saturated soils this is of no consequence, since the bracketed terms are very close to one, thereby making the Terzaghi equation an excellent approximation for saturated soils. But, as Skempton suggests, it is not a good approximation for other porous materials, such as concrete or rock, since the values of C_s/C and $(a \tan \psi)/\tan \phi'$ are too great to be neglected.

The success of the effective stress concept for saturated soils has led many investigators into a search for a similar relationship for unsaturated soils. However, some of the proposed formulations, which will be considered subsequently, have proven essentially impossible to evaluate uniquely and difficult to apply to practical problems (Fredlund and Morganstern, 1977).

Bishop (1959) was the first to propose a formulation to express volume change and shear strength behavior of unsaturated soils. His equation is expressed as follows:

$$\sigma' = \sigma - u_a + \chi \, (u_a - u_w) \qquad (5a)$$

where u_a = pressure in the air or vapor

χ = empirical coefficient

To retain the understanding of the effective stress concept, this equation takes the form

$$\sigma' = \sigma - \{\chi\ u_w + (1 - \chi)\ u_a\} \qquad (5b)$$

or

$$\sigma' = \sigma - u^*$$

where u^* = the equivalent pore pressure

In this form, Equation (5b) shows that effective stress for unsaturated soils consists of two components—one resulting from the total normal pressure, and the other from the pressure exerted by the pore fluids.

The value of the χ parameter, which represents that portion of the pore fluid pressure influencing effective stress, is unity for saturated soils and zero for dry soils, whereas, intermediate values will primarily depend on the degree of saturation (Bishop, et al., 1960). It should be noted though that the χ term is not necessarily the same in statements of effective stress for volume change and shear strength, and that it is also a function of: suction, water content, surface charge on particles, electrolyte composition, particle arrangement, stress path, etc. (Aitchison, 1965).

Bishop, et al. (1960), Jennings (1960), and Bishop and Donald (1961) experimentally determined χ by comparing the effective stress components σ and u_w under changes in applied suction with an identical saturated soil specimen under externally applied pressure. It is tacitly assumed in this procedure that effective stress under conditions of applied suction and externally applied pressure is directly comparable over the whole range of partial saturation.

Jennings and Burland (1962), in their classic paper, disproved this assumption for soils below a critical degree of saturation. They showed that by soaking a one-dimensionally loaded soil specimen (increase in u_w or decrease in σ') either collapse or additional compression can take place. For clays, the critical degree of saturation was found to be about 85 percent; for lower degrees of saturation, it was concluded that Equation (5) does not accurately define soil behavior.

Matyas and Radhakrishna (1968) claim that the χ parameter is not applicable for volume change because volume change data are normally analyzed incrementally in a continuous deformation process, whereas for shear strength, data are analyzed at the failure state. Hence, they conclude that for an effective stress principle to be valid for volume change, it would require comparable behavior of a partially saturated soil element at every stage of its deformation with that of an equivalent fully saturated element. As a result, it is generally conceded that Bishop's equation is not valid for volume change, but is valid for shear strength (Bishop and Blight, 1963). However, this latter contention has never been proved or disproved (Leonards, 1975).

Lambe (1960) was instrumental in formulating an equation for effective stress which considered on a micro scale the static forces exerted between adjacent particles of a particular soil mass. Lambe's generalized equation is as follows:

$$\sigma = \bar{\bar{\sigma}}\, a_m + p_a a_a + u_w a_w + R - A \qquad (6)$$

where σ = total stress

$\bar{\bar{\sigma}}$ = mineral to mineral contact stress

a_m = fraction of the total interparticle area that is mineral to mineral contact

P_a = mineral to air contact stress

a_a = fraction of total interparticle area that is mineral-air contact

u_w = pressure in the water

a_w = fraction of total interparticle area that is mineral-water or water-water contact

R = total interparticle electrical repulsion divided by total interparticle area

A = total interparticle electrical attraction divided by total interparticle area

Lambe's equation shows that for a clay soil under an applied stress regime, the effective stress, or more importantly, the stress that governs soil behavior, is not only dependent on the applied normal stress and the distribution of air, water, and soil, but also on the action of electrical forces between adjacent particles. Mitchell (1976) outlined the interparticle forces (R and A) which influence intergranular stresses; they are: surface and ion hydration, and electrostatic forces (R); electrostatic, and primary valence bonding and cementation forces (A).

Other researchers have proposed similar relationships for effective stress of unsaturated soils. Table 2 outlines

TABLE 2 PROPOSED EFFECTIVE STRESS PRINCIPLES FOR UNSATURATED SOILS

Reference	Equation
Hilf (1956)	$\sigma' = \sigma + u_a + u_c$
Croney, Coleman and Black (1958)	$\sigma' = \sigma - \beta' u_w$
Aitchison (1960)	$\sigma' = \sigma + \psi p''$
Jennings (1960)	$\sigma' = \sigma + \beta p''$
Sridharan (1968)	$\sigma' = \sigma + p_m'' + p_s''$
Aitchison (1973)	$\sigma' = \sigma + x_m'' p_m'' + x_s'' p_s''$
Fredlund (1973)	$\sigma' = \begin{bmatrix} \sigma_x - u_w - p_s'' & \tau_{yx} & \tau_{zx} \\ \tau_{xy} & \sigma_y - u_w - p_s'' & \tau_{zy} \\ \tau_{xz} & \tau_{yz} & \sigma_z - u_w - p_s'' \end{bmatrix} \begin{bmatrix} u_a - u_w & 0 & 0 \\ 0 & u_a - u_w & 0 \\ 0 & 0 & u_a - u_w \end{bmatrix}$

Description of Variables

σ' = effective stress

σ = total stress

u_a = pressure in the air

u_c = capillary pressure

u_w = pore water pressure

$u_a - u_w$ = matrix suction

p'' = pressure deficiency in water

p_m'', p_s'' = matrix and solute suction

β' = bonding factor which is a measure of the number of bonds under tension effective in contributing to soil strength

β, ψ = parameters ranging between zero and one for saturation between zero and one

x_s'', x_m'' = factors ranging from zero to one which are dependent upon stress paths

some of these equations proposed since Bishop's formulation. As shown, the equations proposed by Croney et al. (1958), Aitchison (1960), and Jennings (1960) differ from Equation (5) in two respects: (1) the air in the pore space is assumed to be atmospheric ($u_a = 0$), and (2) the symbol used to modify the pore fluid term is different. Aitchison and Bishop (1960) therefore suggested that the effective stress equation take the general form of Equation (5a), where χ is a parameter identical to ψ, χ, β' and β.

Aitchison (1973) and Sridharan (1968) realized the importance of solute suction (p''_s),or the net repulsion and attraction between clay packets, on soil behavior, as well as the role of matrix suction (p''_m) or the pressure difference across a meniscus, and presented the equations as shown. It can be inferred that these equations consider the phenomena as presented by both Bishop and Lambe.

Fredlund (1973) used multiphase continuum mechanics, involving stress state tensors,to describe effective stress in unsaturated soils. The tensors describe the equilibrium of the solid phase and contractile skin of the meniscus. However, according to Leonards (1975),this is not a rational formulation since the behavior of an unsaturated soil deals with the interaction between the state of stress and the clay fabric. Additionally, since soils behave as particulate materials, they can not be considered as a continuum, especially when trying to examine soil behavior (Mitchell, 1976).

It has been shown that the effective stress concept for unsaturated soils has been dealt with considerably in the engineering literature; however, we are far from formulating a generally valid law for such soils (Leonards, 1975).

Theoretical Considerations of Unsaturated Compression

In 1925, Terzaghi proposed a theory for the one-dimensional consolidation of saturated soils; this is said to be the beginning of soil mechanics. Terzaghi expressed this formulation as:

$$c_v \frac{d^2u}{dz^2} = \frac{du}{dt} \tag{7}$$

where $c_v = \frac{(1 + e)\ k}{a_v\ \gamma_w}$

k = coefficient of permeability

e = void ratio

a_v = coefficient of compressibility

γ_w = unit weight of water

u = excess pore water pressure

z = space variable in the direction of consolidation

t = time

It is this equation which explains the Terzaghi Consolidation Theory or the conventional theory of consolidation which is widely used in engineering practice today.

The mathematical simplicity of Equation (7) is due to continuity considerations; that is, the volume of water expelled from the soil pores is numerically equivalent to the change in total volume of the soil. The solution is not

mathematically simple however, unless certain assumptions are made. The assumptions made by Terzaghi, as indicated by Schiffman et al. (1969) and Lowe (1971) are:

1. The soil skeleton is homogeneous; i.e., a single linear stress-strain and velocity-pressure gradient relationship governs the soil mass.
2. The soil is completely saturated with water.
3. Compressibility of the soil grains and water are negligible.
4. The fluid flow equations follow Darcy's law.
5. a_v and k are constant.
6. The thickness of the layer H for single drainage is constant.
7. One-dimensional flow.
8. Time lag of consolidation is due entirely to the low permeability of the soil.

It is well known that some of these assumptions may be unrealistic or applicable only to the one-dimensional test, especially with respect to soil properties and the dimensionality of compression. Even though it has not proven to be as successful as the effective stress theory for saturated soils, it is mathematically simpler than other theories, i.e., three-dimensional models, etc., and there is a wealth of knowledge based on it (Schiffman, et al., 1969).

Attempts have been made to treat the consolidation of unsaturated soils by modifying Terzaghi's theory. Important

departures from the simplifying assumptions exist however; they are:

1. Compressibility of the pore fluid can not be taken as negligible due to the air content.
2. Variation exists in both air and water permeability.
3. Plastic or viscous resistance effects can not be ignored.

In light of these departures, it is necessary to consider the fundamental relationships known to exist when theoretically treating unsaturated consolidation (Barden, 1974).

Biot (1941) was one of the first to consider the consolidation of unsaturated soils. In the development of a three-dimensional primary consolidation theory, he made the following assumptions:

1. The soil is isotropic.
2. The stress strain relation is irreversible under final equilibrium conditions.
3. The strains are small.
4. Pore water is incompressible.
5. Pore water may contain air bubbles.
6. Darcy's law of water flow is valid.

Like Terzaghi, Biot based his theory on the continuity of volume and expressed it as:

$$\frac{\Delta V_W}{V} = \alpha \frac{\Delta V}{V} + \frac{\Delta u}{Q} \qquad (8)$$

where ΔV_W = volume of water expelled
V = total volume of soil mass
ΔV = total volume change
Δu = change in pore water pressure
α, Q = elasticity constants for soil mass

Biot's formulation clearly indicates that an increment of water volume per bulk volume of soil, $\frac{\Delta V_W}{\Delta V}$, is the linear combination of two stress components—the stress in the soil and the stress in the pore water. Additionally, it incorporates the presence of air in the pore water, since the value of ΔV is affected by the air content.

Barden (1974) claims that Biot's theory is only applicable for soils compacted wet of optimum, or more generally, for soils containing occluded air bubbles that are attached to the soil skeleton and where only water flows. His reasoning stems from Equation (8), implying that the attached gas bubbles merely act to modify the coefficient of compressibility, m_v. Additionally, he states that to obtain the effects of a compressible fluid (gas bubbles in water), it is necessary to consider mass continuity, not volume.

Yoshimi (1958) studied the physical and mechanical mechanisms controlling the consolidation of unsaturated soil. He divided the total compression process into three stages: initial compression, consolidation, and creep. Yoshimi assumed all three stages to occur singly and in the order

stated above. Each stage is defined as:

(1) Initial Compression: the immediate response due to the compression of soil structure and gas as soon as the incremental load is applied.

(2) Consolidation: the part of compression which involves the outflow of pore fluids.

(3) Creep: the part of compression which involves the redistribution of shearing stresses in the adsorbed water and the local rearrangement of the soil particles.

The importance of immediate compression in the unsaturated compression process was noted by Yoshimi and expressed as a ratio β, which is the ratio of initial compression to the total compression. In his treatment of this initial stage, he derived a mathematical expression which takes account of the solubility of air in water and the interfacial tensions between air and water; this expression appears as:

$$\beta + \frac{\beta}{\alpha \;\; \beta} \frac{P_{wo}}{\Delta\sigma} + \left[\frac{\alpha}{\alpha - \beta} - \left[1 - \frac{\beta}{e_o(1 - S_o)} \right]^{1/3} \right] \frac{\Delta p_o}{\Delta\sigma} = 1 \qquad (9)$$

where $\alpha = \frac{e_o}{\Delta e} \left[1 - S_o + HS_o \right]$

e_o = initial void ratio

Δe = total compression in terms of void ratio

S_o = initial degree of saturation

H = volume of dissolved air per unit volume of water

P_{wo} = original absolute pore water pressure

Δp_o = original pore pressure difference $(p_a - p_w)$

$\Delta\sigma$ = change in normal intergranular stress

Yoshimi found the β-value for a nearly saturated Boston Blue Clay and a compacted silty clay to range between 0.30 to 0.42 and 0.78 to 0.98, respectively, when both air solubility and surface tension were ignored ($H = \Delta p_o = 0$). Additionally, he found β was little affected by variations in stress; evidence showed that β varied slightly (0.93 to 0.95), despite large variations in σ_o and $\Delta\sigma$, for the compacted soil.

In view of the foregoing, initial compression may account for a considerable portion of the total compression of a compacted silty clay. It should be noted however that Yoshimi's values were based on an estimated mean radii of curvature (Equation 2b) since no reliable data were available to properly determine the pore water and pore air pressures.

Yoshimi (1958) also developed a series of equations based on time, geometry, stress, and soil properties for the consolidation stage of unsaturated soils. For two conditions of fluid continuity, he expressed these formulations as:

(a) pore water which contains extremely small air bubbles; may be considered a homogeneous, compressible fluid ($S > 95\%$) -

$$\frac{k_w}{S\ V_w} \ \frac{\partial^2 p_w}{\partial z^2} = \frac{\partial n}{\partial t} \qquad (10a)$$

(b) air is in continuous channels; pore water is initially below atmospheric -

$$\frac{k_a}{V_a} \frac{\partial}{\partial z}\left[p_a \ \frac{\partial p_a}{\partial z}\right] = 2\ C_1 p_a \frac{\partial p_a}{dt} + C_2 \ \frac{\partial p_a}{\partial t} \qquad (10b)$$

where k_w, k_a = water and air permeability, respectively

S = degree of saturation

p_a = pore air pressure

p_w = pore water pressure

z = space variable

n = porosity

t = time

V_a = viscosity of air

V_w = viscosity of water

C_1, C_2 = constants related by $n = C_1 p_a + C_2$

For soil with a very small air content (high degree of saturation), Equation (10a) is nearly identical with Terzaghi's equation for saturated soils, and Terzaghi's solution may be used to determine the rate of consolidation. In the case where the outflow of air governs consolidation, Equation (10b) is applicable and can be solved by a method of successive approximations. Yoshimi notes however, that the relative magnitude of consolidation, as compared to initial compression, is probably too small to warrant the time-consuming computations.

Danielson (1963) formulated a general equation for the unsaturated consolidation of clays which considered the viscous resistance (plastic structural resistance) to deformation. The equation was first proposed by Dunn and Nielsen (1959)—as referenced by Danielson (1963)—who confirmed that a logarithmic plot of viscous resistance versus the rate of compression produced essentially a straight line. The form of this equation is:

$$\tau = C_1 \left[- \frac{\partial e}{\partial t} \right]^{C_2} \qquad (11)$$

where τ = viscous resistance

e = void ratio

$\frac{\partial e}{\partial t}$ = rate of compression

C_1, C_2 are constants for a given pressure increment

The value of C_1 is an increasing function with respect to the applied load and is a measure of the degree of closeness of the soil particles. The constant C_2 governs the curvature of the viscous relationship and its value depends on the clay structure, the amount or thickness of adsorbed water, and the type of cation.

Danielson developed a stress equation that incorporated viscous effects in the development of a general differential equation for unsaturated consolidation. Figure 2 illustrates Danielson's approach in terms of Mohr circles.

Figure 2(a) shows the stress condition in a soil element under a consolidation pressure σ_v. The lateral normal stress is denoted by σ_L and the radius of the circle represents the magnitude of the friction component (solid to solid) on the maximum shear plane. The solid friction is defined as the mean principal stress $(\sigma_1 + \sigma_2)/2$ at equilibrium and is dependent on material type and vertical applied stress.

At time t_o an additional load is applied to the sample. As shown in Figure 2(b), σ_v increases slightly due to rapid dissipation of pore pressure; however, the majority of the

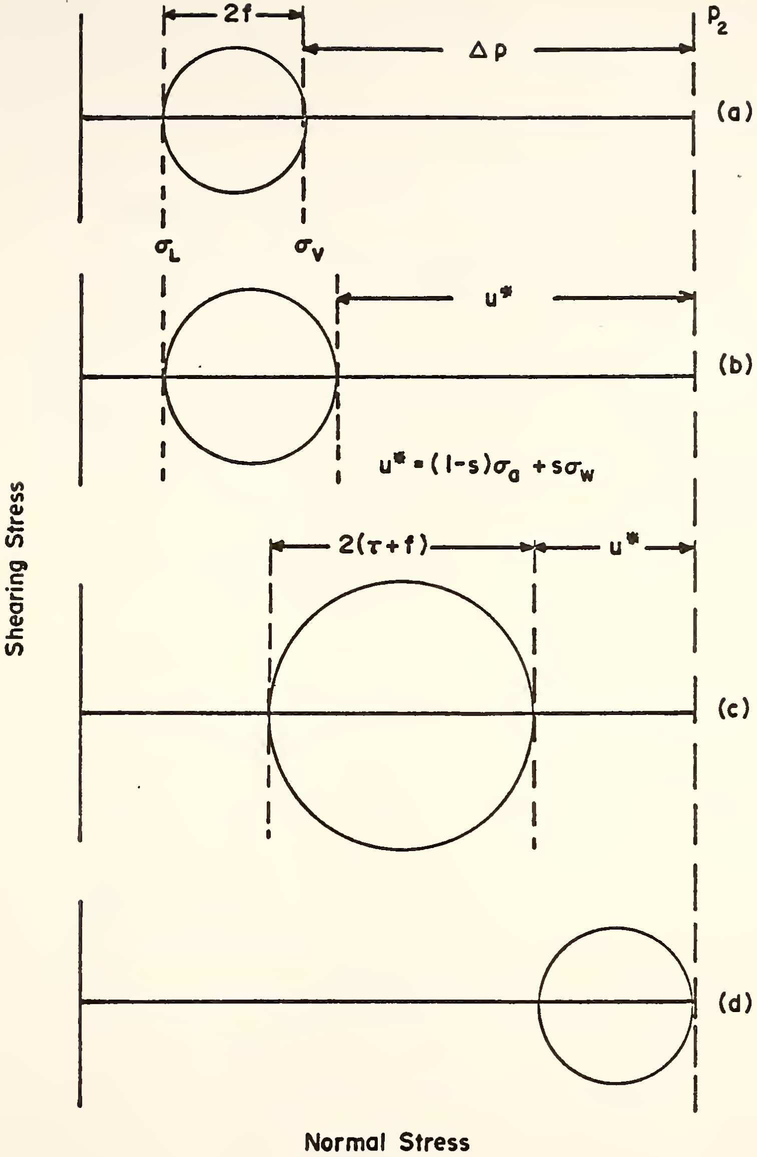

FIGURE 2 MOHR'S CIRCLE OF STRESSES ON AN UNSATURATED SOIL ELEMENT (AFTER DANIELSON, 1963)

load will be carried by the pore pressure. The value of σ_L remains essentially unchanged.

Immediately after load application, viscous resistance, as well as solid friction, play an important role in the deformation process. As a result, the radius of the Mohr circle increases (Figure 2(c)). Finally, when the sample has reached equilibrium, the excess pore pressure will be zero, σ_v will equal p_2, and no viscous resistance will be present. This equilibrium condition is shown in Figure 2(d).

Based on the foregoing, if an intermediate Mohr circle is considered, the stress equation at any time during the unsaturated consolidation process is:

$$p_2 = \sigma_L + 2\ (\tau + f) + u^* \qquad (12)$$

where $u^* = (1-S)\ \sigma_a + S\ \sigma_w$

p_2 = intergranular stress

σ_L = lateral normal stress

τ = viscous resistance

f = solid friction

u^* = pore fluid pressure

S = degree of saturation

σ_a = pore air pressure

σ_w = pore water pressure

Danielson used this stress equation to develop a general solution for the consolidation process for an unsaturated clay.

Barden (1965) realized the difficulty in formulating an overall general equation for the consolidation process.

This is largely due to the complexity of the functions describing the combined effects of porosity, structure, degree of saturation, and effective stress, on the air and water permeability of unsaturated soils. In this connection, Barden treated five idealized compacted clay consolidation processes, which differ depending on the range of partial saturation. The processes are for the following compacted conditions:

(1) Extremely dry clays ($S < 0.5$).
(2) Clay dry of optimum ($0.5 < S < 0.9$).
(3) Clays at optimum ($S = 0.9$).
(4) Clays wet of optimum ($S > 0.9$).
(5) Clays very wet of optimum ($S > 0.95$).

In the treatment of each process, Barden used simple parameters to describe their respective physical conditions, and like Yoshimi, he realized the very different behavior of clays at different degrees of saturation.

One major drawback of Barden's treatment is that only one process is assumed during consolidation. In reality however, a compacted clay may consolidate from process 2, via process 3, into process 4, and this is not considered, although mentioned. Therefore, the writer is in agreement with Matyas and Radhakrishna (1968) who concluded that the volume change characteristics of a partially saturated soil can not be predicted on the basis of any one single equation without reference to the changing state of the soil.

In 1974, Barden made another attempt to explain volume change behavior of compacted clays. For clay compacted dry and wet of optimum, he described the consolidation process of each as follows:

(a) Dry of optimum (continuous air voids) - "Assuming that the initial value of u_a is atmospheric the initial suction will cause the value of u_w to be negative...On applying a load to the soil there will be an initial or immediate compression, and because of the relative stiffness of the soil skeleton and the highly compressible pore-fluid, the values of Δu_a and Δu_w will be small. Thus there will be an increase in u_a and u_w, but in general u_w will remain below atmospheric pressure and hence only air can drain from the soil. Even in cases where u_w does rise above atmospheric pressure, the value of k_a is so much greater than k_w that the flow must be completely dominated by the air...".

(b) Wet of optimum (occluded air bubbles) - "...the material develops pore water pressure, increasing with water content. Since this is also associated with a low value of k_w, consolidation in the classical sense is a real engineering problem involved in the stability analysis of embankments, etc. It has been shown that despite the expansion of air bubbles, the variation of permeability during a consolidation stage is no more marked than in many saturated clays. It is also shown that the compressibility of the pore-fluid should not be a particularly important factor, provided m_v is defined

with respect to the overall settlement. Thus on theoretical grounds it appears that Terzaghi theory should prove adequate".

In the transition from dry to wet, Barden indicates that right up to occlusion, $k_a >> k_w$ and no water flows. Additionally, he suggests occlusion occurs at roughly optimum water content, although there may be regions of continuous air voids with low values of k_a, and that the occlusion process and transition from a dry to a wet process is sudden rather than gradual.

Characteristics of Compacted Fine-Grained Soils

Theories and Structure

The compaction process is a means by which a material is mechanically densified at constant water content. It is distinctly different from consolidation in that the densification process is not accompanied by the expulsion of water, but rather the outflow of air. The externally applied compaction energy, as well as the soil properties, will determine the structure of the compacted mass. The intent of this discussion is to review some of the theories of compaction and the types of compacted clay structures which result.

In 1933, Proctor intended to find a method for determining and limiting the softening, due to changes in saturation, of soil used in constructing earthfill dams. In doing so, he was one of the first to theorize the compaction process of cohesive soils. His theory is two-fold; it considers the combined effects of capillarity and lubrication and is summarized below.

At very low relative moisture contents, a thin film of water surrounds each particle in the compacted mass. Where these films come in contact, surface tension forces draw the particles closer together, thereby increasing the frictional resistance between them. As the molding water content increases, the capillary forces decrease (R_s increases), thus having two effects—a springing apart of adjacent particles and a reduction in frictional resistance due to increased lubrication. The combined effect on the compacted density is: (1) a decrease due to the decrease in capillary forces, and (2) an increase due to lubrication effects. The lubrication effects dominate however, and the combined effect continues until the moisture content, plus a small amount of contained air, become just sufficient to fill the voids. At this point the compacted density is the highest (for this method of compaction); the compacted void ratio, the lowest. A still higher moisture content limits the compaction of the soil and the result is a compacted soil with less density and more voids.

Proctor's instructive conception of the compaction process provided him with a suitable framework for controlling the construction of large embankments subject to changes in saturation. He concluded that at water contents above optimum, additional water is no longer effective as a lubricant; it merely displaces the soil, increases the softening, and decreases the stability. Pertaining to the given application, Proctor suggested that the soil be compacted wet of optimum to provide for a minimum increase in softening with saturation.

Hilf (1956) provided an explanation of the compaction process based on his pore water pressure theory for unsaturated soils. Using the capillary pressure model discussed previously (Equation (1)), he hypothesized that dry soils are difficult to compact because of the high frictional forces caused by high-curvature meniscii. As the water content increases, the capillary forces decrease; consequently, the density increases. Past the optimum moisture content, the density decreases due to the build up of transient air pressure which reduces compaction effectiveness.

The two forementioned theories are conceptually very simple. Additionally, they were considered quite logical for the state of knowledge at that time. In more recent years however, the compaction process has proven to be governed by a number of complex phenomena, namely, capillary pressure, hysteresis, effective stress, osmotic pressure, pore air pressure and pore water pressure. The effects of some of these are discussed next.

Lambe (1958a) realized that the compaction process and colloidal stability involved many soil-water system variables, some of which are:

(1) Electrolyte Concentration.

(2) Ion Valence.

(3) Dielectric Constant.

(4) Temperature.

(5) Size of Hydrated Ion.

(6) pH.

(7) Anion Adsorption.

(8) Water Content.

(9) Pressure.

The interaction of these physio-chemical variables has a marked effect on the structure of compacted clay; that is, dispersion, flocculation or a combination of both.

According to Lambe (1958a), a soil compacted dry of optimum is water deficient; as a result, the high electrolytic concentration depresses the double layer. Moreover, interparticle repulsion decreases, causing flocculation, which results in a low compacted density and a random particle arrangement. Increasing water content expands the double layer (reduction in electrolytic concentration), which, in turn, reduces the degree of flocculation. This permits a more orderly arrangement of particles, as well as, a higher compacted density—the lubrication of particles allows for greater slippage which establishes a denser state. A further increase in water content causes an expansion of the double layer and a continued reduction in the net attractive forces between particles. The compacted density decreases, even though the particle arrangement is more orderly, because the added water has diluted the concentration of soil particles per volume.

Lambe's theory, along with Equation (6), have provided investigators with an adequate framework for understanding the mechanisms controlling compacted clay compressibility. However, a compacted soil subjected to increasing applied

stress, as in a laboratory oedometer test, or to environmental changes, as in an embankment, realizes changes in the system variables that are nearly impossible to determine.

Olson (1963) provided insight into the compaction process by explaining the shape of the moisture-density curve in terms of effective stresses. His main contention for this approach was: (1) Lambe's physio-chemical theory did not have practical applicability, and (2) Proctor's lubrication theory had certain limitations due to knowledge advancement in the soil sciences.

For three conditions of fluid continuity, Olson explained each process as follows (for kneading compaction only):

(1) Dry of Optimum: The effective stresses in the initially loose soil are small because of the low confining pressure, the low B_w-coefficients, and the low χ-coefficient. Upon completion of the process, the coefficient B_w value remains low, thereby preventing the development of significant pore pressures. Additionally, the low χ-value means the pore pressures have little effect on the effective stresses. As the water content is increased (still remaining in the dry range), the pore air and pore water pressures also increase, which reduces the effective stresses between the particles, thereby weakening the soil. The end product is an increase in compacted density.

(2) At Optimum: The same reasoning presented in (1) applies, however, the pressure in the partially or

fully occluded air phase builds up due to the low air permeability value (see Figure 1). When the air voids are no longer continuous, the air permeability drops to zero, and the optimum moisture content (maximum density) is reached.

(3) Wet of Optimum: The explanation is two-fold. First, for a dense soil, pore water pressure peaks at small strains and then decreases continuously with increasing strain. Therefore, it is possible that the pore water pressure increases slightly as the foot pressure is first applied (small strains) and then becomes significantly negative at greater penetration (high strains). The net effect is a resistance to penetration. Second, when the compaction foot penetrates deeply into the soil (simulating the action of a deep footing), the shearing strength of the soil increases, i.e., from six times the undrained strength to ten times. The combined result is a density decrease.

The hypotheses presented thus far have explained the compaction process in terms of the predominant influence of individual clay particles (or clusters). Some have contended however, that the post-compaction characteristics are affected by agglomerations or peds of clay particles, rather than individual ones.

Barden and Sides (1970) attempted to relate the engineering behavior of compacted clay to its structure. Photomicrographs

of the soil structure of two clays revealed that the main difference between samples compacted at different moisture contents was in their macrostructures. Observations revealed an apparently homogeneous structure wet of optimum and 3 mm to 6 mm diameter pellet-like macropeds dry of optimum. These findings led them to the following general analysis of the compaction process:

> At low compaction moisture contents the low dry density is caused by the presence of large air-filled macropores. Additionally, the macropeds, or clusters of clay particles, are able to resist the compaction pressure without much distortion. As the water content is increased, the macropores become filled with soil (easy slippage); the result is an increase in density. As the water content is increased further, the water layers increase in thickness, and the aggregates, easily distorted, fuse together making them indistinguishable. This, in turn, decreases the compacted density.

Hodek (1972) explained the characteristics and engineering behavior of a compacted soil in terms of a deformable aggregate model. He concluded this model to be an appropriate one for use in aiding the interpretation of swell and compaction characteristics for a laboratory static compacted kaolinite. His theory of the compaction process is similar to Barden and Sides' theory.

According to Garcia-Bengochea (1978), pore size distribution measurements for compacted clays have also provided strong evidence for a deformable aggregate model. He cited Bhasin (1975) who found that as the compactive effort increases, the fraction of pores on the dry side of optimum decreases, whereas, on the wet side, the distribution remains the same. These findings bear some interest since they directly affect compacted clay permeability, which, in turn, directly affects the rate of compacted clay compressibility.

Hodek and Lovell (1978a) have proposed a model which explains the achievement of compacted unit weight for the laboratory static compaction of kaolinite. They contend the initial soil structure of the as-molded soil (before compaction) is that of aggregations of different size and water content. The size and distribution of these aggregates play an important role in the compaction process; that is, densification is associated with the decrease in inter-aggregate void ratio due to translation and rotation, the deformation of aggregates into the shape of available voids, and the reduction of intra-aggregate voids. Accordingly, the type of compaction and the aggregate size distribution establish the fluid continuity condition within the mass, and once the air voids are no longer inter-connected, little densification occurs regardless of the input effort. Moreover, they introduce the concept of net energy imparted to the soil during the compaction process. It was found that the net energy required to obtain different conditions on the same moisture-density curve is

inversely proportional to the aggregate size; uncomplicated mathematical models were developed to show this relationship.

Compressibility Characteristics

Unlike shear strength and permeability, the compressibility of compacted clay has not been dealt with extensively in the engineering literature. This may be explained by two reasons: (1) the solution to the problem is not a straightforward adaptation of the Terzaghi consolidation theory for saturated soils, and (2) it is difficult to define the fundamental relationships which govern the compressibility of unsaturated soil under load. This discussion will examine however, the available literature connected with compactive prestress and basic compacted clay compressibility characteristics. A discussion of related subjects—permeability, collapse, swell—will be included where applicable.

An increase in unit weight is the most well-known effect of the compaction process. In connection with compressibility however, this increase may have little effect on the volume change characteristics, just as the void ratio of a compacted soil may have little effect on the strength due the influence of structure. Therefore, it can be said that the mechanical characteristics, e.g., void ratio or density, of a compacted soil may be inadequate for controlling the compressibility of earthen embankments.

During the compaction process (kneading or impact), the soil experiences the load for only a short duration. The energy supplied in this short period is received by: (1) the

soil skeleton, as an intergranular stress, and (2) the pore fluids, as a pressure in each of the phases. Upon completion of the process, there is an induced prestress in the soil which may or may not be equal to the compaction pressure. According to Abeyesekera (1978), it is this value of compactive prestress which is important with respect to compacted clay behavior.

In 1951, Woodsum defined compactive prestress as a term analogous to the preconsolidation pressure of a natural soil; specifically, the apparent pressure effect caused by the compaction process. Lambe (1958b) similarly defined compactive prestress, but realized that its value was affected by other factors, namely, time and chemical changes. For the purposes of this study, the compactive prestress will be defined as the precompression pressure, in terms of total stress, which has been induced in the soil as a result of the compaction process and which is determined on an as-compacted oedometer specimen directly after compaction.

In order to determine compactive prestress, Woodsum (1951) statically compacted soil (Fort Union clay and Mississippi loess) directly in oedometer rings, allowed the soil to come to equilibrium with water under an applied load, and performed the conventional oedometer test. Table 3 presents a partial summary of Woodsum's results.

TABLE 3 PRESTRESS RESULTS OBTAINED BY WOODSUM (1951)

	Compaction Pressure P_c (kg/cm^2)	Confining Pressure P_o (kg/cm^2)	Initial Void Ratio e_o	Prestress Value P_s (kg/cm^2)	Prestress Ratio* P_s/P_c
(1)	5.0	0.4	0.955	0.9	0.18
(2)	5.0	0.8	1.06	0.9	0.18
(3)	10.0	0.4	0.808	1.3	0.13
(4)	10.0	0.8	0.910	1.2	0.12
(5)	15.0	0.4	0.718	1.5	0.10
(6)	15.0	0.8	0.718	2.5	0.17

*Values were determined by the writer.

These data show that as the confining pressure (P_o) remains constant and as the compaction pressure (P_c) increases or initial void ratio (e_o) decreases, the value of prestress increases. Moreover, these data suggest that although the value of prestress increases with increasing compaction pressure, the prestress ratio (P_s/P_c), which is similar to the over-consolidation ratio for saturated soils, varies slightly, and not increasingly as may be expected. In practical terms, this may signify that for a given compaction process and type of soil, the efficiency of the process does not increase with increasing effort.

At the time Woodsum presented these results, there was little information concerning this subject; his findings were truly welcomed. To the author's knowledge, only two other reports—Abeyesekera (1978) and Yoshimi and Osterberg (1963)—mentioned prestress since then.

Abeyesekera (1978) determined the prestress induced by the kneading compaction of a shale material. The material was compacted at pressures ranging between 345 kN/m^2 to 1380 kN/m^2 (50 to 200 psi) and loaded in the as-compacted condition, either incrementally in the oedometer or at constant rate of strain. The elapsed time for each oedometer load increment was ten minutes—the same loading time used by Yoshimi and Osterberg (1963). The estimated prestress was determined in terms of total stress from the void ratio-log pressure curve using the Casagrande construction.

For the seven tests performed, Abeyesekera found the prestress values and the prestress ratio to range between 345 kN/m^2 to 865 kN/m^2 (50 to 126 psi) and 0.49 to 1.0, respectively. The ratio range is greater than Woodsum's (0.1 to 0.2) which could be attributed to the differences between kneading and static methods, shale and clay, unsoaked condition or soaked condition, either singly or in combination. However, some interesting correlations can be made from Abeyesekera's results.

Figure 3(a) shows Abeyesekera's data plotted as the prestress ratio versus the degree of saturation. The degree of saturation was chosen as the abscissa because it characterizes a single point on the moisture density curve; consequently, Figure 3(a) shows the relationship among induced prestress, compaction pressure, moisture content, and dry density on a single plot. If verified, Figure 3(a) may be useful for engineering design and construction decision making. That is, a design or field engineer concerned with compacted clay fill compressibility in a given application, may use a similar figure to manipulate the compaction variables so to obtain a desirable end product. It is the intent of this study to examine more closely the relationships between compactive prestress and the compaction variables for a compacted clay soil; clearly, such a study could prove useful.

Figure 3(b) shows the relationship between initial void ratio and induced prestress for the same material. As can be seen, there is much scatter in the data which may suggest

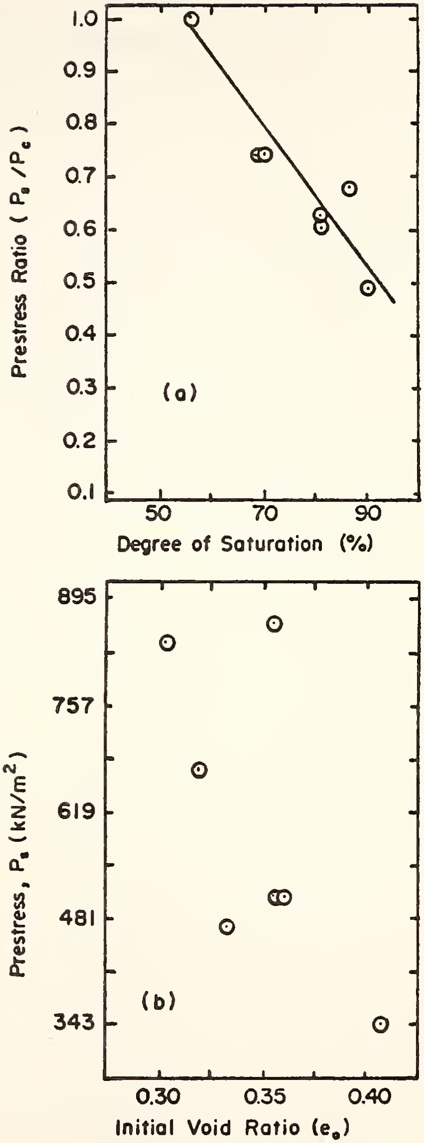

FIGURE 3 RESULTS OF PRESTRESS TESTS ON COMPACTED SHALE

that void ratio is not a sufficient measure of induced prestress. A similar relationship showing the effect of void ratio and compaction pressure may be instructive, however, the data are insufficient.

Table 4 summarizes the results of other investigators who were concerned with the compressibility of compacted materials, but not specifically with compactive prestress. If only the data related to the soils are examined, it can be seen that static compaction methods are the most efficient with respect to induced prestress. Seed, Mitchell and Chan (1960) examined the difference in compaction method on the undrained shear strength of compacted clay; they found: (1) for static compaction—smaller shear strains, lower pore water pressures, higher strength values at low strains, and (2) for kneading compaction—larger shear strains, higher pore water pressures, lower strength at low strains. This explanation appears reasonable for explaining the differences in statically induced prestress and prestress induced by kneading methods.

Wilson (1952) was interested in the effect of water content on the compressibility of a compacted clayey sand. The e-log p curves he showed for two samples—one wet of optimum, the other dry of optimum—indicated the wet compacted sample to be approximately 30 percent more compressible than the dry compacted sample. Wilson attributed this to the higher pore pressures generated in the wetter mass upon loading; consequently, a reduction in the effective stresses resulted in greater deformation: In light of this, Wilson

TABLE 4 COMPACTION PRESSURE AND PRESTRESS (FROM ABEYESEKERA, 1978)

Reference	Material	Compaction Mode	Compaction Pressure P_c (psi)	Dwell Time (seconds)	Prestress Values P_s (psi)	Prestress Ratio P_s/P_c
Campbell (1952)	Bituminous Concrete	Static	2500	60	150 to 210	.06 to .08
Yoshimi and Osterberg (1963)	Silty Clay	Static 20 psi/min	94	280	94	1.00
Mishu (1963)	Residual Clay	Kneading 30 blow/min	95	1	36.1	.38
			125	1	36.1	.29
			170	1	55.6	.33
Abeyesekera (Table D1)	Shale Aggregate	Kneading 30 blow/min	50	1	50	1.00
			100	1	68 to 74	.68 to .74
			200	1	98 to 126	.49 to .63

recommended that cohesive highway embankments be compacted dry of optimum, so as to achieve low volume compressibility.

Leonards (1952), in a discussion of Wilson's article, realized the need for examining the fundamental principles governing the behavior of compacted soil throughout its period of service. Using data obtained by Woodsum (1951), Leonards showed that the compressibility of a highly plastic clay is affected by its confining pressure during contact with water, but that this effect is minimized using higher compaction energies. The data suggest that a compacted sample wetted in the oedometer at a low confining pressure will compress more than a sample of equal void ratio wetted and confined at a higher pressure. Based on this, Leonards concluded that a change in water content resulting from the submergence of a compacted highway or airport pavement fill will be more severe than a corresponding change resulting from capillary action, since the confining pressures in the submerged condition are much lower. This clearly illustrates the effect of service conditions on the ultimate compressibility characteristics of a statically compacted clay.

Lambe (1958b) explained the compressibility characteristics of compacted clay mainly in terms of particle rearrangement and colloidal chemistry, however he does contend that other components—gas change in volume or amount, particle deformation, particle diminution—do come into play. Figure 4 illustrates the reasons for compressibility differences on the wet side and dry side of optimum, as proposed by Lambe,

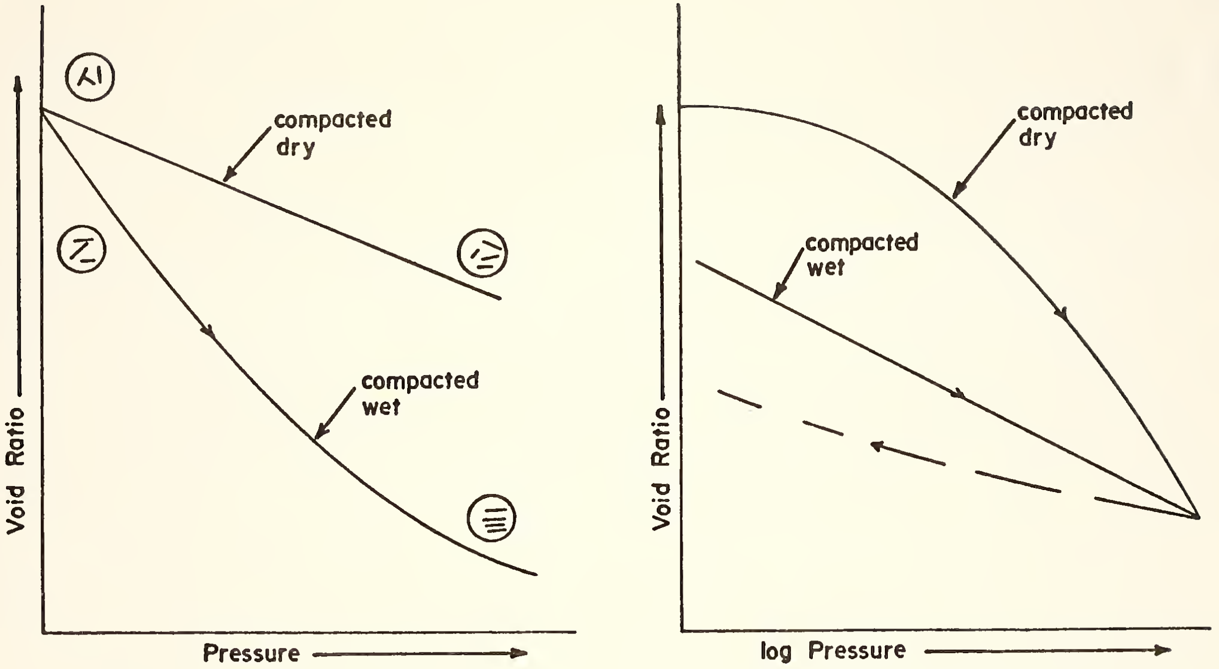

(a) Low Consolidation Pressure

(b) High Consolidation Pressure

FIGURE 4 EFFECT OF ONE-DIMENSIONAL COMPRESSION ON STRUCTURE (AFTER LAMBE, 1958b)

on the basis of changes in soil structure. In the low pressure range (Figure 4(a)), more pressure is required to re-orient the particles of the flocculated structure, therefore the compression that occurs under an increment of load will be greater for the sample compacted wet. However, for a large pressure range (Figure 4(b)), the dry soil will compress more (steeper slope in e-log p curve) as a result of particle re-orientation, but once highly dispersed, will experience essentially the same compression as the wet sample.

Yoshimi (1958) performed a series of one-dimensional compressibility tests on statically compacted samples of Vicksburg silty clay. The object of his experimental analyses was to prove: (1) the pore water is immobile during compression, and (2) the time rate of compressive strain is independent of the soil thickness and drainage conditions.

To prove immobility of water during compression, Yoshimi compacted samples at a water content of 16.7 percent and at a void ratio of 0.65 and compressed them in the oedometer using the standard procedure. Accounting for the water loss to the boundaries under a no-load condition and working under temperature controlled conditions, Yoshimi calculated the net loss of water due to compression to be 0.26 grams, which was 1.2 percent of the total volume change and 0.5 percent of the total amount of water at a final degree of saturation exceeding 97 percent. In light of this, Yoshimi concluded that most of the applied load was carried by the soil structure due to a cushioning effect of the soil air,

and the excess fluid pressure was probably never great enough to exceed the initial pressure in the pore water.

Yoshimi also showed that the time rate of compression is essentially independent of the sample thickness and drainage conditions. In connection with drainage, Yoshimi replaced the porous boundary disks with solid metal disks. The results showed practically no change in the shape of the compression-time curves for the two drainage conditions. Additionally, to determine the effect of sample thickness, Yoshimi compressed compacted samples of different heights and again found that for each load increment, the general shapes of the compression-time curves were almost identical. Based on this, Yoshimi had reasonable assurance that the consolidation process did not play a significant role in overall compression.

Danielson (1963) performed consolidation tests on three compacted soils to define the fundamental relationships which govern the consolidation of an unsaturated soil under load. Based on his findings, Danielson made the following conclusions:

(1) At saturations of 94 percent or less, no outflow of pore water can be expected in any of the soils tested.

(2) The initial compression of an unsaturated sample due to compression of the air accounts for a considerable portion of the total compression, i.e., from 35 percent to 65 percent for the clays studied.

(3) For the same soil, a sample at a higher moisture content compresses to a greater extent than does a

sample at a lower moisture content under the same loading.

(4) The excess pore air pressure is dissipated much more rapidly than the excess pore water pressure in a saturated soil. For the unsaturated case, the pore air pressure appears to be almost entirely dissipated within forty minutes after load application, if not before.

The forementioned conclusions were based on the typical shape of the e-log time curves. Danielson showed that the portion of the curve to about t = 1 minute is characterized by first a decreasing slope and then a slope of constant value. He attributes this shape to the dissipation of the excess pore air pressure in the air due to the initial compression. After t = 1 minute, the rate of deformation $(\frac{de}{dt})$ is constant. This is due to: (1) dissipation of residual pore pressures, (2) the overcoming of viscous resistance, and (3) particle rearrangement. At t = 400 to 600 minutes, depending on the type of clay, the e-log time curve flattens out.

Wahls, et al. (1966) present an excellent review of the work done concerning the compressibility of compacted soils. Most of the information presented has been reviewed herein, however, their summarizing conclusion is worthy of mention. That is, the soil type is undoubtedly one of the basic factors influencing the compressibility characteristics of a compacted cohesive material, but additional factors such as the method of compaction, degree of saturation, and molding water content

will also have significant effects upon the compressibility characteristics.

Hodek and Lovell (1978b) present convincing evidence on the strong relationship between pore size distribution and the observed effects of compaction variables on the principal properties of compacted soil. Based on previous studies, they claim for a clayey soil compacted dry of optimum, the mass consists mostly of large pores, whereas wet of optimum, there are few large pores and many small ones. Additionally, on the dry side, the clay aggregates are shrunken, hard and brittle; on the wet side, swollen and plastic. With respect to compressibility, these structural models support compressibility trends; that is, dry side samples show a brittleness, compress little under low pressures and a good deal under high pressure (all attributed to the collapse of the large voids); whereas, wet side samples, which lack large voids, show an opposite compressibility trend.

EXPERIMENTAL APPARATUS AND PROCEDURE

Soil Studied

The soil used in this study was obtained from the State Road 37 relocation project (No. F-19(3)PE) in Perry County, Indiana. The specific location was station 1005 + 50, 35 feet left (LINE F), which lies approximately 4 miles south of St. Croix and just north of Bandon. See Figure 5. The soil stratigraphy at this location is also shown and was obtained from boring logs issued by the Indiana State Highway Commission (ISHC), Division of Materials and Tests. The soil will hereafter be referred to as St. Croix clay.

The soil was excavated in the fall of 1976 by Purdue and ISHC personnel. It was delivered to the Purdue Soil Mechanics Laboratory and stored in either a 2 cubic meter wooden box or metal containers. Full attempts to maintain the field moisture content proved successful; over a two year period (1976-1978), only one to two percent moisture was lost.

Because of its high cohesiveness and residual-type characteristics, the clay was initially in the form of large chunks or aggregations...the largest being about the size of a shoe box. Consequently, it was necessary to force sieve the material through a U.S. Standard No. 4 sieve (4.76mm), as shown in Figure 6. The fraction passing was used to

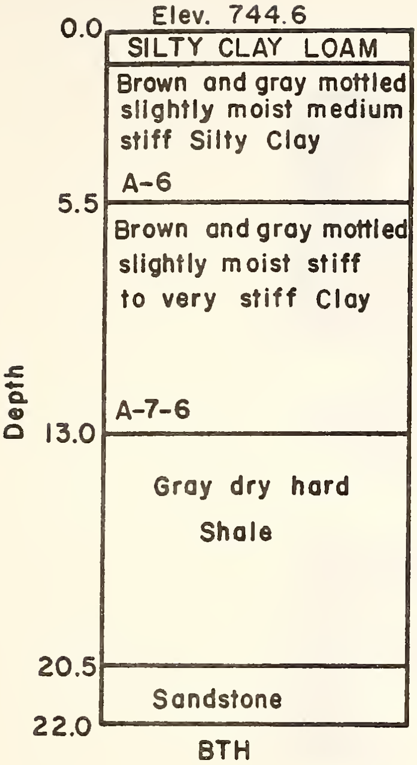
Elev. 744.6
0.0
SILTY CLAY LOAM
Brown and gray mottled slightly moist medium stiff Silty Clay
A-6
5.5
Brown and gray mottled slightly moist stiff to very stiff Clay
A-7-6
13.0
Gray dry hard Shale
20.5
Sandstone
22.0
BTH
Depth

Boring No. 20
State Road 37
1005+50,35' Left (Line F)

(a) Record of Soil Exploration
(ISHC, Division of Materials and Tests)

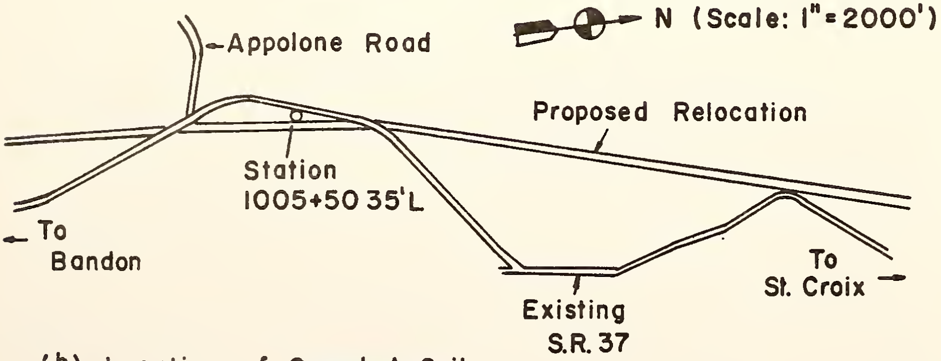

(b) Location of Sampled Soil

FIGURE 5 BORING PROFILE AND LOCATION

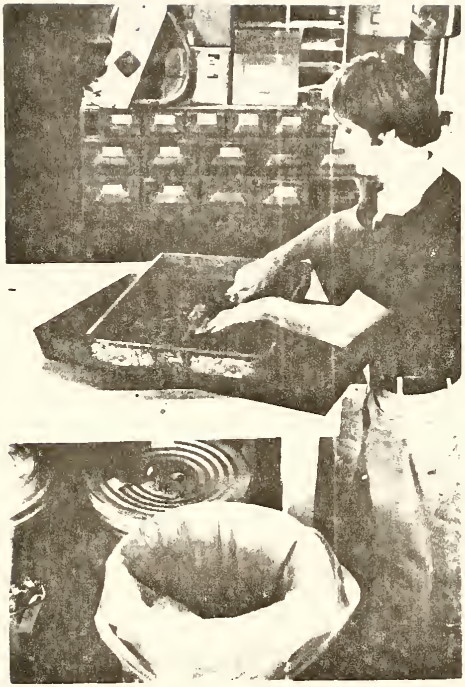

FIGURE 6 ILLUSTRATION OF FORCE SIEVING TECHNIQUE

prepare compacted samples for this study.

The St. Croix clay is medium gray-brown at its natural moisture content. It is classified as a fat clay (CH) and falls within the AASHTO classification of an A-7-6 material. Table 5 gives a general physical description.

TABLE 5. ST. CROIX CLAY CLASSIFICATION

Description	Highly plastic residual Clay (parent material: sandstone-shale)
Soil Classification	
Unified	CH
AASHTO	A-7-6
Index Properties	
Liquid Limit (w_ℓ,%)	53
Plastic Limit (w_p,%)	21
Plasticity Index (I_p,%)	32
Shrinkage Limit (w_s,%)	12
Specific Gravity (G_s)	2.80
Natural Moisture (w_n,%)	20
Clay Size Fraction (%,< 2 μm)	44

Figure 7 illustrates the average grain size distribution determined from 3 hydrometer analyses. As shown, nearly 90 percent of the particles by weight are smaller than 0.074 mm (No. 200 sieve) and approximately 45 percent are within the clay size fraction (< 0.002 mm).

An X-ray diffraction analysis was performed on the clay size fraction: kaolinite was found to be the predominant

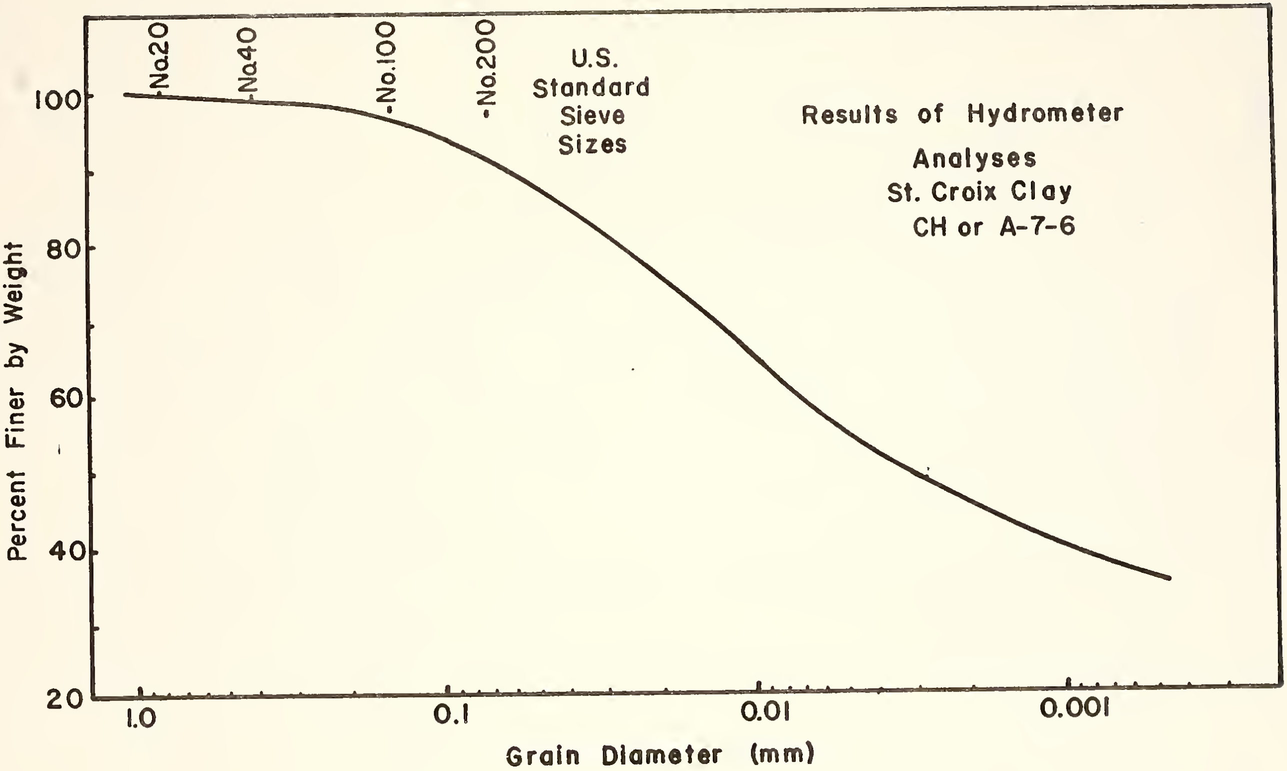

FIGURE 7 GRAIN SIZE DISTRIBUTION

clay mineral, however, montmorillonite was also present in trace amounts.

Sample Preparation

The St. Croix clay was initially broken up by a force sieving method. The collected minus number four material was stored in the laboratory in lined (polyethylene plastic) metal containers. Four days prior to compaction, approximately 2.7 kg (6 lbs.) of this material was sampled for an initial moisture content and sealed in a plastic bag. Directly after the initial moisture content was determined (typically 24 hours after sampling), the soil was either air-dried, i.e., if the initial moisture content was greater than the desired moisture content, or spread on a metal pan—0.45 m x 0.75 m x 0.1 m—for mixing. To achieve the desired moisture content, distilled water was evenly distributed over the soil with a hand-operated atomizer. The soil was frequently mixed with a metal spoon to avoid formation of large lumps.

After mixing, the soil was spooned into a square plastic container—0.3 m x 0.1 m. The container was labelled for identification, wrapped with masking tape to insure air-tightness, and stored in a 0.21 cubic meter (55 gallon) covered plastic humid barrel. In the barrel the soil was allowed to cure for 72 hours; this period was considered suitable for establishing moisture homogeneity.

Compaction and Sampling

Apparatus

The kneading method of compaction was selected for use in this study for the following reasons: (1) the compaction characteristics obtained are comparable, for the same soil, to those obtained by sheepsfoot and pneumatic-type rollers on actual earthen embankments, and (2) the degree of uniformity with respect to moisture content and density is greater than by other methods.

A California-type kneading compactor was used and is shown in Figure 8. It is essentially a semi-automatic device that applies a series of tamps to the soil with a steel shoe. The shoe is shaped like the segment of a circle, is approximately 20 square millimeters (3.1 in.^{2}) in tamping area, and is controlled by a pneumatic-hydraulic system. The energy delivered to the soil is controlled by an air pressure regulator using a calibrated gage. Complete coverage of the sample surface is maintained by a rotating platform; the amount of rotation is approximately 60° between tamps. Gaudette (1960) and Bailey (1976) present additional information on its description and method of operation.

The compaction equipment is shown in Figure 9. It consists mainly of three parts—a main cylinder, a removeable upper collar, and a base stand. The main cylinder is a rigid metal mold—101.6 mm (4 in.) in diameter and 9440 mm^3 (1/30 cu. ft.) in volume. The removeable upper collar is 59 mm

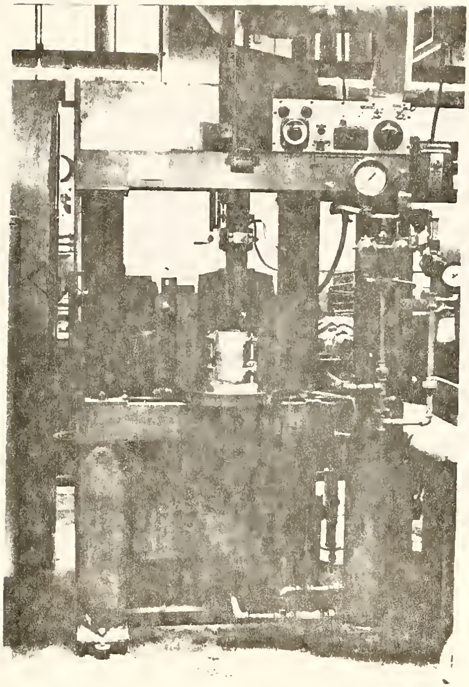

FIGURE 8 CALIFORNIA KNEADING COMPACTOR

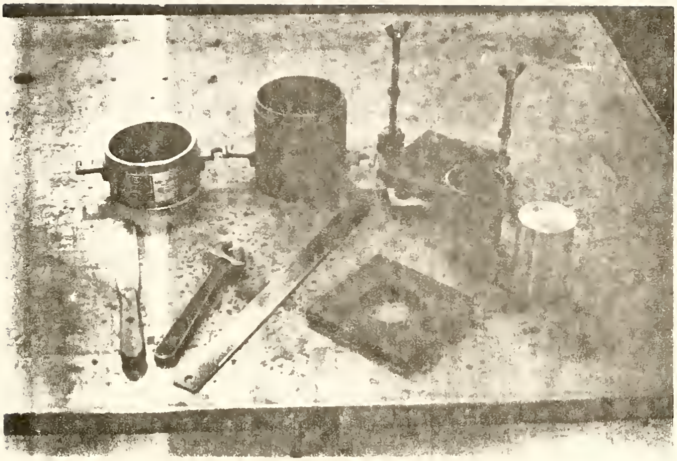

FIGURE 9 COMPACTION, SAMPLING, AND EXTRUDING EQUIPMENT

(2.32 in.) in height and is equal in diameter to the main cylinder.

Also shown in Figure 9 is the apparatus used for sampling and extruding the compacted specimen. It consists of the following: a sharp-edged, seamless, stainless steel tube—88 mm (3.5 in.) in height, 63.3 mm (2.49 in.) in diameter, 2.67 mm (0.1 in.) in wall thickness—used for sampling; an aluminum plug—88 mm in height, 61 mm in diameter—used for extruding the compacted specimen from the tube; a steel attachment piece used for restricting movement of the tube as the soil is being extruded.

Procedure

After the 72 hour curing period, the airtight container was opened and the soil thoroughly mixed. The soil was spooned into the compaction assembly and compacted in 5 approximately equal layers at a rate of 30 tamps per minute per layer. Between layers, the top surface was scarified to insure compacted mass homogeneity. A constant compaction pressure was maintained throughout the process; the value was based on moisture-density relations for the impact method—the results and implications of this procedure will be discussed subsequently.

Following compaction, the entire assembly was dismantled from the compactor, the upper collar and base stand were removed, and the compacted mass was trimmed to the dimensions of the main cylinder. The compacted mass (plus cylinder)

was weighed to the nearest 0.1 g, following which, it was removed from the cylinder by a hydraulic jacking procedure.

The free specimen was placed directly inside a split-mold cylinder of identical height. This mold was circumferentially secured to the sample by attached upper and lower bolts. The steel sampling tube—lubricated with silicone oil on the inside surface—was placed on top of the specimen and hydraulically pressed into the sample. The bolts were periodically loosened to allow for lateral displacement during tube insertion. This procedure is illustrated in Figure 10.

After sampling, the tube was trimmed from the split-mold, sealed in a plastic bag, and stored in a humid decanter for immediate use. Representative portions of the trimmings were collected for "as-compacted" moisture content determination.

Discussion

The kneading method of compaction, as indicated previously, was used in this study to model actual field conditions. Typically however, density and water content are the prescribed elements in an end result approach and are based on results obtained by the laboratory impact method. It was therefore considered appropriate to use the impact moisture-density relations as a base reference for the kneading method.

The moisture-density curves for the three basic impact energy levels used are shown in Figure 11. Each energy level is characterized as follows:

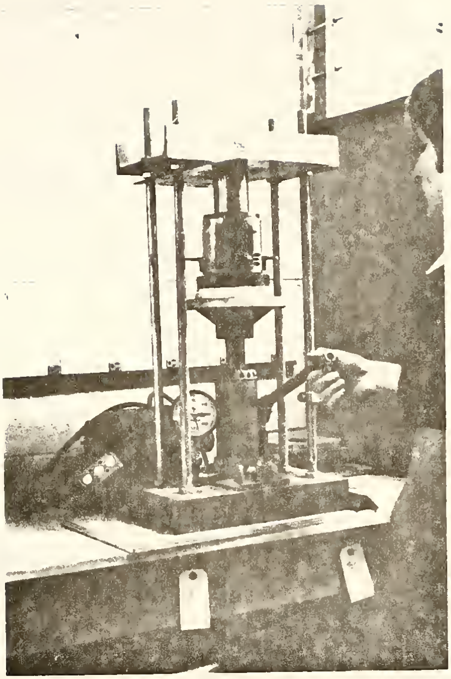

FIGURE 10 SAMPLING OF COMPACTED SPECIMEN

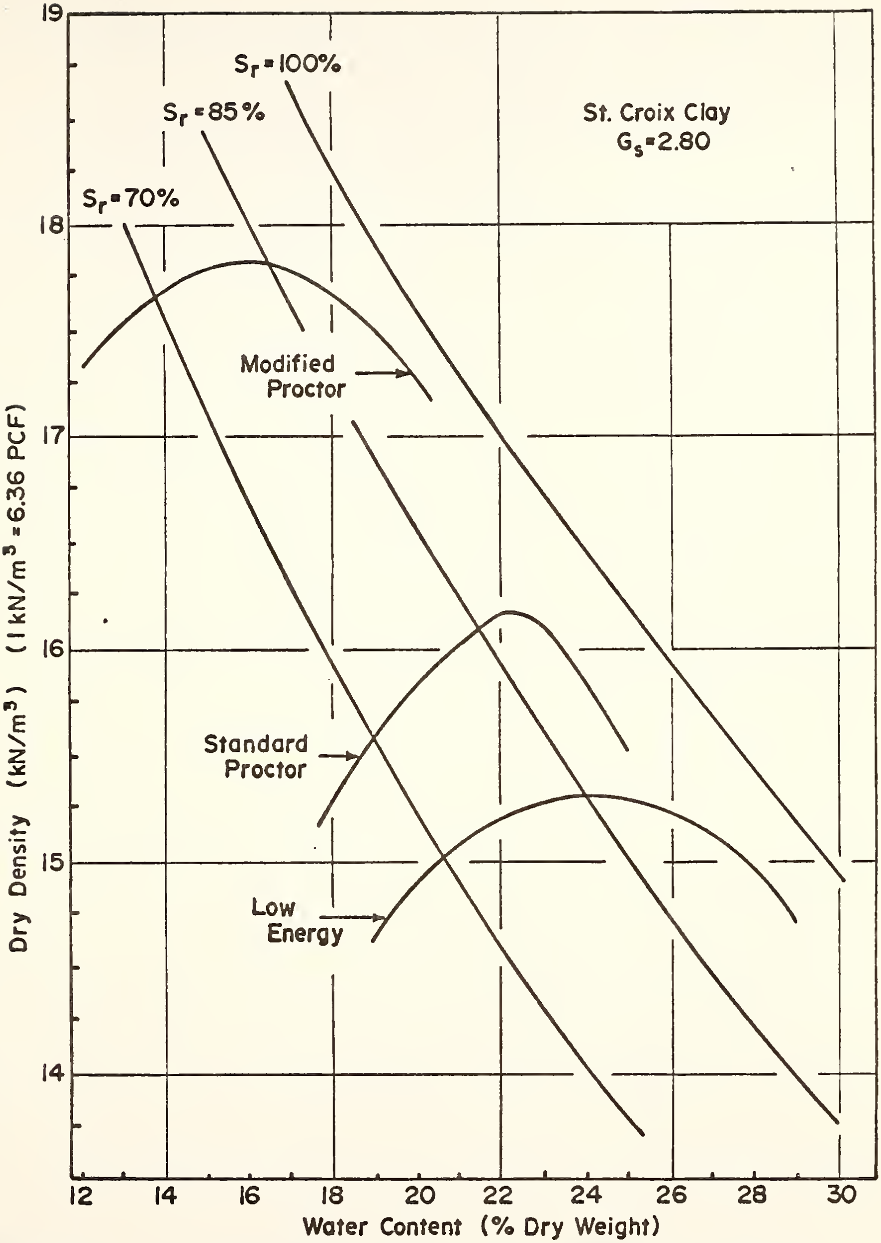

FIGURE 11 MOISTURE-DENSITY-ENERGY RELATIONS FOR IMPACT METHOD.

(1) Low Energy Proctor - 304.8 mm (12 in.) drop, 24.5N (5.5 lb) rammer, 3 layers, 15 blows per layer.

(2) Standard Proctor - 304.8 mm drop, 24.5N rammer, 3 layers, 25 blows per layer.

(3) Modified Proctor - 457.2 mm (18 in.) drop, 44.5N (10 lb) rammer, 3 layers, 25 blows per layer.

The compaction assembly and procedure were as specified in AASHTO T99-70, however fresh samples were used for each point on the curve.

The number of data points obtained for these impact levels is large and are therefore not shown in Figure 11. (See Table A1 in Appendix A for a complete listing of the data). Instead, each curve illustrates the moisture-density statistical function determined from a least squares method. For all three levels the data points match quite closely to the statistical curves, in fact, the coefficient of multiple determination (R^2) for each was 0.99.

A series of kneading compaction tests were performed on the St. Croix clay using different compaction pressures. For each pressure a moisture-density relation was obtained for a range of moisture contents between 4 percent wet and dry of optimum. These relations were corresponded approximately to the three impact levels to select a kneading compaction pressure that would produce the same densities at equivalent water contents; Mishu (1963), Reed (1977) and Garcia-Bengochea (1978) followed a similar procedure. The

differences between the methods with respect to compacted structure and pore fluid pressures were not considered in this study.

According to Bailey (1976), the energy supplied to the sample during kneading compaction is divided into four stages; they are:

(1) The compaction foot descends to the sample surface and pushes into the soil.

(2) Foot pressure is restricted by lateral constraint causing the ram pressure to build up to a preselected level.

(3) The ram pressure is maintained for a short period of time, then decreases.

(4) The ram pressure decreases to zero, and the compaction foot ascends from the sample surface.

In light of this 4 stage process, to accurately quantify the net energy delivered to the soil, an apparatus able to record time- displacement and force-time relationships for each tamp would be required. In this study no attempt was made to quantify this energy; instead, the maximum dynamic foot pressure, determined using a proving ring, was used. The relation between this foot pressure and gage pressure is shown in Figure 12.

The two most common occurrences with the kneading method were: (1) variations in density for soil compacted at similar moisture content and compaction pressure, and

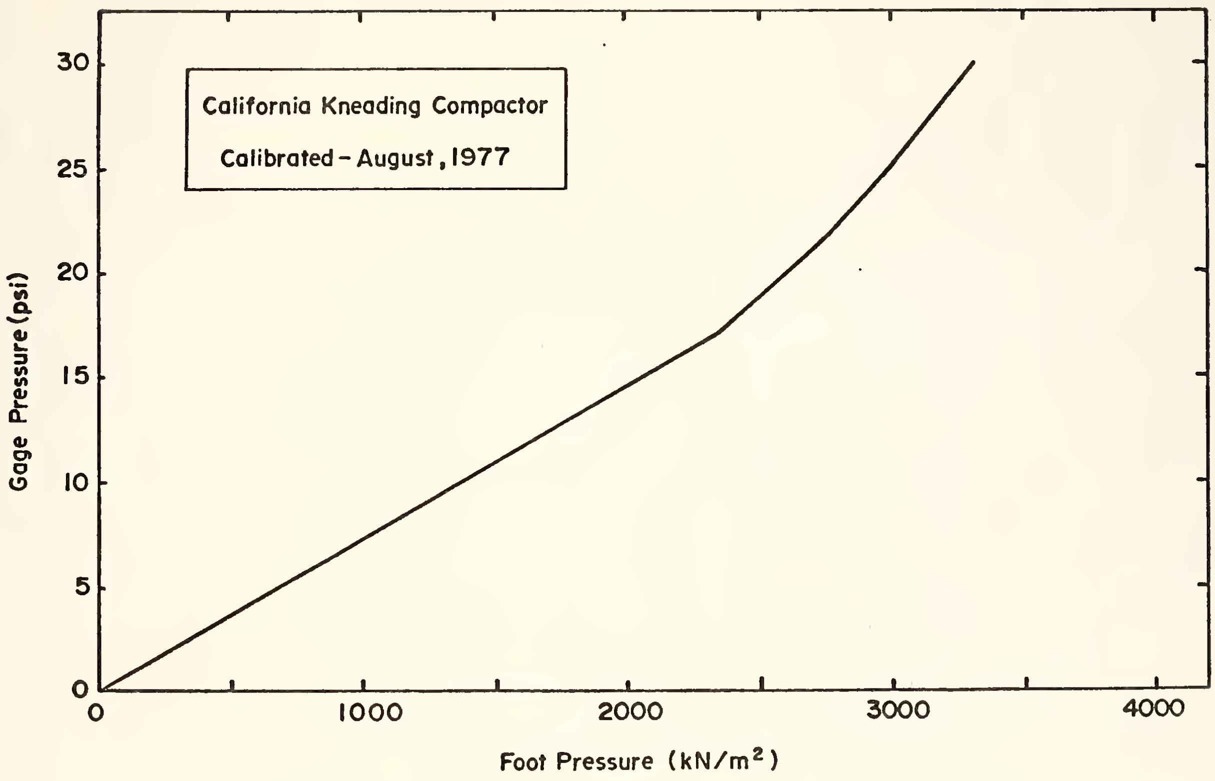

FIGURE 12 DYNAMIC FOOT PRESSURE VS. GAGE PRESSURE

(2) the loss of moisture during the compaction process. The former occurrence has been indicated by others—Woodsum (1951) and Garcia-Bengochea (1978)—and is attributable to the seasonal effects of temperature and humidity on the applied foot pressure, especially at low compaction pressures. The latter occurrence can not be totally prevented, but moisture loss can be minimized by keeping the as-molded soil covered during the compaction process and by expediting the procedure.

As-Compacted Compressibility

Apparatus

A Karol-Warner fixed ring consolidation cell was used in this study; it will be referred to as an "oedometer" in subsequent discussions. It is made completely of brass, except for the loading piston, which is stainless steel. The capability of safely withstanding large backpressures, i.e., 1035 kN/m^2 (150 psi), is its major feature.

The oedometer ring is 63.5 mm (2.50 in) in diameter, 2.54 mm (1 in) in height, and 19.1 mm (0.75 in) in wall thickness. It is not designed to eliminate or reduce wall friction, therefore a silicone lubricant (vacuum grease) was applied before each test. The ring as well as the complete assembly is shown in Figure 13.

Two medium-porous bronze stones—6.35 mm (0.25 in) thick—allowed pore fluid dissipation, during compression, at the top and bottom of the sample. The top stone diameter was slightly less than the ring diameter; this reduced the

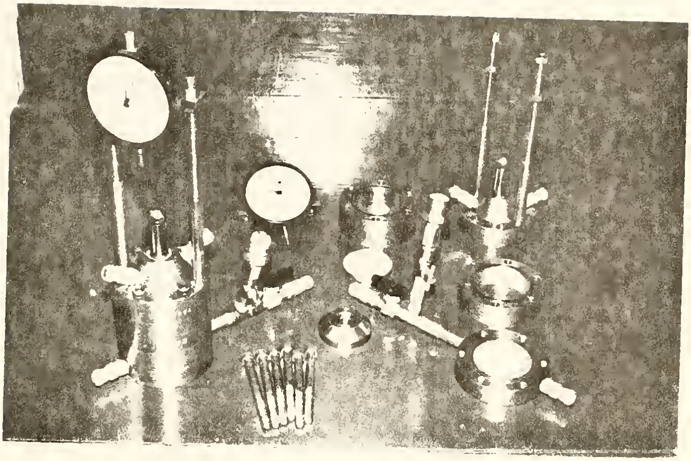

FIGURE 13 KAROL-WARNER CONSOLIDATION APPARATUS

risk of the stone catching on the side of the ring during compression. Single sheets of medium porous filter paper separated the stones from the sample. (Corrundum porous stones were used initially because of their relative cheapness and non-corrosive characteristics, however they were not as durable and often broke during loading).

The loading frame used to compress the sample is shown in Figure 14. It is a lever arm-weight type loading system capable of performing six oedometer tests simultaneously; however, in this study only one as-compacted compressibility test was run at a single time. The mechanical advantage of the system is a 10:1 load ratio for the back hanger and a 40:1 load ratio for the front hanger. The maximum design capacity of the frame is 25.1 kN (2560 kg), which provided a maximum vertical stress of about 8000 kN/m^2 (81.6 kg/cm^2).

The sample compression was measured by a Federal dial gage. The gage measures deflection to the nearest 0.0001 inch (.00254 mm) and has a maximum throw of 10.16 mm (0.4 in). During compression the gage stem is in contact with the loading yoke and measures the movement of the piston, which, in turn, measures sample compression.

Procedure

The tube sample was hydraulically extruded, using the aluminum plug and metal attachment piece (see Figure 9), directly into the oedometer ring. The upper and lower faces of the specimen were trimmed with a steel straight edge

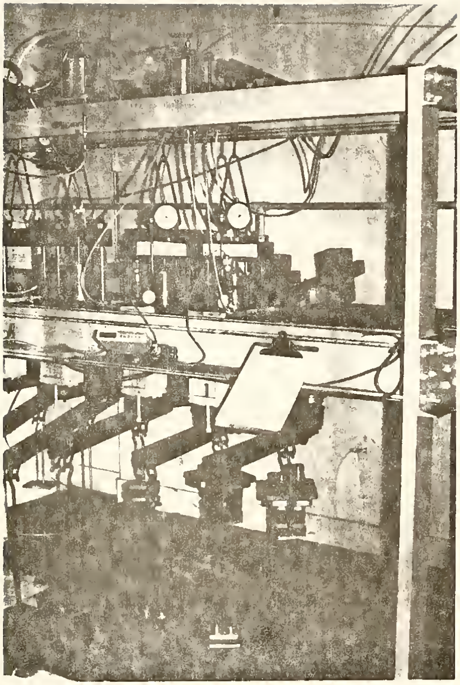

FIGURE 14 LOADING FRAME

using the top and bottom of the ring as guides. The trimmings were collected for "tube sample" moisture content determination.

The sample was weighed (without the ring) to the nearest 0.01 g, and its average height based on four separate measurements (90° apart) was determined using a vernier caliper. The sample was seated against the bottom porous stone; the other porous stone was placed on top of the specimen—both stones were air-dried. Once the specimen was in place, the loading platten, as well as a saturated strip of cotton (used to reduce moisture loss by evaporation), were placed on the top stone. The oedometer was completely assembled, and the loading piston was seated firmly in its position on the platten. The oedometer was placed on the loading frame, the dial gage was mounted, and a seating load of 9.81 kN/m^2 (0.1 kg/cm^2) was applied. Up to this point, all dial gage readings were ignored.

Following the seating load adjustment period (typically 10 minutes), the applied pressure was increased, using a load increment ratio (LIR) of 0.5, to: 15.2, 22.6, 34.0, 49.5, 76.5 kN/m^2, etc., until the prestress value for the particular sample could be well defined. The duration of each load was 10 minutes, during which, dial readings were typically recorded at 0, 0.1, 0.5, 1, 2, 4, 8 and 10 minutes. At the end of the last load, the weights were removed from the frame, the oedometer assembly dismantled, and a final moisture content taken.

Discussion

Trimming the tube sample to the top and bottom of the ring was difficult. Samples compacted dry of optimum tended to crumble very easily when trimmed, which usually resulted in larger voids at the top and bottom of the sample. Samples compacted wet of optimum remained intact, however, tended to pull from the side of the ring in the direction of trimming motion. Other researchers have eliminated this procedure by compacting samples directly into the oedometer rings, however the purpose of their investigations was different from the one reported herein.

Aside from minimizing evaporation from the sample during compression, little was done to maintain isothermal conditions in the testing area. This may be of concern since altering soil specimen temperature can produce effects similar to changes in stress history, as well as changes in pore water pressure (Plum and Esrig, 1969). However, throughout the 3 month as-compacted testing program, ambient temperature was 22° ± 3°C. Furthermore, during each test, which typically took 2-1/2 to 3 hours, the variation was much less. In light of this, it is felt that changes in temperature did not affect the reported results.

The 10 minute load duration criterion was based principally on the findings of Yoshimi (1958). During one-dimensional compression tests on statically compacted Vicksburg silty clay, he observed that most of the compression

occurs within a few minutes after load application. Figure 15 illustrates his findings.

Figure 15(a) shows the amount of compression versus time for different load increments. As can be seen by the shapes of each curve, a relatively large amount of compression takes place within the first 4 minutes, following which, a relatively small amount occurs. Figure 15(b) shows the relation between log time and relative compression (the ratio of compression at time = t to the compression at time = 1000 minutes). At a time = 10 minutes, the relative compression value is approximately 0.85. Additionally, at this same time a change in slope occurs, which may mark the transition between the full expulsion of air and creep. Based on these results, a ten minute load duration was selected.

To determine what load increment ratio to use for the as-compacted compression test, it was decided that the following requirements should be met:

(1) A large portion of the compression must take place within 10 minutes.

(2) As few loads as possible would be used, to limit moisture loss by evaporation.

(3) The prestress value could be accurately defined using the Casagrande construction.

If an LIR = 1 were used, requirements (1) and (2) would be satisfied, however, requirement (3) may not, based on the results of Leonards and Girault (1961) for determining the

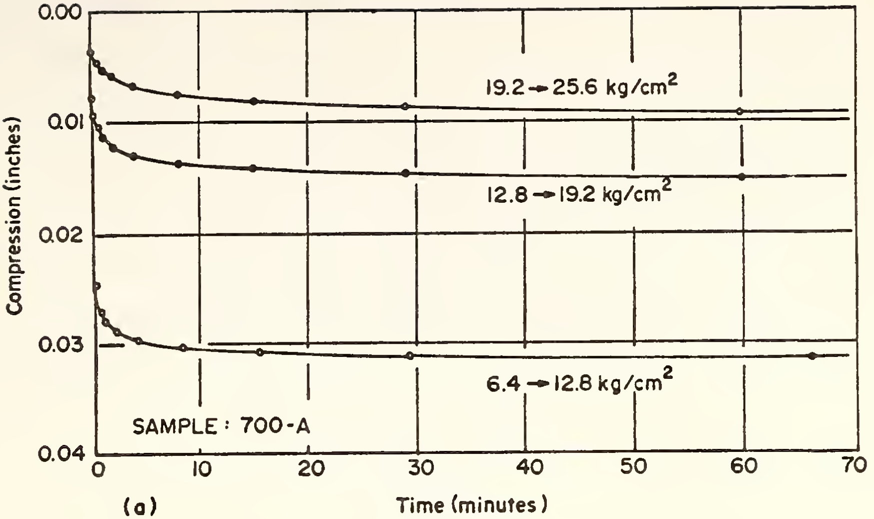

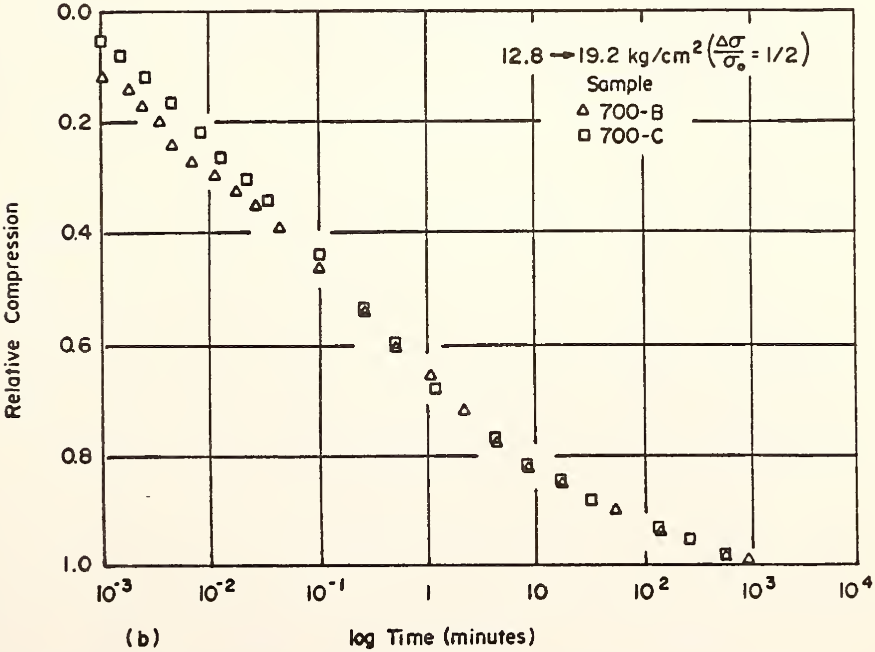

FIGURE 15 COMPRESSION VS. TIME (AFTER YOSHIMI, 1958)

preconsolidation value for saturated soils. If a LIR = 0.1 or 0.2 were used, requirement (3) would be satisfied, but not requirements (1) and (2) (Yoshimi, 1958). Ideally, a load increment ratio equal to actual field loading conditions should be used, however, it is dependent on a given application and may be difficult to determine. Therefore, an LIR = 0.5 was chosen, since it most suitably matched the requirements.

Soaked Compressibility

Apparatus

The oedometer and loading frame previously described were also used to determine the soaked compressibility characteristics; for a description of each assembly, see the previous section.

A Tyco AB pore pressure transducer was used to measure pore pressures during consolidation and back pressures during saturation. The transducer has the capacity to safely measure up to 3450 kN/m^2 (500 psi), which was well beyond the maximum required. The device is made of a series of strain gages which measure the deflection of a diaphragm. Pressure exerted on the diaphragm causes it to deflect, thereby changing the electrical resistance of the gages. The accuracy of the transducer is rated at 1 percent over the full pressure range at normal temperature; it was found to be quite accurate and reliable.

The pressures were recorded with a Hewlett-Packard Digital Voltmeter (Model 3476A). The device was convenient because of its compactness and simple operation.

A closed-system back pressuring device developed by Garcia-Bengochea (1978) was used for back pressuring the oedometer samples (see Figure 16). The apparatus is arranged such that two samples could be back pressured simultaneously, either from one regulator or separately from two. An admirable feature of this apparatus is the calibrated standpipes; they were useful for determining saturation, as will be discussed subsequently.

A de-airing system was used to remove air from the oedometer. It consisted of a vacuum regulator, a vacuum pump, an aspirator, and a de-aired water reservoir. The use of this apparatus was not essential, however it did expedite the saturation process.

Procedure

The compacted specimen was assembled in the oedometer as described in the previous section. It was compressed (LIR = 0.5, load duration = 10 minutes) in the as-compacted condition until a vertical pressure of either 160, 320, or 480 kN/m^2 was applied, whereupon, it was allowed to compress for 30 minutes. At the end of this sustained loading period, the de-airing apparatus was connected to the oedometer at its top and bottom. Thirty-five kN/m^2 (5 psi) of vacuum was applied and maintained for approximately 1 hour. This

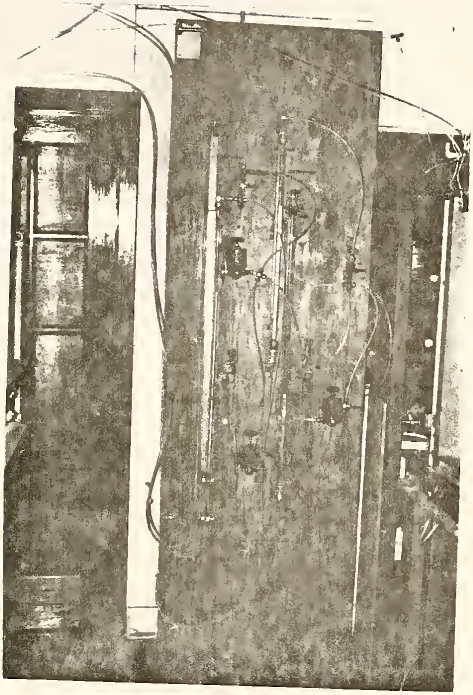

FIGURE 16 BACK PRESSURE SATURATION DEVICE

procedure was helpful in removing air from the initially air-dried porous stones and from the cell chamber. An overhead reservoir filled with de-aired water was then connected to the top and bottom of the cell. The vacuum pressure sucked the water through the cell, thereby filling it with water without entering air. Once filled, the de-airing apparatus and the overhead reservoir were disconnected from the oedometer. The sample, now in contact with water, was allowed to attain equilibrium. During this period the pore pressure transducer was connected to the base of the oedometer cell.

After equilibrium was reached, the back pressure device was connected to the top and bottom of the cell. The back pressure was incremented 70 kN/m^2 (10 psi) every hour until a maximum pressure of 965 kN/m^2 (140 psi) was applied. The sample was then permitted to adjust under full back pressure for a period of 48 to 72 hours. At the end of the adjustment period, the back pressure supplied to the bottom of the cell was disconnected, however back pressure was still maintained at the top.

The sample was unloaded from the original sustained load to 76.4 kN/m^2 using a LIR = 1.0. The sample was then reloaded, using a load increment ratio of 0.5, to: 114.54, 171.52, 257.33, 386.1, 579.15, 868.72, 1303.08, and 1954.6 kN/m^2. Dial readings were recorded during loading and unloading at the conventional times. The duration of each load was based on t_{100} values determined from pore pressure

measurements. Pore pressure measurements were made at the bottom of the sample, and the sample drained singly at the top. At the end of the last load, the back pressuring apparatus was disconnected, the weights were removed from the frame, the oedometer was dismantled, and a final moisture content was taken.

Discussion

Soaked compressibility tests on the compacted St. Croix clay were performed to determine long term compressibility characteristics of actual embankments. In order to simulate field loading and environmental conditions, the soil was initially tested in the as-compacted condition to a sustained load. This load—either 160, 320, or 480 kN/m^2—represents the pressure exerted by an equivalent embankment height of 7.8 m (25 ft.), 15.6 m (50 ft.), and 23.5 m (75 ft.), respectively. (A wet unit weight of 20.9 kN/m^3 (133 pcf) was used which is slightly greater than the maximum at Standard Proctor).

As indicated previously, the back pressure was incremented 70 kN/m^2 every hour until the maximum pressure (965 kN/m^2) was reached. Lowe, Zaccheo, and Feldman (1964) suggest incrementing every 30 minutes, therefore twice this time was considered reasonable.

Lowe and Johnson (1960) and Black and Lee (1973) presented theoretical curves which show the back pressure required to bring an unsaturated sample from an initial

degree of saturation to a final degree of saturation. For the range of saturation greater than approximately 80 percent, the maximum back pressure used in this procedure, according to the theoretical curves, was sufficient for achieving full saturation; however, for lower degrees of saturation, i.e., within the dry of optimum range, greater amounts of back pressure would theoretically be required. As will be shown in the next chapter, the maximum used in this study was adequate.

After 36 hours of sustained loading and maximum back pressure, two approaches were taken to determine saturation. In the first approach, which was performed every five hours, the drainage lines from the oedometer were closed, and a 0.5 kg weight was applied. After 2 to 5 minutes after application, the pore water pressure response was recorded and the value of $\Delta u/\Delta\sigma$ determined. If three successive attempts gave the same $\Delta u/\Delta\sigma$ ratio, the back pressure was incremented to 1035 kN/m^2 (150 psi). After 3 hours the change in water level in the pressurized standpipe was recorded. If the change was negligible, i.e., less than 1 mm in height, the soaked compressibility test was begun. If not, the forementioned procedure was repeated, until these requirements were met.

RESULTS AND DISCUSSION OF RESULTS

As-Compacted Compressibility

Compaction

The moisture-density-energy relations for the Low Energy, Standard and Modified Proctor impact levels were previously shown in Figure 11. As mentioned, the kneading compaction curves were corresponded accordingly. The correspondence for each level is illustrated in Figure 17.

In this Figure, observe that for a given kneading compaction pressure, an increase in water content has a greater effect on the compacted dry density than a similar increase for a nearly corresponding impact level. Also observe that large increases in density result, particularly in the dry of optimum range, from nominal increases in compaction pressure.

In view of the above, to obtain an equivalent density using the kneading method, it was necessary to: (1) maintain the gage pressure exactly at the required pressure, and (2) prevent the loss of moisture during the compaction process. However, even with strict monitoring and control, the end-result density differed from the desired end-value density by 0.15 to 0.30 kN/m^3 (1 to 2 pcf), thereby indicating the inherent difficulties associated with meeting

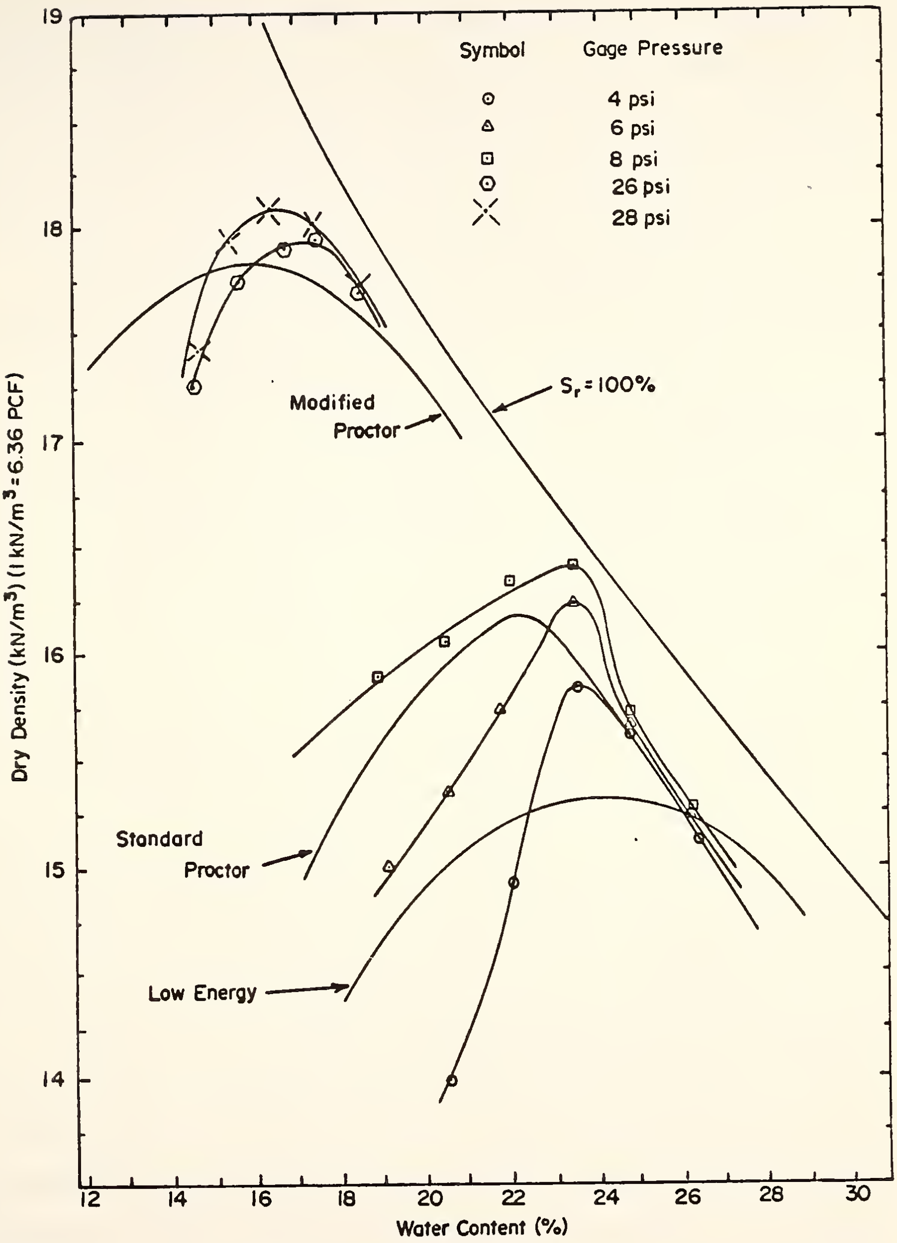

FIGURE 17 CORRESPONDENCE BETWEEN KNEADING AND IMPACT METHODS

these requirements. The factors which may have affected these differences were discussed previously. Additionally, it is not impossible that uncharacteristic material may have been stored and sampled for use, due the limited areal extent and depth of the St. Croix clay deposit (See Figure 5).

The compaction variables used to characterize each as-compacted compressibility test sample are defined as follows:

(1) Water Content (w,%) - the average of the as-compacted and tube sample moisture determinations.

(2) Dry Density (γ_d, kN/m^3) - the dry density of the oedometer sample computed from its unit weight, water content (w), and volume. (See Special Notes and Conversions Section for explanation of the units).

(3) Compaction Pressure (P_c, kN/m^2) - the maximum dynamic kneading foot pressure applied during compaction, expressed nominally.

The other computed variables were initial degree of saturation (S_r, %) and initial void ratio (e_o). Both were calculated from (1) and (2) of the above.

The compaction water contents ranged between 4 percent wet and dry of optimum and were based on the results of the impact method. Their specific values within this range were selected arbitrarily to account for the expected variation in water contents among field-compacted samples of the same soil.

As previously stated, the dry density variable refers to the oedometer sample density rather than the compacted mold density. (Table A2 in Appendix A lists a comparison of both). This density was used due the single or combined effects of trimming and sampling. That is, trimming often caused voids in the brittle dry-of-optimum samples, and the release of mold confinement prior to sampling caused swelling in the wet-of-optimum samples.

Thirty-two as-compacted compressibility tests were performed; the values of the previously defined compaction variables are listed in Table 6. In this Table, as well as subsequent discussions, the sample number characters are defined as follows: L, S, M—the compaction condition corresponding to the equivalent Low Energy, Standard Proctor, and Modified Proctor impact levels, respectively; D, O, or W—dry, at, or wet-of-optimum conditions, respectively; 1, 2, ..., etc.—the sample number for that condition. For example, a sample designated by MD1 characterizes the first (1) sample compacted to a dry (D) of optimum condition using an equivalent Modified Proctor (M) kneading compaction pressure.

Compression vs. Time Relations

The compressibility of compacted clays and other partially saturated soils generally occurs in three stages (Yoshimi, 1958); they are: (1) Initial Compression - the immediate response due to the compression of the soil skeleton and the

TABLE 6 INITIAL COMPACTION VARIABLES FOR AS-COMPACTED COMPRESSIBILITY SAMPLES

Sample No.	Water Content (%)	Dry Density $\gamma_d (kN/m^3)$	Compaction Pressure $P_c (kN/m^2)$	Degree of Saturation S_r (%)	Initial Void Ratio e_o
LD1	20.60	13.97	460	59.77	0.9649
LD2	20.60	14.85	525	65.26	0.8838
LD3	20.51	14.27	426	62.15	0.9240
LO1	23.26	15.74	426	80.14	0.8126
LO2	23.85	15.77	558	89.62	0.7451
LO3	24.27	14.91	683	80.68	0.8423
LW2	27.94	14.88	525	92.47	0.8460
LW3	26.98	14.82	657	88.42	0.8544
SD4	18.95	15.26	788	66.40	0.7990
SD8	19.38	14.62	788	61.82	0.8770
SD9	19.59	15.06	788	66.58	0.8238
SD10	19.37	15.65	788	71.87	0.7545
SO3	21.37	15.76	657	80.61	0.7423
SO8	21.71	15.78	657	82.02	0.7411
SO9	21.21	15.99	657	82.70	0.7180
SO11	21.65	15.72	814	81.12	0.7473
SO12	22.32	16.15	788	89.20	0.7066
SO13	22.67	16.25	762	92.92	0.6905
SO16	22.68	15.97	762	88.18	0.7202
SW2	25.38	15.24	722	88.67	0.8014
SW3	25.71	15.13	722	88.27	0.8155
SW4	25.05	15.42	722	89.80	0.7810
SW6	24.72	15.64	722	91.49	0.7565
SW7	24.87	15.38	722	88.66	0.7854
SW8	24.71	15.68	722	92.08	0.7514
MD1	14.67	18.31	3191	82.10	0.5003
MD2	13.96	17.65	3071	70.23	0.5565
MO1	16.20	17.97	2905	85.90	0.5281
MO2	15.71	18.10	2735	85.10	0.5168
MW1	19.59	16.99	2466	87.85	0.6243
MW3	19.74	16.87	2439	88.05	0.6277
MW5	19.57	16.86	2466	87.18	0.6285

pore-air phase; (2) Consolidation - the compression resulting from the outflow of pore fluids; (3) Creep - the rearrangement of soil particles or aggregations under a constant applied stress. It is likely that each stage acts in combination, however, in this discussion, each will be considered as acting singly. (The compressibility of the oedometer apparatus was accounted for in all subsequent discussions).

Figure 18 shows a series of typical[1] compression-time relations for samples compressed from initially dry of optimum conditions. For each load increment shown, a large amount of compression occurs within the first minute of loading, with very little compression occurring thereafter. Yoshimi (1958) observed similar behavior for a compacted silty clay (Figure 15) and attributed each to the following: Initially rapid compression - the extremely rapid dissipation of excess pore air pressure ($\Delta u_a > 0$, $\Delta u_w < 0$), as well as the initial compression of the pore air and soil skeleton; Subsequent negligible compression - the dissipation of residual pore air pressure and soil particle rearrangement.

Similar relations for samples compressed from initially near optimum conditions are shown in Figure 19. Observe that the duration of each load was 60 minutes. Of interest is that these relations and the ones shown in Figure 18 are quite similar. That is, both sets of curves show initially large compression within the first minute, followed by nominal compression in subsequent minutes. These data may

---

[1] Some curves are omitted for clarity

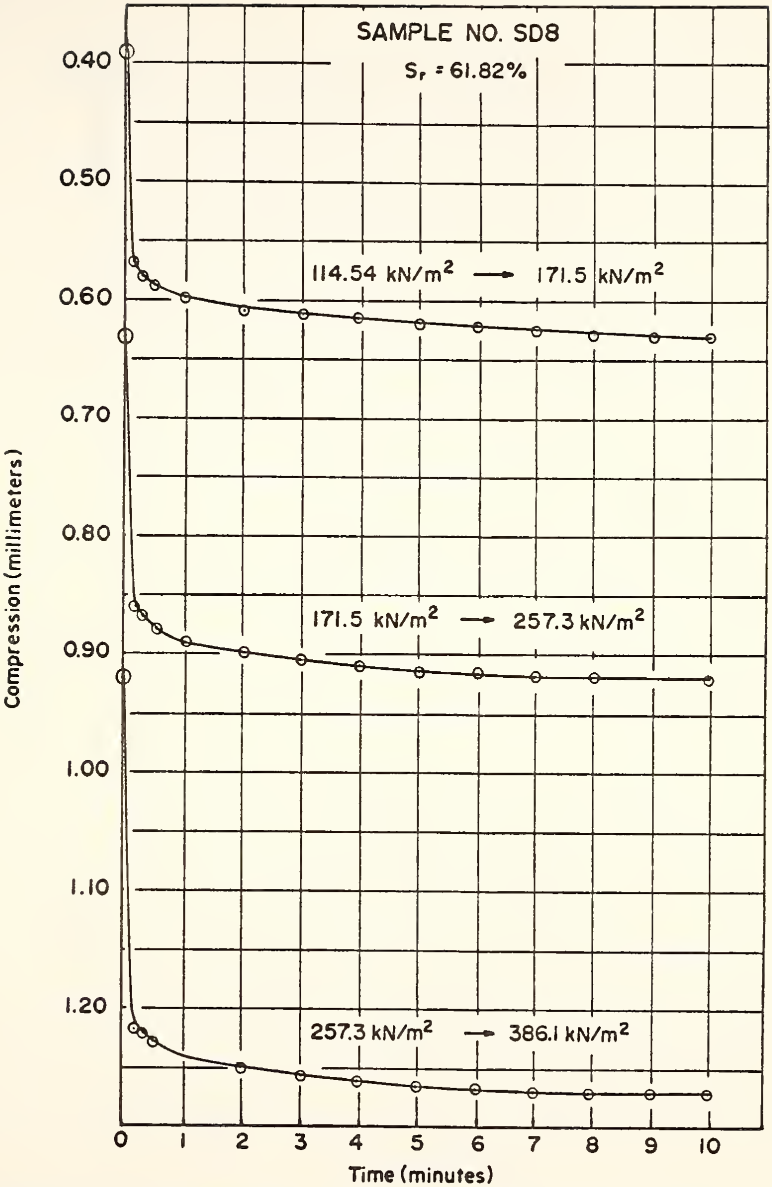

FIGURE 18 COMPRESSION VS. TIME (DRY OF OPTIMUM)

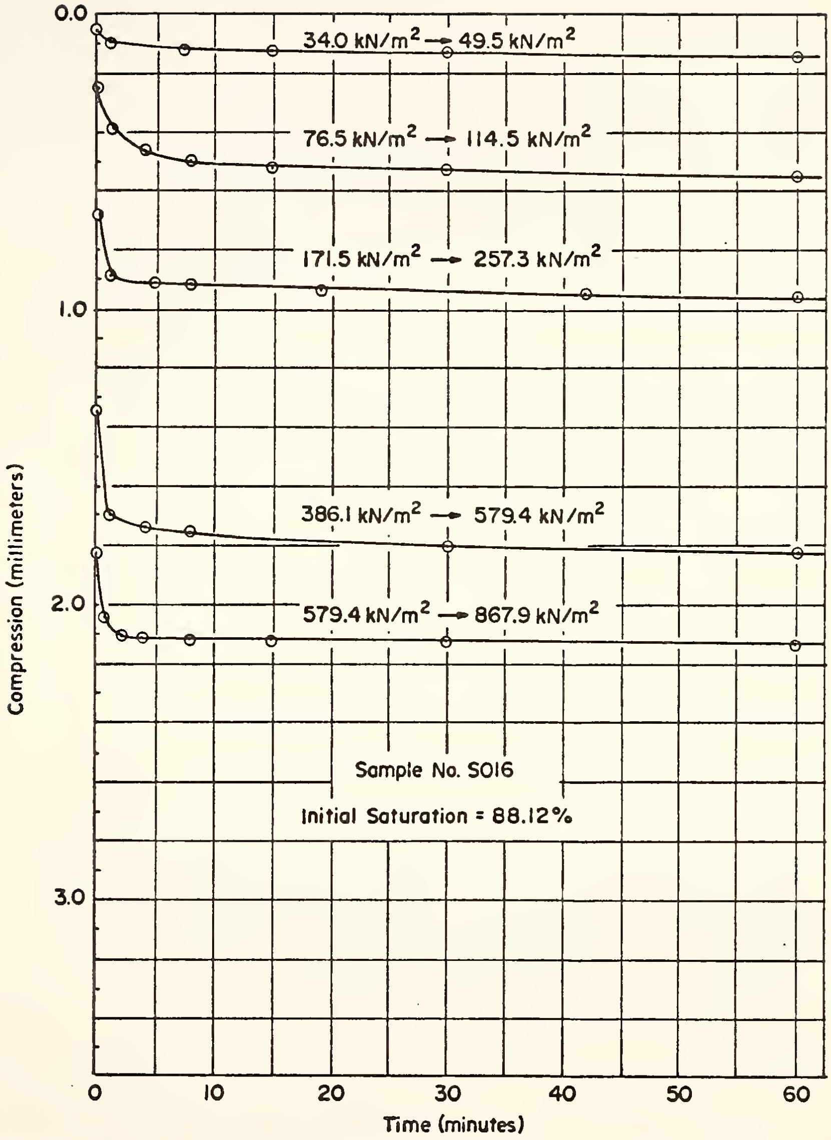

FIGURE 19 COMPRESSION VS. TIME (NEAR OPTIMUM)

suggest that samples compacted dry and at optimum exhibit similar fluid continuity conditions, i.e., continuity of pore air.

To facilitate a more direct comparison, Figure 20 shows the relative compression (compression at time = t divided by the total compression at time = 10 minutes) plotted against time. For the two samples just discussed (SD8, SO16), the magnitudes of relative compression are virtually the same at each successive time plotted. It is believed that this would not occur if the compression of both samples was not dominated by the outflow of pore air ($\Delta u_w < 0$); specifically, if the air voids were not interconnected (Yoshimi, 1958).

Figure 20 also shows the magnitude of relative compression with time for an initially wet of optimum sample—LW2. In comparison, the wet-side sample exhibits the least amount of relative compression within the 10 minute period. This may suggest either of three processes governing wet-side compression: (1) the pore air is occluded, the pore water pressure is less than atmospheric, and compression is governed by the rearrangement of soil particle or aggregations at constant water content, (2) the pore air is occluded, pore water pressure is greater than zero, compression is governed by the outflow of pore water and contained air, or (3) the air voids are continuous, the pore water is less than atmospheric, and compression is governed by the outflow of air, but at a reduced permeability due the high degree of saturation (Barden, 1974).

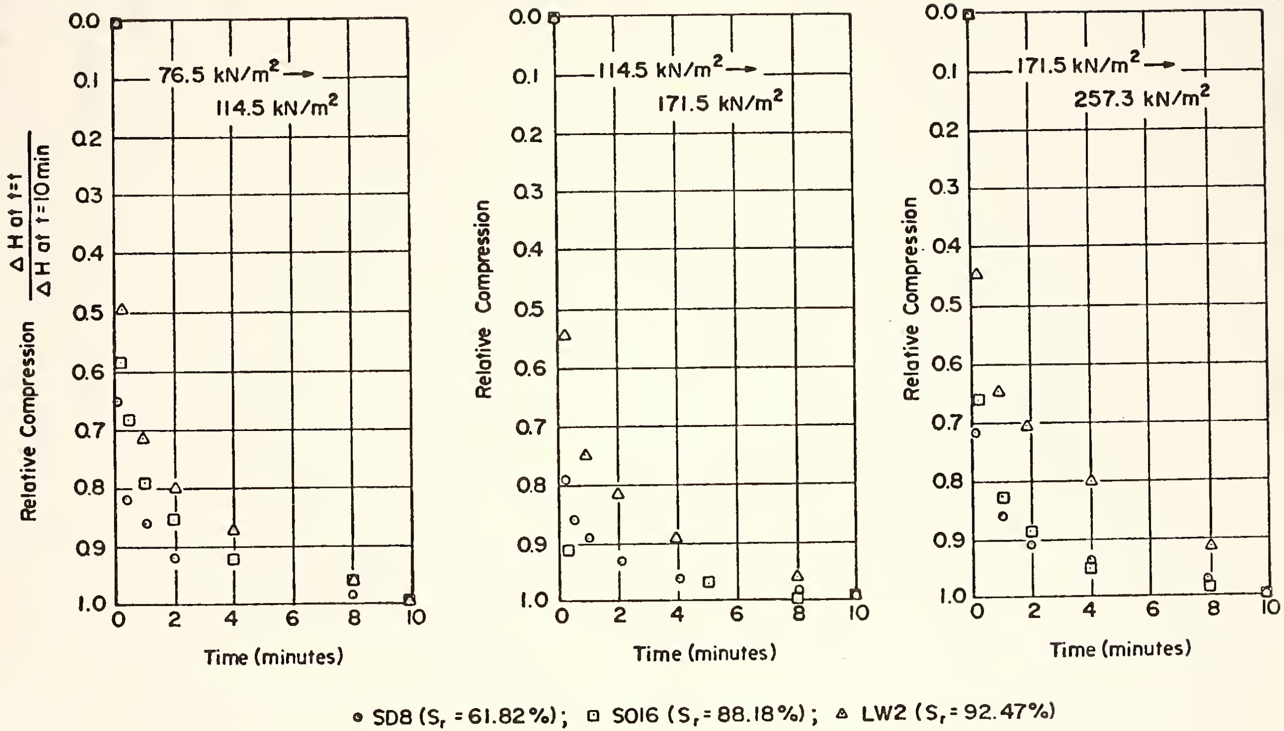

FIGURE 20 COMPARISON OF RELATIVE COMPRESSIONS FOR DRY, WET, AND AT OPTIMUM SAMPLES

In this connection, Yoshimi (1958) and Danielson (1963) found no outflow of pore water in compacted samples compressed to final saturations of 94 to 97 percent, respectively. (Unfortunately, in this study, the final degree of saturation could not be accurately determined due the uncontrolled effects of evaporation on moisture loss). It is therefore unlikely that the compression of sample LW2 was governed by process (2). However, during compression, if the degree of saturation had become sufficiently high, i.e., $S_r > 97$ percent, process (2) may have occurred via process (1) or (3).

Compressibility Characteristics

The purpose of compaction is to improve the engineering properties of the material in a given application. The effect of the important compaction variables on compressibility behavior has been well-documented by others: Woodsum, 1951; Wilson, 1952; Leonards, 1952; Lambe, 1958b; Yoshimi and Osterberg, 1963; Mishu, 1963. In the following, the observed as-compacted compressibility behavior will be discussed briefly and in connection with some of the recent evidence concerning compacted clay pore sizes. (In this and subsequent discussions, consolidation will refer to the outflow of pore water and/or pore air; however, in the classical sense, it is only used to describe the outflow of pore water).

Figure 21 shows the effects of increasing water content and degree of saturation on compressibility behavior for samples compacted to equivalent Low Energy conditions. As

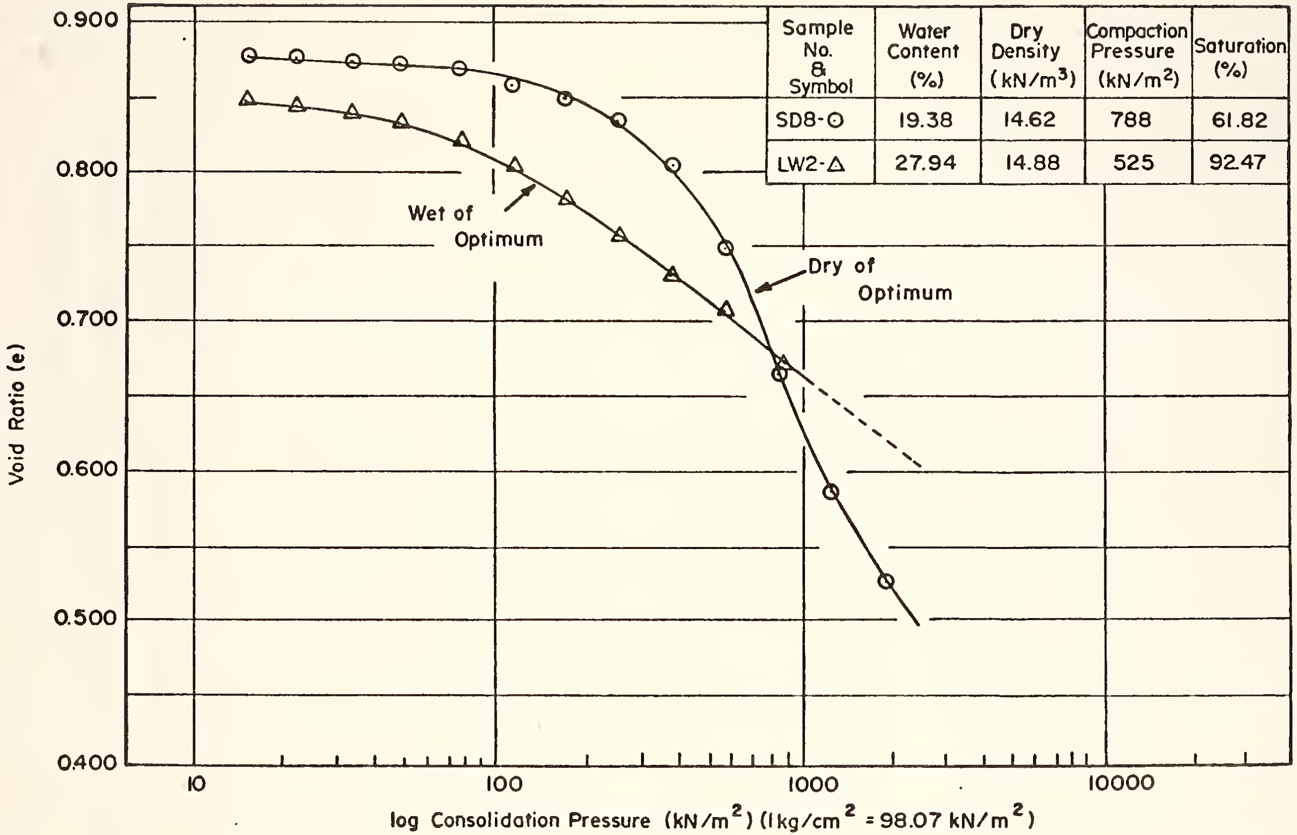

Sample No. & Symbol	Water Content (%)	Dry Density (kN/m^3)	Compaction Pressure (kN/m^2)	Saturation (%)
SD8-⊙	19.38	14.62	788	61.82
LW2-△	27.94	14.88	525	92.47

FIGURE 21 EFFECT OF MOISTURE CONTENT ON COMPRESSIBILITY (LOW ENERGY)

may be inferred, there is a marked difference in the compressibility behavior for wet and dry-side samples depending on the range of consolidation pressure considered. That is, in the low pressure range (20 to 200 kN/m^2), the wet-side sample is more compressible than the dry-side sample, whereas, in the high range (> 200 kN/m^2), the opposite is true. Similar behavior is illustrated in Figure 22 for wet and dry-side Standard Proctor samples and Figure C1 for wet and dry-side Modified samples.

Lambe (1958a,b) explained this behavior in terms of compacted clay structure, colloidal chemistry, and soil particle rearrangement. However, more recently, Hodek and Lovell (1978b) examined this behavior in terms of pore size distribution, pore size magnitude, and deformable aggregate theory. Based on supporting evidence (Hodek, 1972; Reed, 1977; Garcia-Bengochea, 1978), their explanation can be stated as follows:

(1) Dry-side compressibility - the pores are typically large and numerous; the clay aggregates are shrunken, hard and brittle; compressibility is governed by the collapse of large pores under straining.

(2) Wet-side compressibility - the pores are small and numerous; the clay aggregates are swollen and plastic; compressibility is governed by the fusing of aggregates under load.

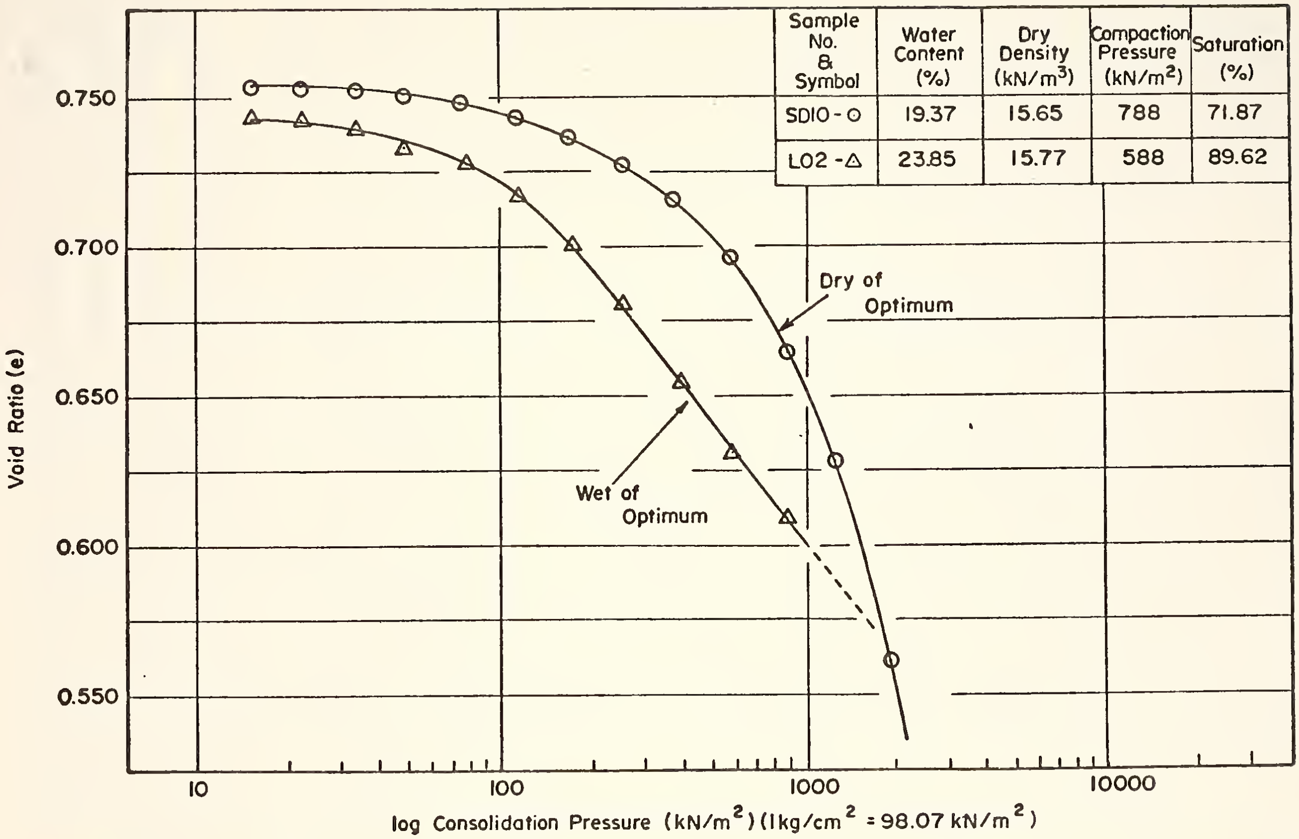

Sample No. & Symbol	Water Content (%)	Dry Density (kN/m^3)	Compaction Pressure (kN/m^2)	Saturation (%)
SD10 - ○	19.37	15.65	788	71.87
L02 - △	23.85	15.77	588	89.62

FIGURE 22 EFFECT OF MOISTURE CONTENT ON COMPRESSIBILITY (STANDARD PROCTOR)

In view of this explanation, a dry-side sample would compress less in the low pressure range due the large intergranular forces resulting from the many well-developed meniscii. However, on loading, these forces are overcome, and the brittle aggregates displace into adjacent pores. Consequently, a large amount of compression occurs due the large amount of available interaggregate pore space. On the other hand, a wet-side sample compresses more in the low pressure range due the smaller number of developed meniscii (high degree of saturation) and less in the higher range due the relatively small number of large interaggregate pores.

Figure 23 illustrates the effect of increasing compaction pressure on the compressibility behavior of initially dry compacted samples. A general observation is that the slope of the curves within the respective high pressure ranges becomes steeper, i.e., increasingly more negative, with decreasing compaction pressure. With respect to the structural models previously discussed, this suggests that for dry-side samples, the magnitude and frequency of the large pore mode decreases with increasing compaction pressure.

If a similar comparison is made for the wet-side samples of Figure 24, then it may be said that increased compaction pressure does not alter compressibility behavior to as great a degree as the dry-side samples of Figure 23. Moreover, it suggests that the magnitude and frequency of the large

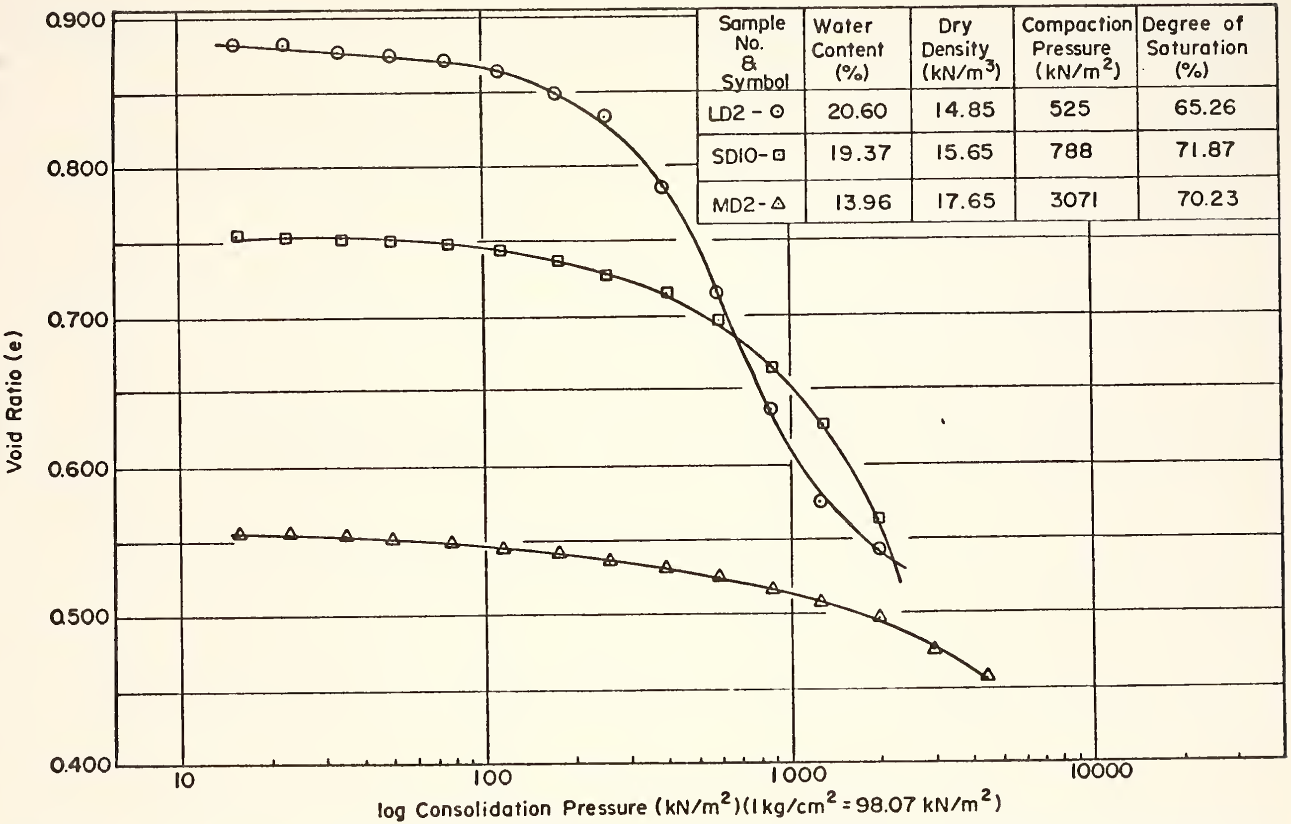

Sample No. & Symbol	Water Content (%)	Dry Density (kN/m³)	Compaction Pressure (kN/m²)	Degree of Saturation (%)
LD2 - ⊙	20.60	14.85	525	65.26
SD10 - ⊡	19.37	15.65	788	71.87
MD2 - △	13.96	17.65	3071	70.23

FIGURE 23 EFFECT OF COMPACTIVE EFFORT ON COMPRESSIBILITY (DRY OF OPTIMUM)

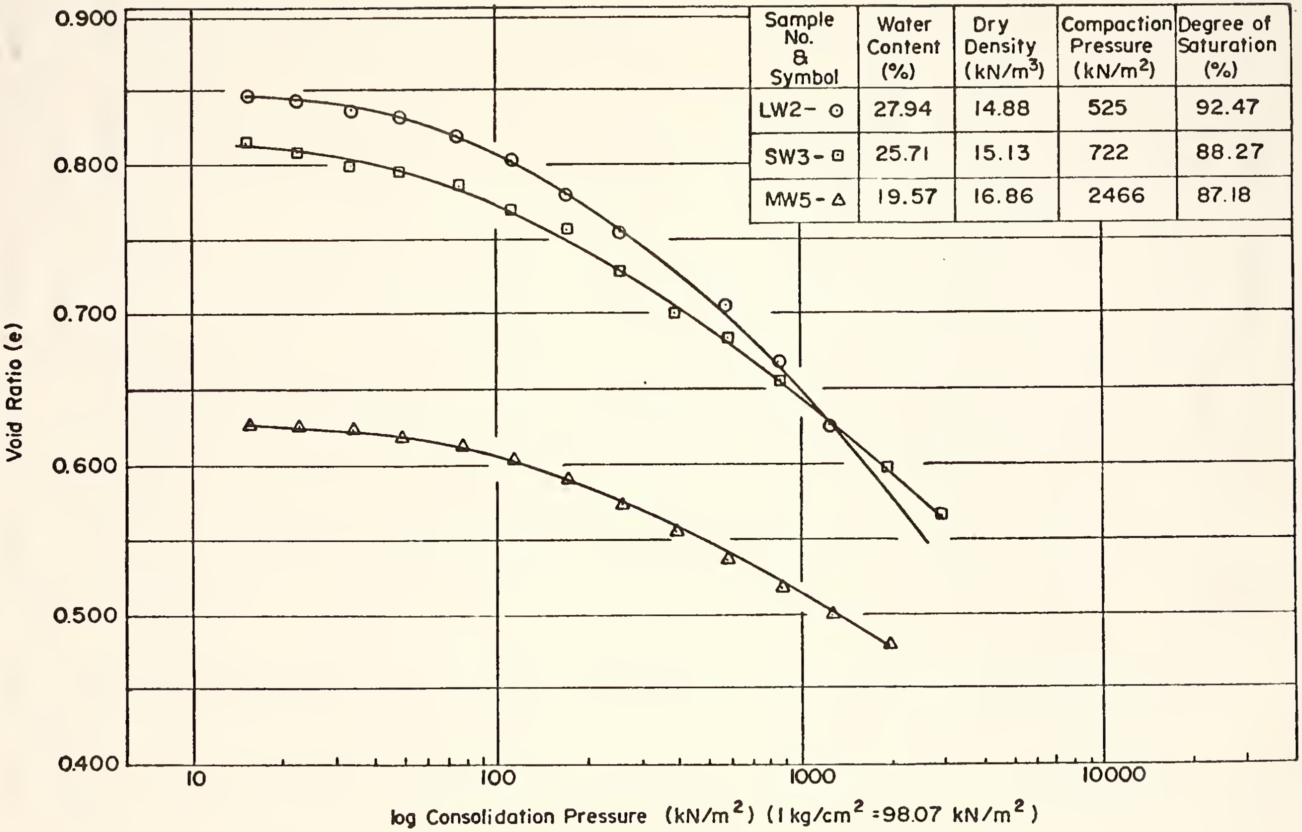

Sample No. & Symbol	Water Content (%)	Dry Density (kN/m³)	Compaction Pressure (kN/m²)	Degree of Saturation (%)
LW2- ⊙	27.94	14.88	525	92.47
SW3- ⊡	25.71	15.13	722	88.27
MW5- △	19.57	16.86	2466	87.18

FIGURE 24 EFFECT OF COMPACTIVE EFFORT ON COMPRESSIBILITY (WET OF OPTIMUM)

pore mode is little affected by increased compaction pressure.

For samples compacted near optimum, Figure C2 illustrates similar trends as established for the dry-side samples of Figure 23.

According to Garcia-Bengochea (1978), Bhasin (1975) found that the fraction of pores for dry compacted clays decreases with increasing effort. Similarly, for wet compacted clays, this fraction remains unchanged. Based on the foregoing, it is therefore believed that macrostructure is truly an important factor contributing to compacted clay compressibility.

Compactive Prestress

The results presented in the previous section illustrated the compressibility behavior within specific ranges of applied pressure. However, an important characteristic not considered was the value of compactive prestress. Clearly, its value could serve useful in design, since the compressibility behavior of the mass may be different at embankment confining pressures above and below this value. That is, as may have been shown in Figures 21 to 24, each specific value of compactive prestress, as determined in the manner presented below, is the approximate pressure value below and above which low range compressibility behavior and high range compressibility behavior respectively occur.

The values of compactive prestress (P_s) and prestress ratio ($^{P}s/P_c$) for each of the 32 as-compacted compressibility

test samples are listed in Table 7. Each value of compactive prestress was determined from its corresponding e-log p curve using the Casagrande approximation commonly employed for determining the most probable preconsolidation pressure for saturated soils. In the strictest sense, its use may be unjustified. However, the current state of the art is such that very little is known of the fundamental relationships governing unsaturated compression. Consequently, the use of this method, or any other method, will in the classical sense be unjustified.

Figure 25 shows the values of compactive prestress plotted at their respective values of water content, dry density, and equivalent impact effort level. Note that many of the densities do not correspond to a particular impact level density. This illustrates the combined effects of sampling, trimming, and the inherent difficulties on obtaining the desired end-value density, as previously discussed. The 87 percent saturation curve was arbitrarily selected and plotted in this Figure, and for the purpose of this discussion, will be referred to as a means of separating wet and dry compaction conditions.

From this Figure, certain general conclusions may be made with respect to the capacity for prestressing; they are:

(a) For dry of optimum conditions, $S_r < 87\%$:

(1) At a given equivalent impact effort level, as the water content increases, the value of compactive prestress decreases.

TABLE 7 VALUES OF COMPACTIVE PRESTRESS AND PRESTRESS RATIO

Sample No.	Compactive Prestress P_s (kN/m^2)	Compaction Pressure P_c (kN/m^2)	Prestress Ratio P_s/P_c	Degree of Saturation S_r (%)*
LD1	290	460	0.63	59.8
LD2	315	525	0.60	65.3
LD3	220	426	0.52	62.2
LO1	185	426	0.43	80.1
LO2	155	588	0.26	89.6
LO3	85	683	0.12	80.7
LW2	76	525	0.14	92.5
LW3	72	657	0.11	88.4
SD4	505	788	0.64	66.4
SD8	470	788	0.60	61.8
SD9	490	788	0.62	66.6
SD10	500	788	0.63	71.9
SO3	410	657	0.62	80.6
SO8	340	657	0.52	82.0
SO9	235	657	0.36	82.7
SO11	105	814	0.13	81.1
SO12	95	788	0.12	89.2
SO13	105	762	0.14	92.9
SO16	125	762	0.16	88.2
SW2	95	722	0.13	88.7
SW3	135	722	0.19	88.3
SW4	80	722	0.11	89.8
SW6	160	722	0.22	91.5
SW7	90	722	0.12	88.7
SW8	55	722	0.08	92.1
MD1	830	3191	0.26	82.1
MD2	1120	3071	0.36	70.2
MO1	1030	2905	0.35	85.9
MO2	1100	2753	0.40	85.1
MW1	85	2466	0.03	87.9
MW3	86	2439	0.04	88.1
MW5	150	2466	0.01	87.2

* The degrees of saturation were rounded to the nearest tenth; these values were plotted in Figure 25.

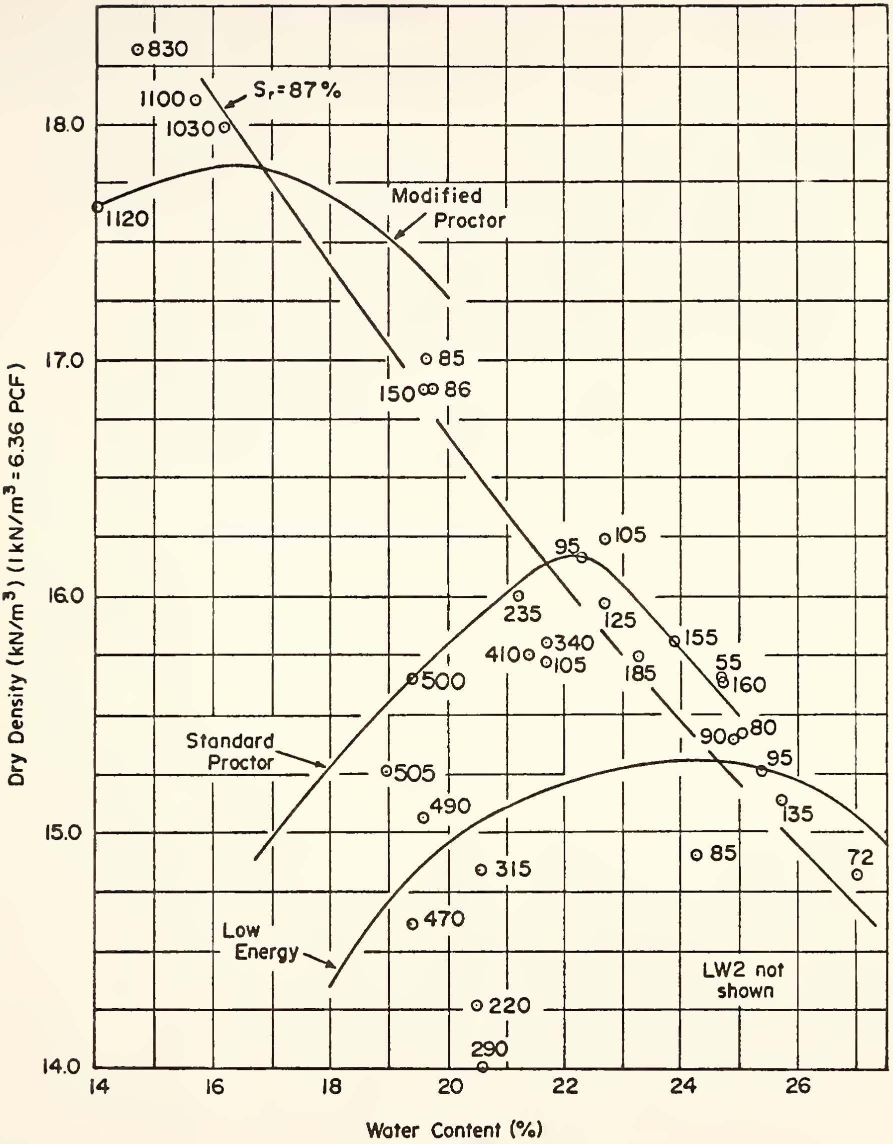

FIGURE 25 PRESTRESS VALUES (kN/m²) FOR AS-COMPACTED COMPRESSIBILITY TESTS

(2) As the equivalent impact effort increases, the value of compactive prestress also increases.

(b) For wet of optimum conditions, $S_r > 87\%$:

(1) At a given equivalent impact effort level, the capacity for prestressing is small and remains virtually unchanged with increasing water content.

(2) As the equivalent impact effort level increases, the capacity for prestressing is virtually unchanged.

(These general conclusions are based on the assumption that the method for determining compactive prestress was suitably accurate. It should be noted that difficulties existed with using the Casagrande procedure for wet-side samples due the remolded-like characteristics of the e-log p curves).

The above suggests that at dry-side water contents, the capacity for prestressing is largely affected by compaction water content and compaction pressure. According to Lambe (1961) however, an increase in compaction pressure causes an increase in pore water pressure; consequently, the compacted clay structure is more dispersed, and the result is a lower value of compactive prestress. The general conclusions stated herein indicate otherwise. That is, the compactive prestress values for dry-side samples increase with increasing compaction pressure. This observation will be dis-

cussed in a later section dealing with the compactive prestress prediction model.

Additionally, it was observed in Figure 25 that compactive prestress is little affected by water content and compaction pressure for initially wet samples. This is largely due the small differences in pore water pressure that result from a change in these variables.

Figure 3 showed the relationship between prestress ratio and degree of saturation for a compacted shale; Figure 26 shows a similar plot for compacted St. Croix clay. Although the functional relationship is not accurately defined, it does suggest that the prestress ratio decreases with increasing saturation, as was the case in Figure 3. Additionally, for the partial range of saturation considered in this study, Figure 26 shows that the prestress ratio is always less than one, which may indicate that not all of the energy delivered is achieving densification.

In this connection, it is important to realize that the compaction pressures reported herein are only nominal pressures; that is, they are the pressures expended by the kneading compactor during the compaction process. Therefore, the actual prestress ratios, i.e., compactive prestress/effective compaction pressure, are more than likely greater than the values presented here.

It is realized that no one single compaction variable can explain the effects of compaction on compactive prestress. Its value is governed by a complexity of factors, some of

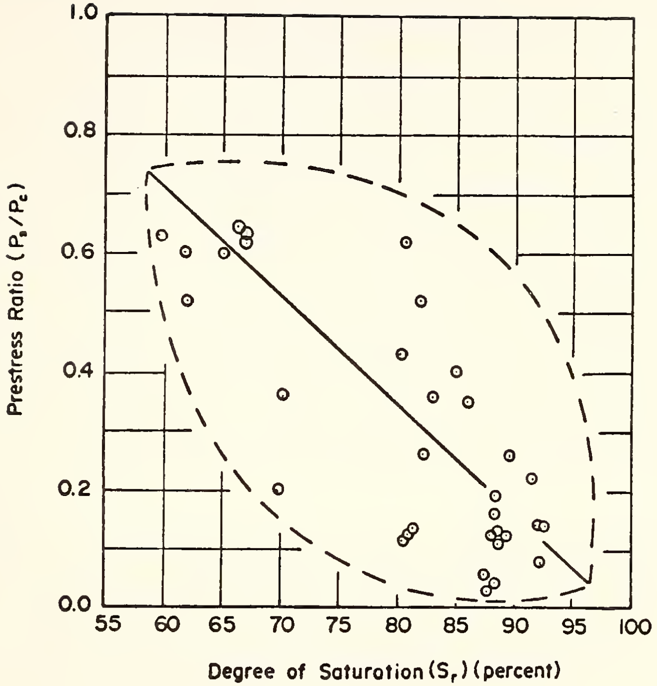

FIGURE 26 PRESTRESS RATIO VS. DEGREE OF SATURATION

which may be difficult to quantify. In the last part of this chapter, statistical methods will be used to better examine the relationship between the initial compaction variables and compactive prestress for compacted St. Croix clay.

Soaked Compressibility

Compaction

The compaction data for the 17 soaked compressibility samples are listed in Table 8. Each variable, e.g., water content, dry density, compaction pressure, initial degree of saturation, and initial void ratio are as previously defined for the as-compacted compressibility samples. Additionally, the occurrences associated with compacting, sampling, and trimming were common to those previously reported.

Figure 27 shows the location of each sample with respect to its initial water content, dry density, and equivalent impact energy level. This Figure may be useful as a quick reference for subsequent discussions.

Each soaked compressibility sample is designated by three letters: the first two characterize the equivalent desired impact level and the desired end-result compaction condition, respectively; the last letter—A, B, or C—characterizes the sustained load during saturation for equivalent embankment heights of A = 7.8 m (25 ft), B = 15.6 m (50 ft), C = 23.5 m (75 ft). For example, a soaked sample designated by the characters—SDA—indicates that the

TABLE 8 INITIAL COMPACTION VARIABLES FOR SOAKED COMPRESSIBILITY SAMPLES

Sample No.	Water Content (%)	Dry Density γ_d (kN/m^3)	Compaction Pressure P_c (kN/m^2)	Degree of Saturation S_r (%)	Initial Void Ratio e_o
SDA	18.56	14.66	788	59.46	0.8738
SDB	18.66	15.14	788	64.16	0.8143
SDC	19.00	15.22	788	66.15	0.8042
SOA	22.40	16.01	788	87.63	0.7157
SOB	22.50	16.05	788	88.60	0.7111
SOC	23.32	15.76	788	87.90	0.7427
SWA	24.50	15.67	657	91.08	0.7532
SWB	24.58	15.75	657	92.56	0.7435
LDB	21.22	12.93	361	52.86	1.1240
LDC	20.51	14.27	427	62.15	0.9240
LOA	25.68	15.09	394	87.62	0.8206
LOC	24.20	14.72	394	78.29	0.8654
LWC	24.27	14.91	683	80.68	0.8423
MDB	14.39	17.64	3161	72.36	0.5568
MOA	15.66	18.08	2905	84.52	0.5188
MOB	13.53	17.57	3161	67.24	0.5633
MWA	18.86	17.40	2466	91.33	0.5782

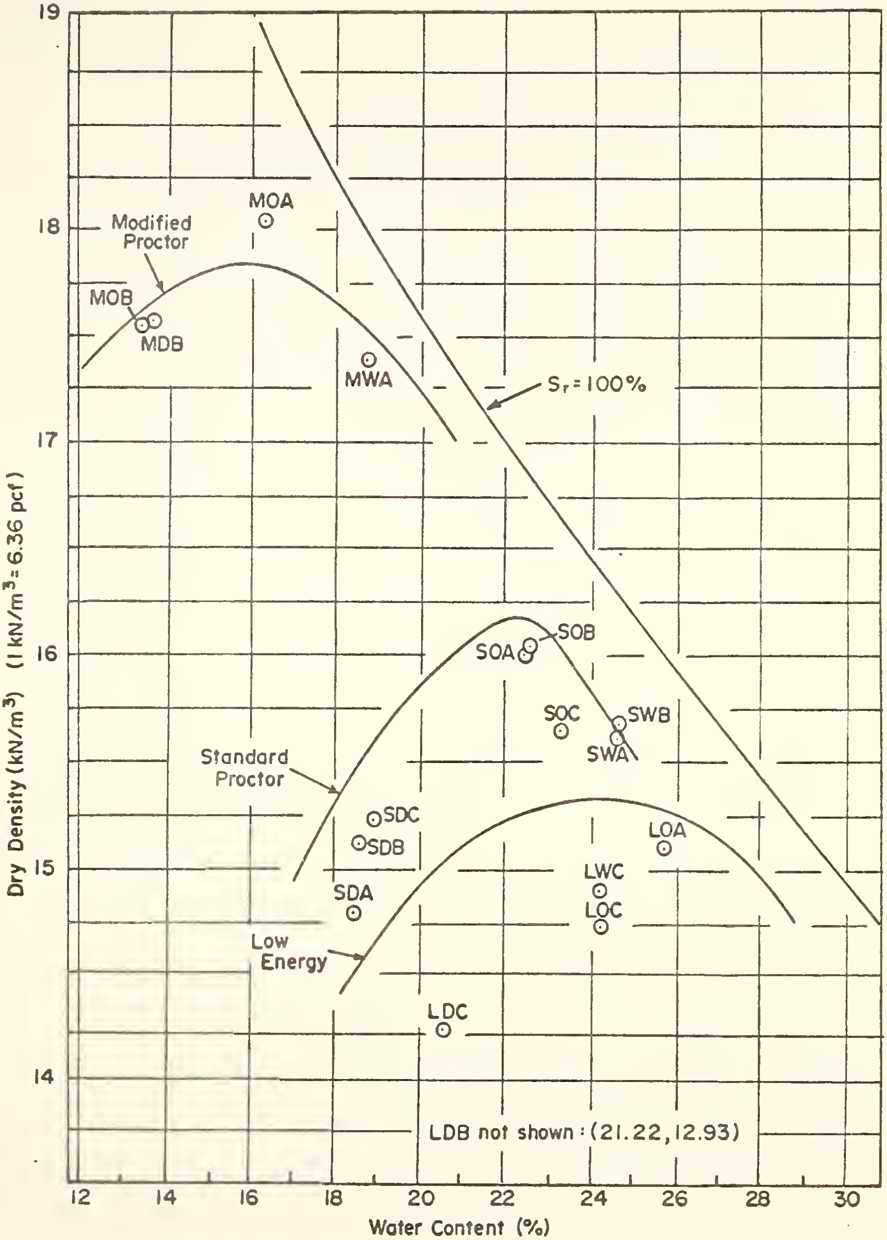

FIGURE 27 INITIAL MOISTURE-DENSITY CONDITION FOR SOAKED COMPRESSIBILITY TESTS

sample was initially compacted at an equivalent Standard (S) Proctor impact level, to an initially dry (D) of optimum condition, and incrementally loaded and soaked at an applied pressure corresponding to an embankment height of 7.8 m (A).

Compression and Pore Pressure Measurements

In order for the fully saturated compressibility characteristics of compacted St. Croix clay to be examined, it was necessary to: (1) saturate each oedometer specimen with back pressure, and (2) maintain this pressure in the pore fluid throughout the soaked test. Other procedures, i.e., flooding and percolation, have been used for similar purposes in other investigations, however, the complete removal or solutioning of entrapped air by such methods is unlikely. This discussion focuses on the success of using back pressure to achieve full saturation, as well as the relations, and implications thereof, obtained during incremental loading.

Table 9 lists typical ratios of maximum excess pore water pressure to the load increment applied or removed; this ratio is expressed as $\Delta u_{max}/\Delta\sigma$. By strict definition, it is different from the B-parameter proposed by Skempton (1954) in that Δu was measured under drained conditions. It is useful however, as a method for verifying full saturation, as is shown below.

For the representative samples of Table 9, the value of $\Delta u_{max}/\Delta\sigma$ was typically less than unity within the unloading

TABLE 9 RATIOS OF MAXIMUM EXCESS PORE WATER PRESSURE TO PRESSURE INCREMENT

Applied Load	$\Delta u_{max}/\Delta\sigma$		Applied Load	$\Delta u_{max}/\Delta\sigma$		Applied Load	$\Delta u_{max}/\Delta\sigma$	
(kN/m^2)	MOA	MWA	(kN/m^2)	SDB	SWB	(kN/m^2)	LDC	LWC
160.0	----	----	320.0	----	----	480.0	----	----
114.5	0.70	0.84	171.5	0.91	0.80	386.1	0.74	0.71
76.5	----	1.00	76.5	1.00	0.96	171.5	0.87	0.90
114.5	0.54	0.72	114.5	0.60	0.64	76.5	1.97	0.64
171.5	0.55	0.76	171.5	0.93	1.00	114.5	0.72	1.00
257.4	0.63	0.84	257.4	1.04	1.08	171.5	1.00	1.00
386.1	0.75	1.00	386.1	1.00	1.00	257.3	1.00	1.00
579.2	0.83	0.97	579.2	0.98	0.98	386.1	1.00	1.00
868.7	0.84	0.97	868.7	1.03	1.01	579.2	1.00	1.00
1303.1	0.84	0.97	1303.1	1.02	1.03	868.7	1.02	1.00
1954.6	0.77	----	1954.6	0.80	----	1303.1	1.00	----

and recompression range. (The first applied load value—160, 320, or 480 kN/m^2—is the sustained embankment load during saturation; all other values refer to the loads incremented to or decremented to during the soaked test). According to Girault (1960) and Crawford (1964), this can be attributed to air coming out of solution upon load removal and/or the inaccuracies of the pore pressure measuring device.

Also listed in Table 9 are values greater than unity. Girault (1960) obtained values as high as 1.10 for the same loading frame apparatus (Figure 14) and attributed it to a slight dynamic effect on load application. However, except for sample MOA, which will be discussed subsequently, the ratios obtained for increments exceeding the previously sustained embankment load are typically one; that is, the pore pressure responded equally to the applied loading increment.

Ratios obtained for samples compacted to initially dry and optimum Modified conditions are represented by sample MOA in Table 9. All of the values listed are significantly less than one, and when compared to the values previously discussed may suggest incomplete saturation. Wissa (1969) found however, that the skeleton compressibility of highly overconsolidated saturated soils approaches that of water; consequently, the maximum theoretical value of $\Delta u/\Delta\sigma$ can be considerably less than one, i.e., as low as 0.65 for very stiff saturated soils. Assuming complete saturation, these data may then suggest that the Modified soil skeleton, for initially dry and optimum samples, is less compressible than

that of Low Energy, Standard Proctor, and wet Modified samples. In view of the higher compaction pressures required to obtain these conditions (See Figure 17), Wissa's findings seem applicable.

The relations shown in Figure 28 are typical soaked compression versus log time curves. Each curve has a characteristic Type I shape, as proposed by Leonards and Girault (1961). The division of consolidation into primary and secondary components is illustrated by two techniques—the usual Casagrande approximation and pore water pressure measurements. As shown, the amount of compression at the end of primary consolidation (R_{100}), as determined by both methods is nearly identical. Additionally, the time for full dissipation of pore pressure to occur (t_{100} value at $\Delta u = 0$) corresponds well with the Casagrande t_{100} value; however, typically the former time was 15 percent less.

Figure 29 illustrates typical pore pressure build-up and dissipation curves for three samples initially compacted at different initial conditions, for the load increment shown. In all cases, the maximum value of $\Delta u/\Delta\sigma$ was not reached until some time after load application. Accordingly, this may be due to the following: (1) low soil permeability, (2) the compressibility of the soil skeleton, (3) the influence of side friction, or (4) the flexibility of the pore pressure measuring system—either singly or in combination.

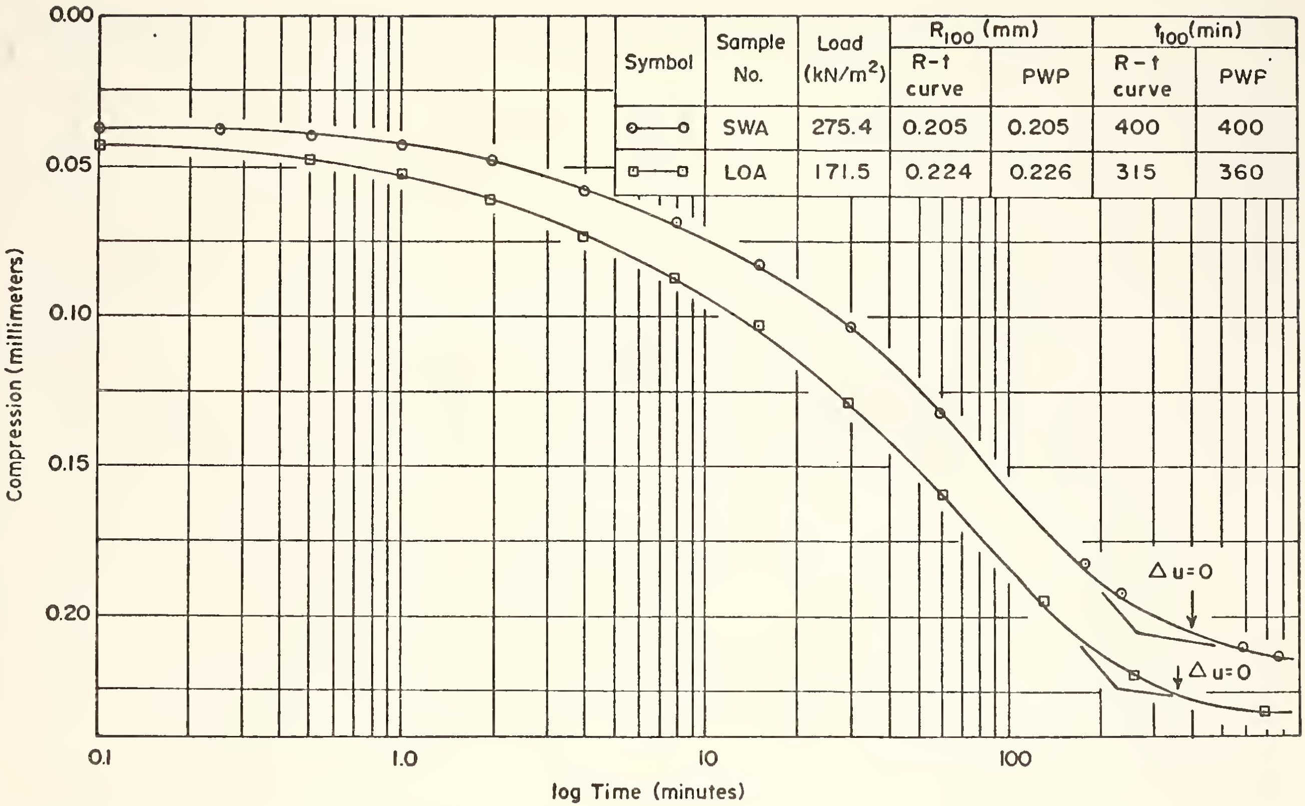

Symbol	Sample No.	Load (kN/m^2)	R_{100} (mm)		t_{100}(min)	
			R–t curve	PWP	R–t curve	PWF
○—○	SWA	275.4	0.205	0.205	400	400
□—□	LOA	171.5	0.224	0.226	315	360

FIGURE 28 COMPARISON OF METHODS FOR OBTAINING R_{100} AND T_{100}

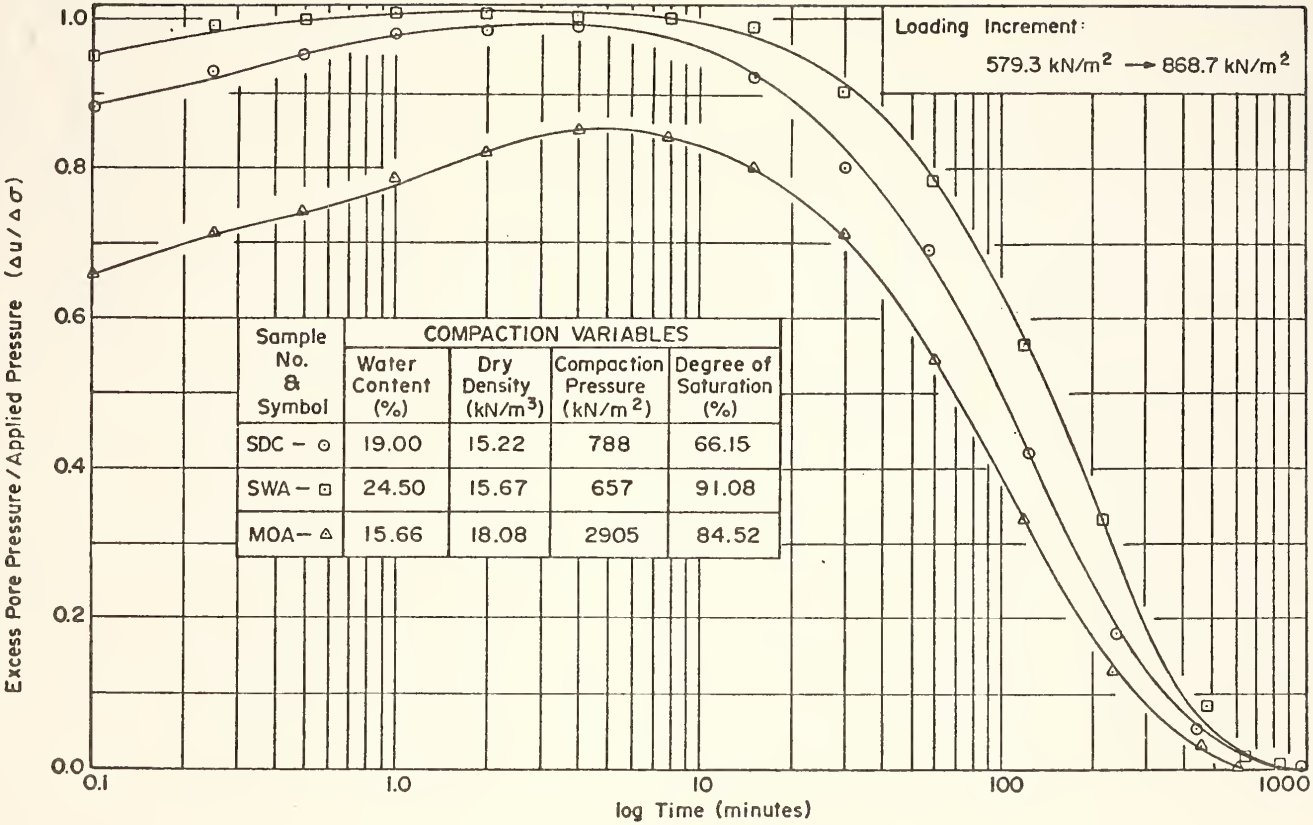

Sample No. & Symbol	COMPACTION VARIABLES			
	Water Content (%)	Dry Density (kN/m³)	Compaction Pressure (kN/m²)	Degree of Saturation (%)
SDC – ⊙	19.00	15.22	788	66.15
SWA – ⊡	24.50	15.67	657	91.08
MOA – ◬	15.66	18.08	2905	84.52

FIGURE 29 TYPICAL PORE PRESSURE BUILD-UP AND DISSIPATION CURVES

As can be seen from this Figure, the time for the Modified sample (lower curve) to reach its maximum value is greater than that for the two Standard samples (top curves), and in connection with Wissa's (1969) findings, may suggest that skeleton compressibility is at least one major factor contributing to the delayed build up effect.

Based on the foregoing, it is suggested that future soaked compressibility studies on St. Croix clay incorporate a saturation procedure similar to the one reported herein. Additionally, because the Casagrande construction provides a very good approximation for the end of primary consolidation (for the load increment ratio used), doubly-drained oedometer tests may be warranted. Such a procedure will considerably reduce the duration of each test, which in this study, was typically 1-1/2 to 2 weeks.

Volume Change on Saturation

During the service life of an earthen embankment, environmental changes may effect an increase or decrease in the volume of the mass. As a result, the compacted material will undergo changes in void ratio and saturation which may be undesirable in the given application. The one-dimensional percent volume changes ($\Delta V/V_o$) which occurred on incremental loading and wetting will be examined hereafter. ($\Delta V/V_o$ = $\Delta e/1+e_o$, where Δe = change in void ratio on saturation, and e_o = initial void ratio).

Figure 30(a) shows the relationship between percent volume change on wetting ($\Delta V/V_o$), initial void ratio (e_o), and the sustained load on saturation (P_o). In general, for a given sustained load, the percent increase in volume increases with decreasing initial void ratio, and the percent decrease in volume increases with increasing initial void ratio. Abeyesekera (1978) obtained similar results for an isotropically-consolidated compacted shale. (Figure C3(b) shows similar trends for $\Delta V/V_o$ values based on the void ratio before soaking (e_1), i.e., $\Delta V/V_o = \Delta e/1+e_1$).

To facilitate a more instructive comparison among these variables, Figure 30(b) shows the same data plotted in a different manner. Observe for a P_o equal to 320 kN/m^2, as the void ratio increases, there is less tendency toward volume increase, and once the critical void ratio is reached (value of e_o at $\Delta V/V_o = 0$), there is an increasing tendency toward volume decrease. This is similar to the trends stated above. However, note for the two other P_o values, i.e., 160 kN/m^2 and 480 kN/m^2, this is not the case. That is, the percent increase and decrease in volume does not occur with decreasing and increasing void ratio, respectively. (Note that an increase in volume is indicated by a negative sign; a decrease, by a positive sign. This convention was used throughout due the limited number of swell data).

Mishu (1963) determined the percent volume change on wetting for a residual clay using a similar procedure to the one reported herein, however, no back pressure was employed.

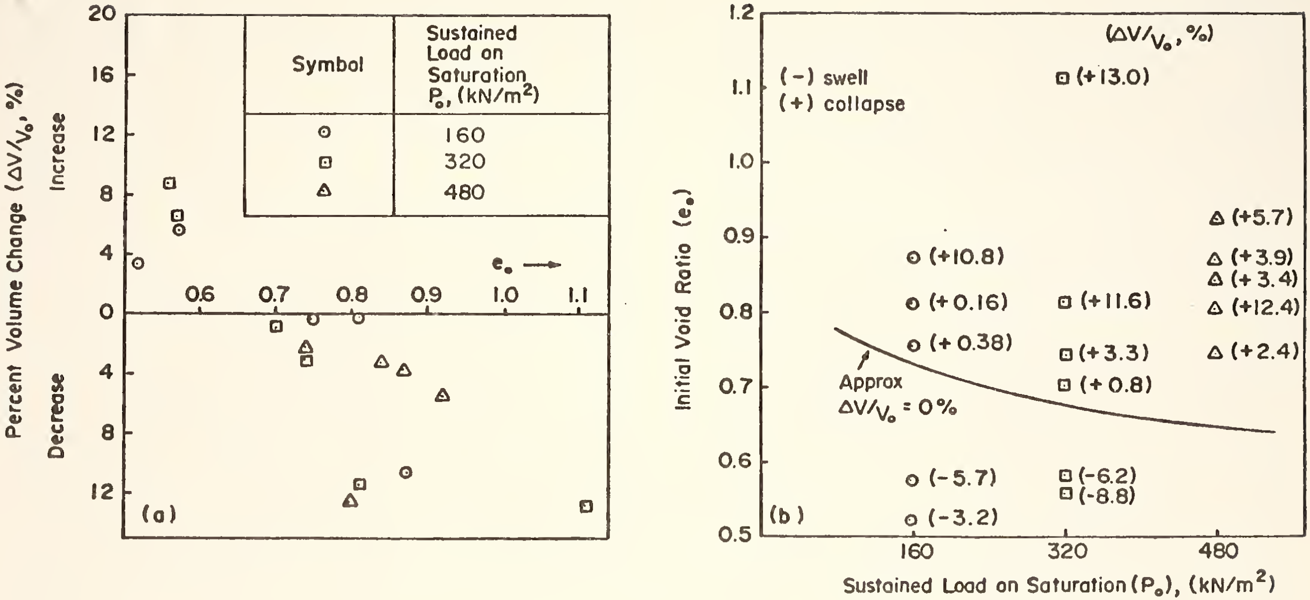

FIGURE 30 VOLUME CHANGE UNDER LOAD ON SATURATION

Some of his results for a given kneading compaction gage pressure (7 psi) are shown in Table 10.

In this Table, observe that for each degree of saturation listed, a maximum collapse value is obtained at some intermediate load rather than at the maximum load, as designated by each asterisk. Additionally observe that as the saturation increases, the value of the intermediate load causing maximum collapse decreases.

In connection with the compactive prestress discussion, it was also found that compactive prestress decreased with increasing water content or saturation. Therefore, if both observations are combined, it may be hypothesized that the volume change on wetting is clearly a function of whether loading and saturation occur at a value above or below some critical value, which may be the compactive prestress. It is therefore uncertain as to the usefulness of such graphs as Figure 30(b) without due consideration of the compactive prestress value.

In all the cases reported herein, the change in volume occurred during the initial wetting period, with little to no change occurring during the incrementing of back pressure. Additionally, depending on the initial compaction condition, the volume change was either sudden or time dependent. That is, samples compacted to equivalent Low Energy and Standard Proctor dry conditions, collapsed instantly on wetting; those compacted to equivalent Modified dry conditions, swelled

TABLE 10 MISHU'S (1963) RESULTS FOR ONE-DIMENSIONAL VOLUME CHANGE ON WETTING

Pressure On Sample (tsf)	$\Delta V/V_o$ in percent S_r = 43%	 S_r = 64%	 S_r = 89%
0.1	+ 2.0	+ 1.2	+ 0.5
1.0	- 4.0	0.0	- 0.4*
2.0	-11.0	- 1.0*	- 0.3
3.0	-13.5*	- 0.9	0.0
4.0	-12.5	---	---
5.0	-11.5	---	---

(+) indicates volume increase; (-) indicates volume decrease.

* indicates maximum collapse value for the given S_r value.

suddenly on wetting; whereas those compacted to all other conditions, increased or decreased in volume within 1 to 4 hours after wetting.

The collapse phenomenon was first recognized by Jennings and Burland (1962) and indicated an apparent contradiction to the effective stress law as stated by Equation 5. Interestingly, under a constant total stress, an increase in pore pressure reduces the effective stress, and an increase in volume should result rather than a decrease in volume. Matyas et al. (1968) contend that this contradictory behavior is the result of decreasing matrix suction ($u_a - u_w$) on wetting, which, in turn, has a two-fold effect on structure—a reduction in intergranular stress (volume decrease) and a reduction in soil stiffness (volume increase). The net effect is a volume decrease.

If their explanation is combined with the more recent evidence pertaining to compacted clay macrostructure (Hodek and Lovell, 1978b and Barden and Sides, 1970), then the observed collapse phenomenon may be stated as in the following paragraph.

The dry compacted soil has numerous large inter-aggregate pores. On wetting, the surface tension meniscii and flocculated clay buttresses between aggregates are destroyed and become more dispersed, respectively. Consequently, the aggregates will fuse and displace into the available pore spaces. The soil structure resulting from loading,

wetting, and subsequent collapse will resemble that of a wet compacted sample, i.e., with fewer number of inter-aggregate pores and a more dispersed macrostructure.

Similarly, the volume change behavior of samples compacted to other initial conditions may be explained in terms of compacted clay structure. Equivalent Low Energy and Standard Proctor wet-side and at-optimum samples exhibited little volume change on wetting due the initially more dispersed structure, the smaller number of large pores, and the few developed meniscii. On the other hand, all Modified samples swelled on wetting, and according to Hodek (1972), this is the result of: (1) local softening at aggregate contacts (volume decrease), (2) expansion of the double layer (volume increase), and (3) rearrangement of the soil skeleton (volume decrease), with the effect of (2) outweighing the sum total of (1) and (3).

Compressibility Characteristics

Typical results of the soaked compressibility tests are illustrated by the e-log p curves of Figures 31 to 34. (A complete listing of the data can be found in Table B2 of Appendix B). For each curve, the stress-deformation behavior is outlined as follows: a dashed curve—the as-compacted loading; a solid vertical line—volume change on wetting; a solid curve—soaked unloading and reloading. From these curves, inferences can be made in connection with soaked compressibility characteristics, as-compacted compressibility

characteristics, and volume change on wetting characteristics. These will be discussed in the following.

Figure 31 makes the comparison of samples compressed from very similar initial dry-side conditions, but incrementally loaded and saturated at different vertical confining pressures. For the three samples shown, the amount of volume change on wetting ranges between 11 and 12 percent (based on initial void ratio). A first observation would conclude that the percent change in volume is independent of confinement. However, as indicated by each of the dashed as-compacted curves, none of the samples were loaded past their respective prestress values. In connection with a previous discussion, one may expect less percent change in volume with increased confinement.

To facilitate a direct comparison between as-compacted and soaked compressibility behavior, values of secant moduli were computed within specific pressure ranges. Additionally, within the soaked virgin compression regions, i.e., approximate straight line portions, the values of compression index (C_c) were determined. Comparisons of compressibility behavior based on these values are shown below. (All of the values presented herein are reported as their absolute values).

For the as-compacted curve of sample SDC in Figure 31, the secant modulus is approximately 0.05 within the 75 kN/m^2 to 480 kN/m^2 pressure range. Similarly, for the soaked curve, it is 0.10. Clearly, this indicates that in this

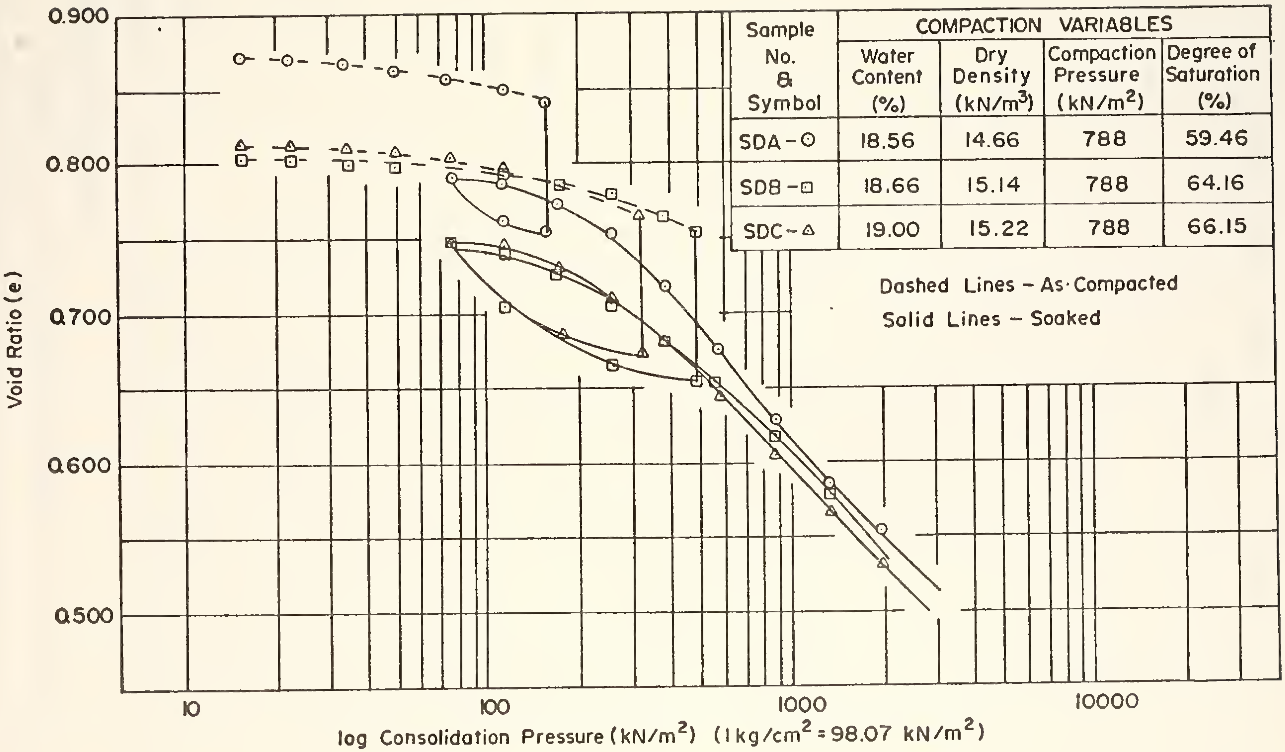

Sample No. & Symbol	COMPACTION VARIABLES			
	Water Content (%)	Dry Density (kN/m³)	Compaction Pressure (kN/m²)	Degree of Saturation (%)
SDA – ⊙	18.56	14.66	788	59.46
SDB – ⊡	18.66	15.14	788	64.16
SDC – △	19.00	15.22	788	66.15

FIGURE 31 EFFECT OF CONFINEMENT ON SOAKED COMPRESSIBILITY BEHAVIOR (DRY OF OPTIMUM)

pressure region, the soaked soil is more compressible than the as-compacted soil, and may be attributed to the greater as-compacted resistance to deformation due the negative values of pore water pressure.

Figure 32 makes the comparison between samples compacted to different initial conditions, but loaded and saturated at similar confining pressures. The values of C_c (320 to 1300 kN/m^2 pressure range) for samples LDB and SWB are 0.19 and 0.16, respectively. This indicates that in the virgin compression range, the dry-side sample (LDB) is more compressible than the wet-side sample (SWB). However, these values are not very different, and may indicate similar macrostructures due loading, wetting, and subsequent collapse.

Figure 33 shows the effects of increasing confinement (on soaking) on compressibility for initially wet-side Standard Proctor samples. Of interest is that the values of C_c range between 0.195 and 0.202, and may indicate, for these conditions, the independence of soaked virgin compressibility on confinement. Similarly, for the dry-side samples of Figure 31, the C_c values range between 0.210 and 0.230. This range is slightly greater than for the wet-side samples. Of additional interest is that the dry-side samples are more compressible in their respective ranges than the wet-side samples. This was also found to be the case for the as-compacted samples.

Figure 34 illustrates the effect of increased compaction pressure on as-compacted and soaked compressibility behavior

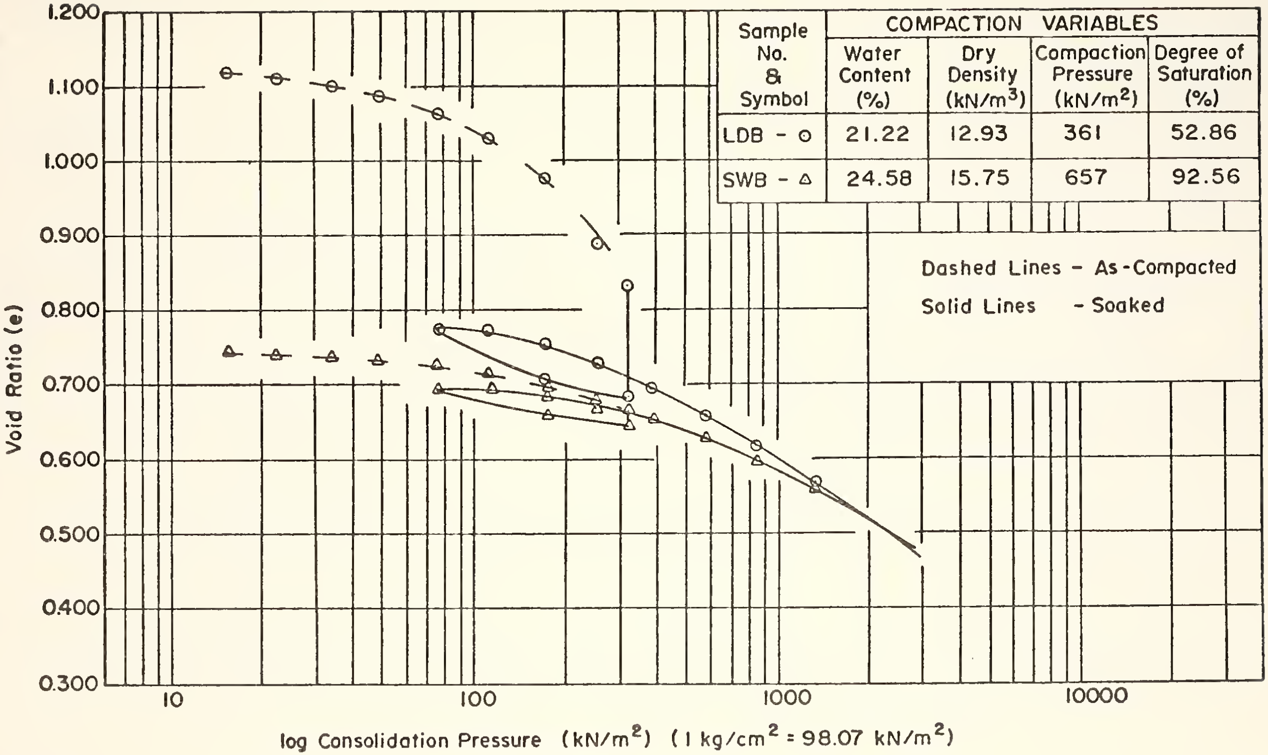

FIGURE 32 COMPARISON OF SOAKED COMPRESSIBILITY BEHAVIOR FOR LOW ENERGY AND STANDARD PROCTOR SAMPLES

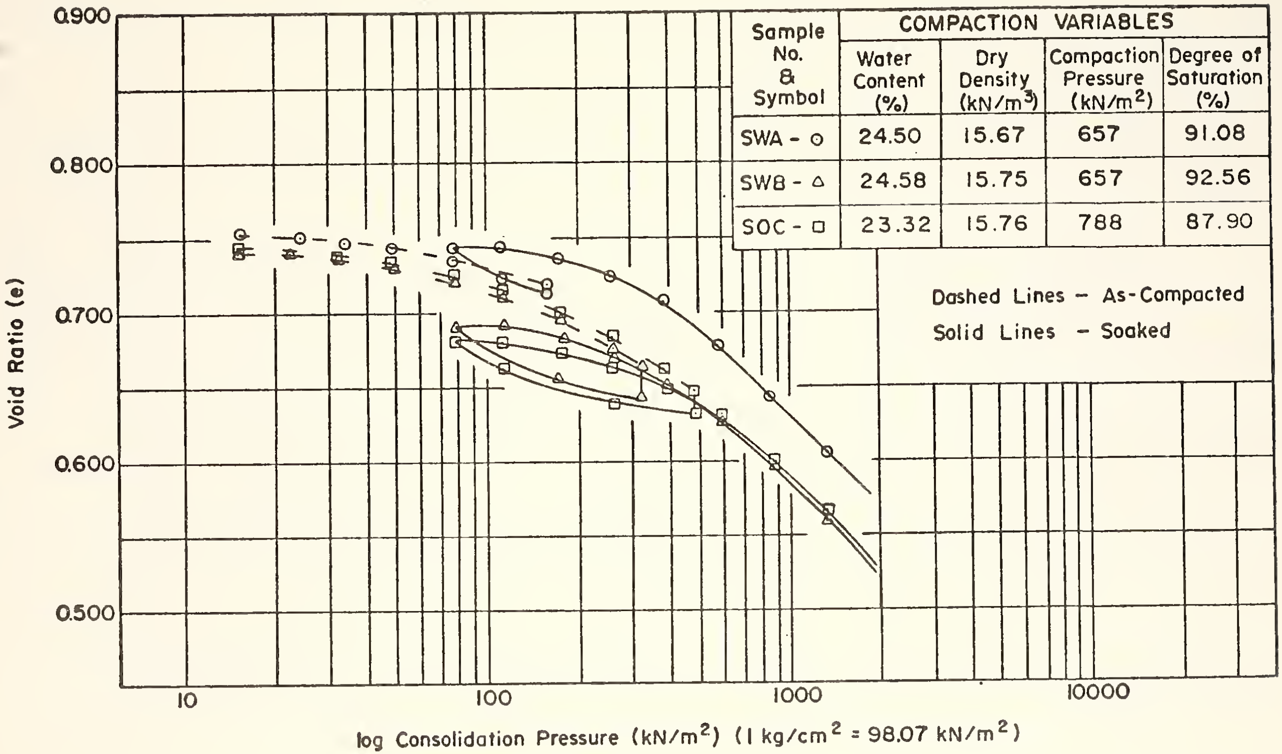

Sample No. & Symbol	COMPACTION VARIABLES			
	Water Content (%)	Dry Density (kN/m³)	Compaction Pressure (kN/m²)	Degree of Saturation (%)
SWA - ⊙	24.50	15.67	657	91.08
SWB - △	24.58	15.75	657	92.56
SOC - □	23.32	15.76	788	87.90

FIGURE 33 EFFECT OF CONFINEMENT ON SOAKED COMPRESSIBILITY BEHAVIOR (WET OF OPTIMUM)

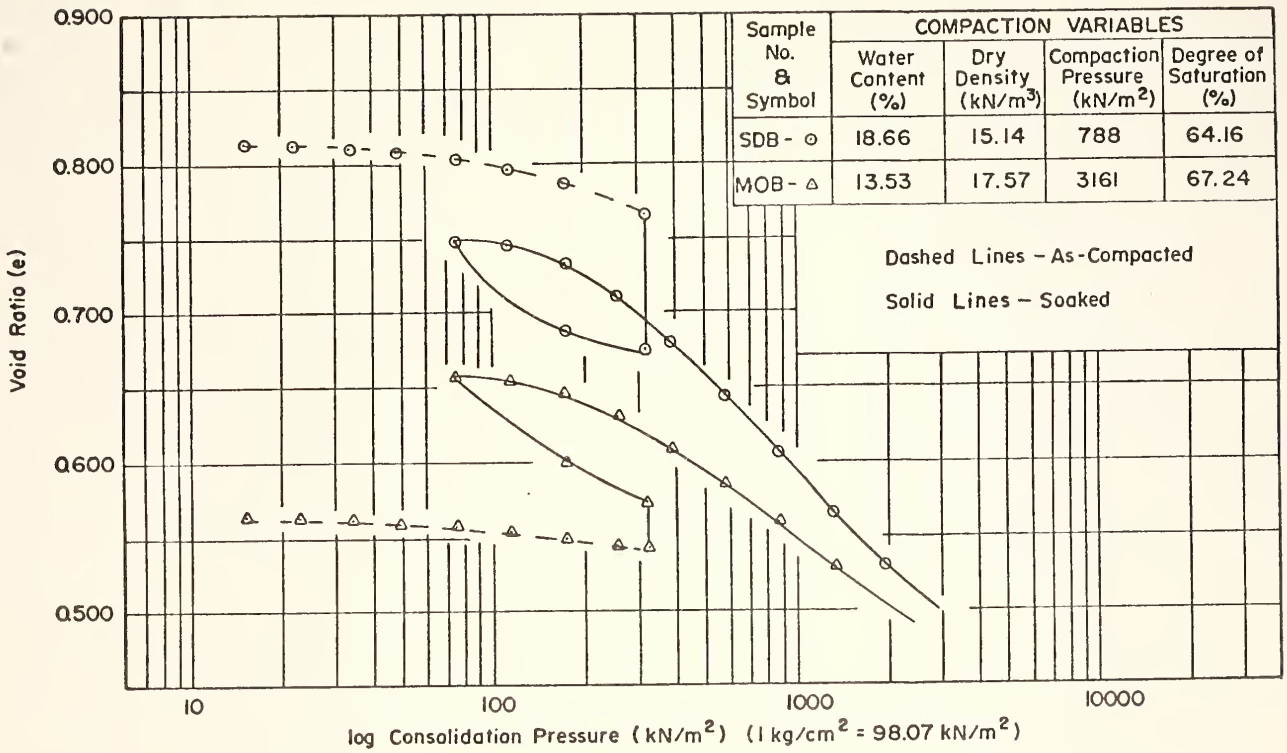

Sample No. & Symbol	COMPACTION VARIABLES			
	Water Content (%)	Dry Density (kN/m³)	Compaction Pressure (kN/m²)	Degree of Saturation (%)
SDB - ⊙	18.66	15.14	788	64.16
MOB - △	13.53	17.57	3161	67.24

FIGURE 34 EFFECT OF COMPACTION PRESSURE ON SOAKED COMPRESSIBILITY BEHAVIOR (DRY OF OPTIMUM)

for initially dry of optimum samples. Within the 75 kN/m^2 to 320 kN/m^2 pressure range, the secant moduli for the as-compacted and soaked curves are 0.60 and 0.90 for sample SDB and 0.25 and 0.62 for sample (MOB), respectively. In both cases, the soaked soil is more compressible than the as-compacted soil. Additionally, within the virgin compression region, the values of C_c are 0.21 (SDB) and 0.15 (MDB). Clearly, the Modified sample is less compressible in this range, which may be due the higher rigidity of the initial soil structure.

For initially wet of optimum samples, the effect of increasing compaction pressure is illustrated in Figure C4. For the Standard Proctor equivalent condition (sample SWA), the value of C_c is approximately 0.20, as was reported in the discussion of Figure 33. For the Modified sample, the value is approximately 0.13. As was the case for the dry-side comparison of Figure 34, the equivalent Modified specimen is less compressible in its corresponding virgin range than the Standard Proctor specimen. Moreover, these data suggest that the initially wet-side samples remain less compressible in the high (or virgin) range than the initially dry-side samples even after loading, wetting, and subsequent volume change.

(Table 11 presents a summary of the soaked compressibility characteristics just discussed, as well as the as-compacted compressibility characteristics discussed earlier).

TABLE 11 SUMMARY TABLE OF AS-COMPACTED AND SOAKED COMPRESSIBILITY BEHAVIOR

Condition	Compressibility Behavior
As-Compacted	
Water Content	Wet-side more compressible in low pressure range, dry-side in the high pressure range.
Compaction Pressure	For dry-side condition, an increase in compaction pressure, decreases high pressure range compressibility. For wet-side conditions, similar trends exist, but to a lesser degree.
Soaked*	
Vs. As-Compacted	In the low pressure range, as-compacted less compressible than soaked.
Water Content	Dry-side more compressible than wet-side in their respective virgin compression pressure ranges.
Confinement	Virgin compressibility decreases with increasing confinement on saturation for dry-side conditions. For wet-side conditions, there is little change in virgin compressibility behavior with increased confinement.
Compaction Pressure	For dry and wet-side conditions, an increase in compaction pressure reduces virgin compressibility.

* Dry and wet refer to the initial compaction condition.

One characteristic of soaked compressibility behavior is illustrated by the stress-deformation curve for sample SWA in Figure 33. Observe that the void ratio at the end of saturation is less than the void ratio at the same pressure on reloading. This indicates that a certain degree of swelling has progressed with time. No explanation can be offered as to why this phenomenon occurs, however the fact that each sample was not allowed to swell freely under zero load before reloading may be a contributing factor. That is, due the limitations of the testing apparatus, the samples could not be unloaded beyond the 76 kN/m^2 applied load value.

Statistical Correlations

Multiple regression is a statistical technique used by researchers, scientists, and engineers to study the relationship between a dependent variable and a set of independent variables. Moreover, its basic goal is to establish a linear model of independent variables that can accurately predict, control, or describe a dependent response.

Consider the _general linear regression model_ of the form

$$Y_i = \beta_o + \beta_1 X_{i1} + \beta_2 X_{i2} + \ldots + \beta_{p-1} X_{ip-1} + \varepsilon_i \qquad (13)$$

In this Equation, the β-coefficients represent the partial regression parameters; the X-values, the independent variables; ε_i, the error term; Y_i, the dependent variable. The statistical form of this model is linear with p-1 independent variables and is applicable in cases when more

than one independent variable influence the response value (Y_i). Additionally, it is considered a general regression form, since nonlinear independent variables, such as a polynomial (X^n), a logarithm (logX), or a cross product (X_1X_2), may be transformed accordingly into linear form.

It is impossible to determine the error term (ε_i) in Equation 13, since some of the factors influencing the dependent variable are unknown or incalculable. However, if certain basic assumptions are made with respect to this term, and if the regression coefficients are selected in such a way that the sum of squared residuals ($\Sigma(Y_i - \hat{Y}_i)$) are minimized, the estimated response function for Equation (13) can be written as

$$\hat{Y}_i = b_o + b_1x_1 + b_2x_2 + \ldots + b_{p-1}x_{p-1} \qquad (14)$$

where $\hat{Y}_i$ is the estimated mean response of Y_i, and the b_o, b_1, b_2, ..., b_{p-1} are the estimated partial regression coefficients. It is this model along with its inferences and restrictions that was considered applicable for use in this analysis. Regarding multiple regression, relevant discussions can be found in Neter and Wasserman (1974), Draper and Smith (1966), and Nie, et al. (1975).

The predictive models presented herein were developed using SPSS (Statistical Package for the Social Sciences) procedural programs on Purdue University software. It should be mentioned that any best model identified by these programs is highly dependent on the procedure used, and an

equivalent model may not be established given another set of procedures. Each successive procedure incorporated in this analysis is described in the following.

The first phase of the isolation process involved plotting the independent variables against the dependent variable. (These variables will be discussed later). This was facilitated using the SPSS procedure SCATTERGRAM. If the scatter plots showed a linear relationship, the independent variable was considered highly correlated with the dependent variable. If a linear trend was not found, the independent variable was considered statistically insignificant.

The next step was to isolate a subset of the independent variables considered highly correlated with the dependent variable, so that an optimal expression with as few variables as possible could be established. This was achieved using the automatic SPSS search procedure——STEPWISE. This procedure combines a forward inclusion of independent variables to the model and a backward deletion of independent variables already in the model at each successive step. Additionally, it conducts a statistical test to screen out any independent variable that is too highly correlated with the independent variables already in the model. Other search procedures, such as DRRSQU (a Purdue University all possible regressions program) could have been employed, however, the correlation screening ability, the large number of independent variables that could be examined, the relative low expense——all made the STEPWISE procedure more desirable.

The final step of the isolation process was to obtain the best estimated prediction model from the subset of independent variables isolated by the STEPWISE procedure. This was done using the SPSS procedure REGRESSION (developed by Nie, et al., 1975). Various regression equations were obtained using different combinations. That is, if X_1, X_2, and X_3 were the independent variables isolated by the STEPWISE procedure, then linear regression models were established for the dependent variables in terms of X_1, X_2, X_3, X_1 and X_2, X_1 and X_3, X_2 and X_3, and X_1, X_2, X_3. From these, the procedure for selecting the "best" model was based on the following statistical criteria:

(a) For the overall multiple regression equation:

(1) The coefficient of multiple determination (R^2) is greater than 0.65; that is, at least 65 percent of the variation must be explained by the variables included in the model.

(2) The coefficient of multiple determination (R_a^2) must increase with each additional independent variable entered in the model.

(3) The overall F-test at the $\alpha = 0.05$ significance level must be met. (This tests for multiple linearity of the model).

(b) For the partial regression coefficients:

(1) The F-test for each partial regression coefficient at the $\alpha = 0.05$ significance level

must be met. (This tests whether an independent variable should be dropped from the model).

(2) The coefficients of partial determination ($r_{i\cdot jk}$) are significant.

(3) The 95 percent confidence limit for each b_i is small and does not cross zero. (This restriction is similar to (1)).

(c) For the computed residuals:

(1) The scatter plots of the residuals vs. the independent variables(s) show normal constancy of variance trends.

(2) The residuals are normally distributed random variables; that is, the values of $e_i/\sqrt{MSE}$ (residuals divided by the error root mean square) must range between ± 3.

In the case when all criteria were suitably met by more than one model, the model with the fewest number of variables was selected, provided there was no appreciable difference, i.e., less than 5 percent, in either of the R^2 or R_a^2 values.

Results of Statistical Analysis

The "best" estimated prediction models were isolated in accordance with the procedure and criteria outlined previously. Two dependent variables—compactive prestress (P_s) and one-dimensional percent volume change on saturation ($\Delta V/V_o$)—were regressed in separate analyses. The in-

dependent variables used were the earlier defined compaction variables, i.e., water content, dry density, compaction pressure, initial degree of saturation, initial void ratio, and equivalent embankment pressure on wetting (for $\Delta V/V_o$ only), as well as their squares, square roots, base 10 logarithms, cross products, and combinations thereof. In total, approximately 200 different independent variables were used separately in each analysis. The values of the dependent variable and the linear form of the independent variables used are listed in Tables 12 and 13.

Based on the foregoing, the following prediction models were selected:

(a) For Compactive Prestress, ($\hat{P}_s$):

$$\hat{P}_s = -343.13 - 0.0020w^2 \cdot P_c + 48.91\ P_c^{1/2} \qquad (15)$$

where $\hat{P}_s$ = estimated value of compactive prestress in kN/m^2

$w^2 \cdot P_c$ = interaction term between water content (%) squared and compaction pressure (kN/m^2)

$P_c^{1/2}$ = the square root of compaction pressure $(kN/m^2)^{1/2}$

(b) For 1-D Percent Volume Change on Saturation, ($\Delta \hat{V}/V_o$):

$$\Delta \hat{V}/V_o = 25.47 - 0.872w - 0.0048\ P_c \qquad (16)$$

where $\Delta \hat{V}/V_o$ = estimated value of 1-D percent volume change on wetting (%)

w = water content (%)

TABLE 12 COMPACTION VARIABLES FOR COMPACTIVE PRESTRESS STATISTICAL ANALYSIS

Sample No.	Compactive Prestress P_s (kN/m^2)	Water Content w (%)	Dry Density γ_d (kN/m^3)	Compaction Pressure P_c (kN/m^2)	Degree of Saturation S_r (%)	Initial Void Ratio e_o
LD1	290	20.60	13.97	460	59.77	0.9649
LD2	315	20.60	14.85	525	65.26	0.8838
LD3	220	20.51	14.27	426	62.15	0.9240
LO1	185	23.26	15.74	426	80.14	0.8126
LO2	155	23.85	15.77	558	89.62	0.7451
LO3	85	24.27	14.91	683	80.68	0.8423
LW2	76	27.94	14.88	525	92.47	0.8460
LW3	72	26.98	14.82	657	88.42	0.8544
SD4	505	18.95	15.26	788	66.40	0.7990
SD8	470	19.38	14.62	788	61.82	0.8770
SD9	490	19.59	15.06	788	66.58	0.8238
SD10	500	19.37	15.65	788	71.87	0.7545
SO3	410	21.37	15.76	657	80.61	0.7423
SO8	340	21.71	15.78	657	82.02	0.7411
SO9	235	21.21	15.99	657	82.70	0.7180
SO11	105	21.65	15.72	814	81.12	0.7473
SO12	95	22.32	16.15	788	89.20	0.7066
SO13	105	22.67	16.25	762	92.92	0.6905
SO16	125	22.68	15.97	762	88.18	0.7202
SW2	95	25.38	15.24	722	88.67	0.8014
SW3	135	25.71	15.13	722	88.27	0.8155
SW4	80	25.05	15.42	722	89.80	0.7810
SW6	160	24.72	15.64	722	91.49	0.7565
SW7	90	24.87	15.38	722	88.66	0.7854
SW8	55	24.71	15.68	722	92.08	0.7514
MD1	830	14.67	18.31	3191	82.10	0.5003
MD2	1120	13.96	17.65	3071	70.23	0.5565
MO1	1030	16.20	17.97	2905	85.90	0.5281
MO2	1100	15.71	18.10	2735	85.10	0.5168
MW1	85	19.59	16.99	2466	87.85	0.6243
MW3	86	19.74	16.87	2439	88.05	0.6277
MW5	150	19.57	16.86	2466	87.18	0.6285

TABLE 13 COMPACTION VARIABLES FOR ONE-DIMENSIONAL PERCENT VOLUME CHANGE ON SATURATION STATISTICAL ANALYSIS

Sample No.	Percent Volume Change $\Delta V/V_o$* (%)	Water Content w(%)	Dry Density γ_d(kN/m^3)	Compaction Pressure P_c(kN/m^2)	Degree of Saturation S_r(%)	Initial Void Ratio e_o	Embankment Pressure P_o(kN/m^2)
SDA	5.13	18.56	14.66	788	59.46	0.8738	160
SDB	5.36	18.66	15.14	788	64.16	0.8143	320
SDC	5.62	19.00	15.22	788	66.15	0.8042	480
SOA	----	22.40	16.01	788	87.63	0.7157	160
SOB	----	22.50	16.05	788	88.60	0.7111	320
SOC	1.06	23.32	15.76	788	87.90	0.7427	480
SWA	0.17	24.50	15.67	657	91.08	0.7532	160
SWB	1.45	24.58	15.75	657	92.56	0.7435	320
LDB	8.29	21.22	12.93	361	52.86	1.1240	320
LDC	3.13	20.51	14.27	427	62.15	0.9240	480
LOA	0.74	25.68	15.09	394	87.62	0.8206	160
LOC	1.96	24.20	14.72	394	78.29	0.8654	480
LWC	1.90	24.27	14.91	683	80.68	0.8423	480
MDB	-3.21	14.39	17.64	3161	72.36	0.5568	320
MOA	-1.09	15.66	18.08	2905	84.52	0.5188	160
MOB	-2.28	13.53	17.57	3161	67.24	0.5633	320
MWA	-2.12	18.86	17.40	2466	91.33	0.5782	160

* Values were computed from $\Delta V/V_o = H/H_o = \Delta e/1+e_1$, where Δe = volume change during soaking, e_1 = void ratio before soaking.

P_c = compaction pressure (kN/m^2)

The pertinent statistical data associated with each of these models is presented in Table 14. From the R^2 values listed, it may be inferred that much of the variation is explained by the independent variables included in each of the models; specifically, 88 percent for $\hat{P}_s$ and 86 percent for $\Delta\hat{V}/V_o$. ($100(R^2)$ values of 0 and 100 percent indicate that none and all of the variation is explained by the independent variables in the model, respectively). Additionally, as shown in Table 14, all of the other statistical criteria are suitably met. That is, for each model, the overall and partial F-test values are significant and greater than the decision rule; the partial determination coefficients are significant; the 95 percent confidence limits for each partial regression coefficient are small and do not cross zero.

An inherent assumption in regression analysis is that the error component or residuals are normally distributed random variables with mean zero and constant variance σ^2. For the models expressed as Equations (15) and (16), this assumption is verified in Figures 35 and 36.

Parts (a), (b), and (c) of these Figures show the relationship between the residuals and each of the variables included in the model. None of the relations show a conical, linear, or quadratic trend, which suggest that the constancy of variance criterion is suitably met (Neter and Wasserman, 1974).

TABLE 14 STATISTICAL DATA FOR PREDICTION EQUATIONS

Statistical Criteria	PREDICTION EQUATIONS Compactive Prestress $\hat{P}_s = -343.12-0.0020w^2 \cdot P_c+48.91P_c^{1/2}$	 1-D Volume Change $\Delta\hat{V}/V_o = 25.47-0.872w-0.0048P_c$
Coefficient of Multiple Determination (R^2)	0.88	0.86
Adjusted Coefficient of Multiple Determination (R_a^2)	0.87	0.83
Overall F-Test	103.24	36.23
Partial F-Test		
$w^2 \cdot P_c$	116.14	-----
$P_c^{1/2}$	119.42	-----
	------	29.03
E	------	66.84
Coefficient of Partial Determination*		
$r^2(\hat{P}_s \ w^2P_c \cdot P_c^{1/2})$	0.80	-----
$r^2(\hat{P}_s \ P_c^{1/2} . w^2P_c)$	0.87	-----
$r^2(\Delta\hat{V}/V_o w \cdot P_c)$	------	0.70
$r^2(\Delta\hat{V}/V_o \ P_c \cdot w)$	------	0.81

*$r(Y\Delta \ X_1 \cdot X_2)$ = coefficient of partial determination between Y and X_1 when X_2 is in the model

TABLE 14 (Continued)

Statistical Criteria	PREDICTION EQUATIONS Compactive Prestress $\hat{P}_s = -343.12-0.0020w^2 \cdot P_c+48.91P_c^{1/2}$	 1-D Volume Change $\Delta\hat{V}/V_o = 25.47-0.872w-0.0048P_c$
95% Confidence Limits		
w^2P_c	-.0024,-.0016	-----
$P_c^{1/2}$	41.82, 55.99	-----
Constant ($\hat{P}_s$)	-466.8, -219.4	-----
w	-----	-1.22, -0.520
P_c	-----	-.0061, -.0035
Constant	-----	16.87, 34.06

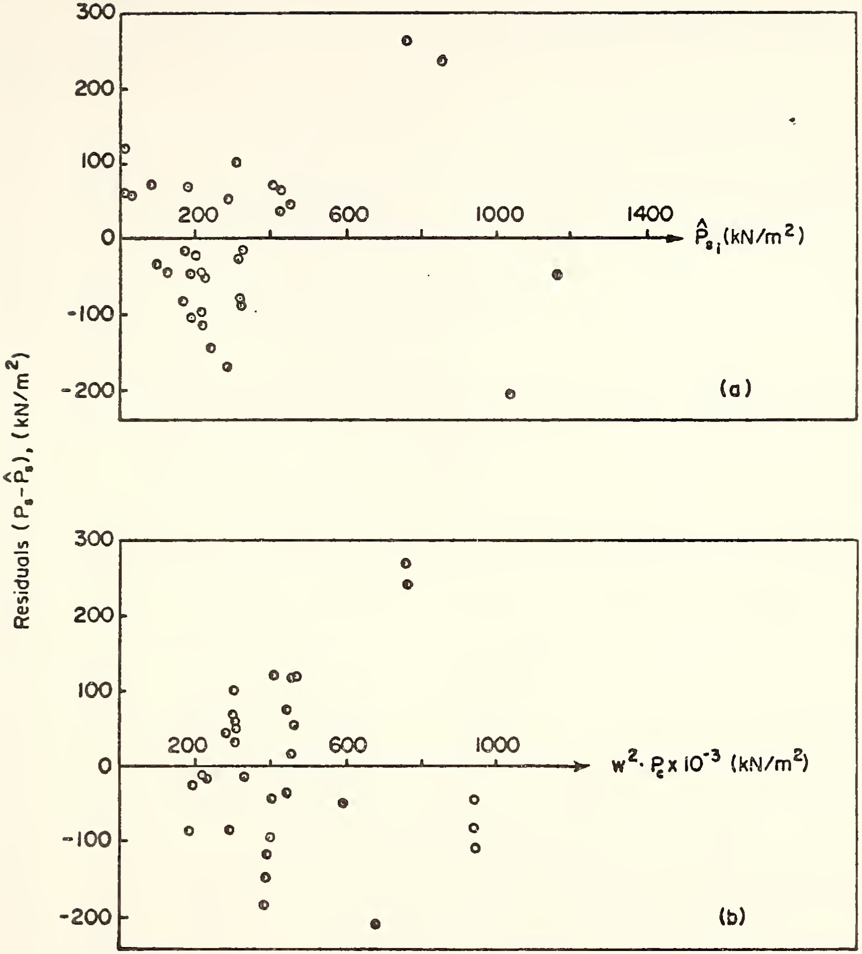

FIGURE 35 RESIDUAL ANALYSIS FOR COMPACTIVE PRESTRESS PREDICTION EQUATION

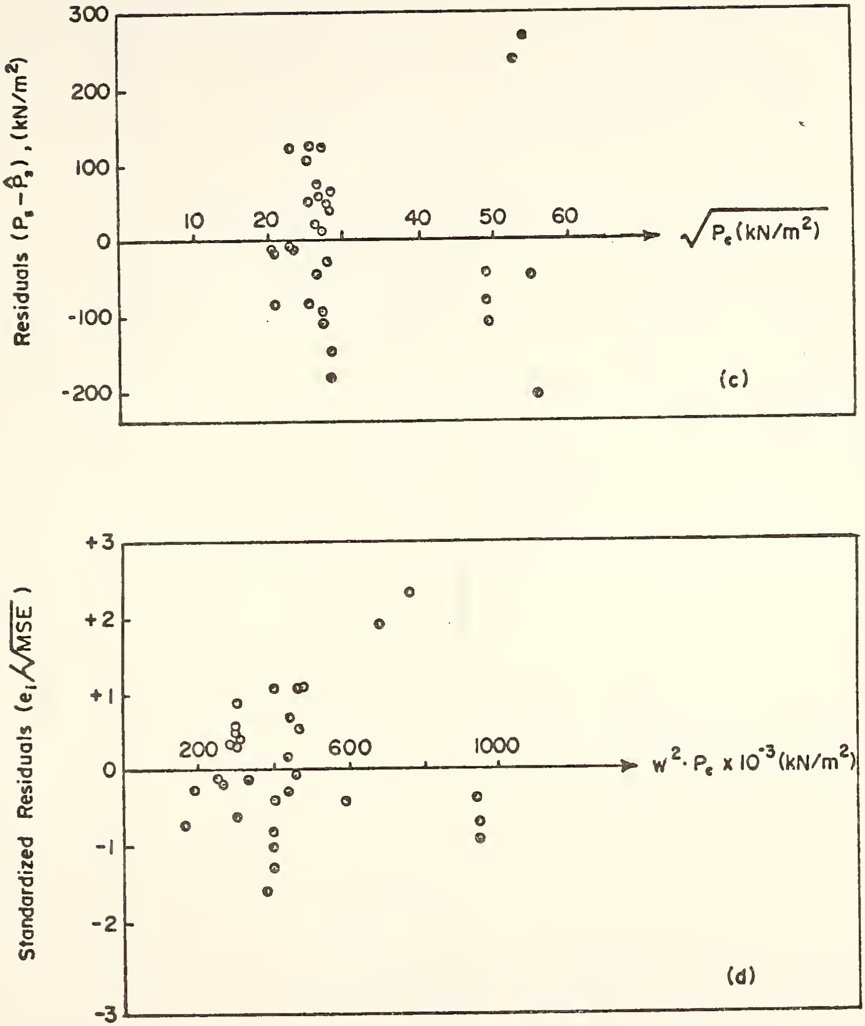

FIGURE 35 CONTINUED

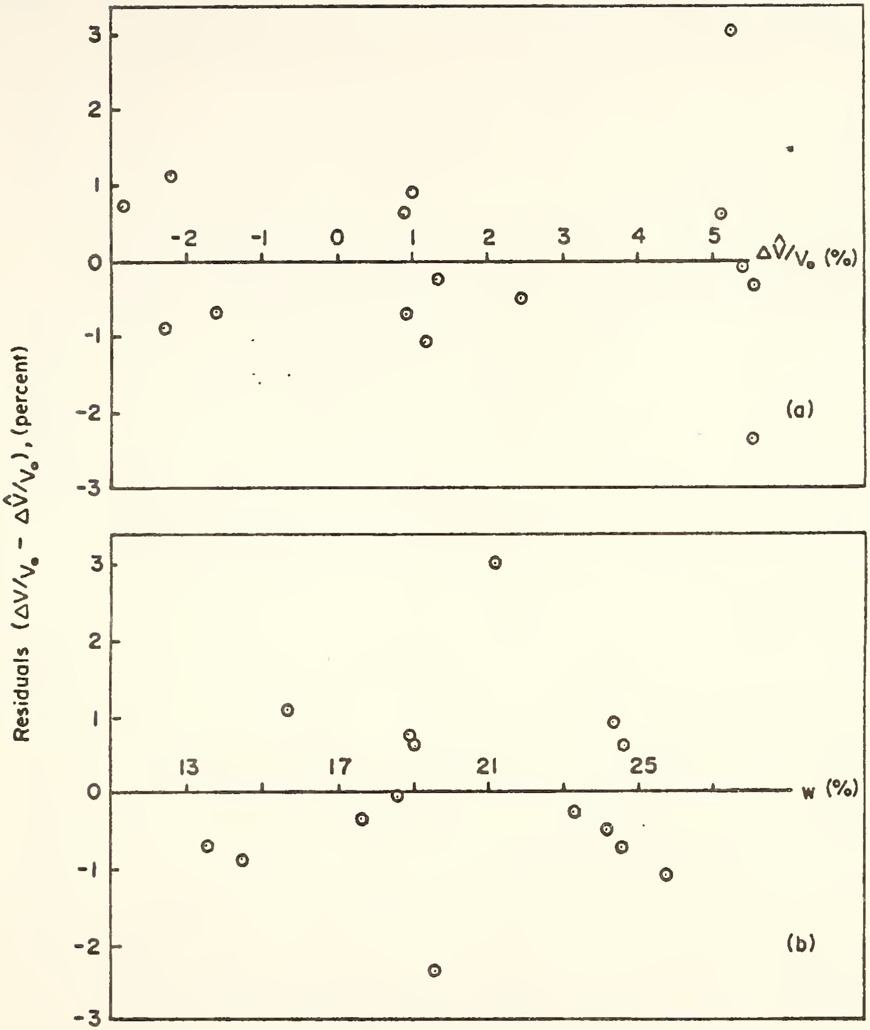

FIGURE 36 RESIDUAL ANALYSIS FOR ONE-DIMENSIONAL PERCENT VOLUME CHANGE ON WETTING

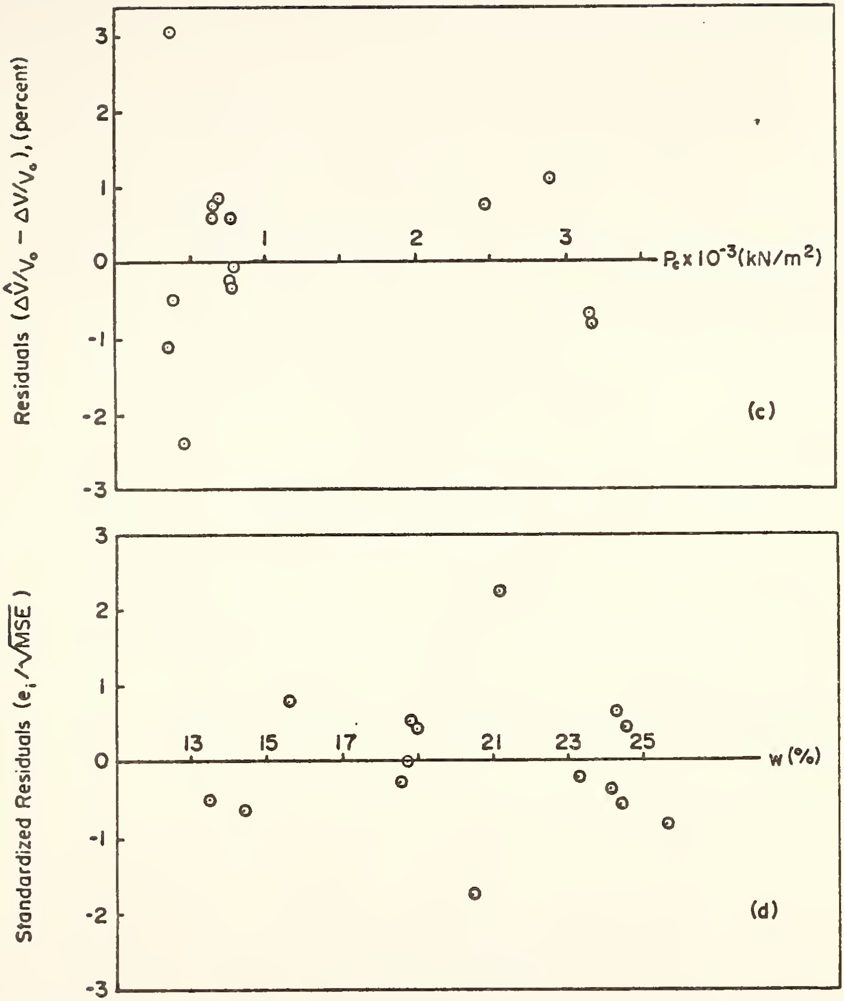

FIGURE 36 CONTINUED

Additionally, the standardized residuals ($^{e}i/\sqrt{MSE}$), plotted in (d) of each Figure, lie within ± 3, thereby indicating normality.

In view of the above, it is felt that both models are statistically accurate. A discussion of each model with respect to its physical significance and practical application follows. (An examination of the prediction variances was beyond the scope of this study. Its evaluation in future studies may be warranted. See Scott, 1977).

Discussion of Prediction Models

In the previous section, the estimated compactive prestress model ($\hat{P}_s$) was expressed as Equation (15). This Equation is valuable in that it allows one to predict the laboratory induced prestress in terms of the compaction variables, viz., water content and compaction pressure. A graphical representation of this relationship is presented in Figure 37.

In this Figure, observe for a given water content, the estimated compactive prestress increases with increasing compaction pressure. Woodsum (1951) and Abeyesekera (1978) obtained similar results, as shown in Tables 3 and 4. Also observe for a given compaction pressure, an increase in water content is accompanied by a decrease in compactive prestress. More clearly, at a given effort level, an increase in water content reduces the capacity for prestressing.

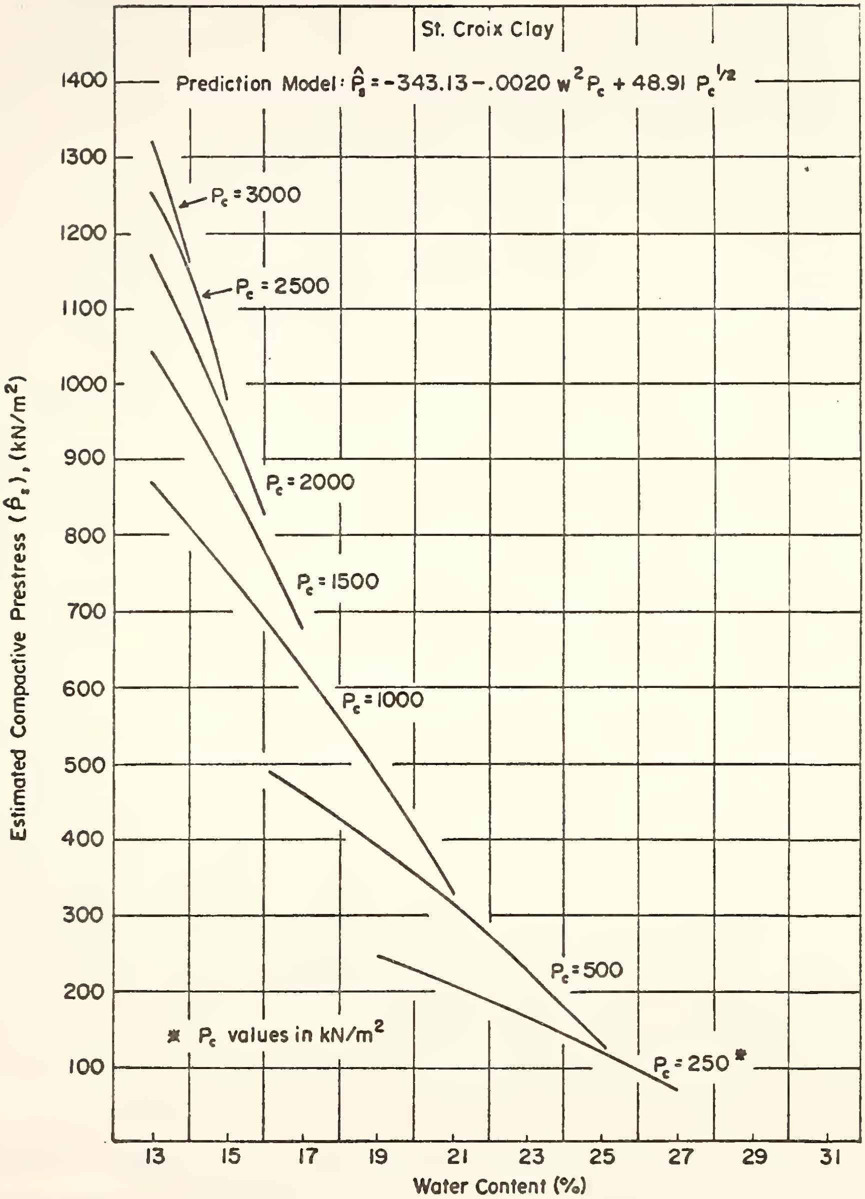

FIGURE 37 PREDICTION OF COMPACTIVE PRESTRESS

Interestingly, Garcia-Bengochea (1978) determined that permeability, as well as the frequency and magnitude of the large pore mode, also decreased with increasing water content. If these findings can be applied to compacted St. Croix clay, then they suggest that compactive prestress also varies with the characteristics of the large pore mode. That is to say, a decrease in the magnitude or frequency of the large pore mode, results in a decrease in compactive prestress.

More importantly however, is the relationship between these variables and the values of negative pore water pressure established during the kneading process. The interaction term in Equation (15) illustrates the effect of water content on the response. Note that the regression coefficient for this term is a negative value. Clearly, this indicates that as the water content increases, say dry to wet of some optimum value, the value of compactive prestress decreases. As previously reported, other investigators (Lambe, 1961 and Olson, et al., 1965) found that an increase in water content, for a given compaction pressure, increases the pore water pressure to a less negative value, and thereby reduces the capacity for prestressing. Based on this, the influence of water content is well-established by this Equation.

The effects of increasing compaction pressure on the response value ($\hat{P}_s$) has been discussed and is suitably illustrated in Figure 37. According to Lambe (1961), the pore water pressures established during compaction increase, i.e., become less negative, with increasing compaction

effort. Therefore, one may expect a decrease in the capacity for prestressing due the more dispersed structure (high u_w value). It is therefore unlikely that compaction pressure influences the prestress response value in the same manner as water content.

It may be recalled that Figure 29 illustrated the relative stiffnesses among equivalent Modified and Standard Proctor soaked samples. If these same findings can be applied herein, they suggest that the net effect of compaction pressure in Equation (15) is on the soil skeleton rigidity. That is, as the compaction pressure increases, the soil skeleton rigidity also increases. Consequently, in one-dimensional compression, much of the load is supported by the stiff skeleton, and the net result is less compression and a higher prestress value.

From the above, it may be realized that both water content and compaction pressure jointly affect the response value. That is, their effects on compactive prestress are more than likely complementary and must be considered in combination.

Shown in Figure 38 is the relationship between the one-dimensional percent volume change on wetting ($\Delta\hat{V}/V_o$), as expressed by Equation (16). This Figure forecasts the collapse and swell behavior by the linear combination of water content and compaction pressure. Moreover, it shows for a given water content, as the compaction pressure is increased, there is less tendency toward collapse (volume decrease) and

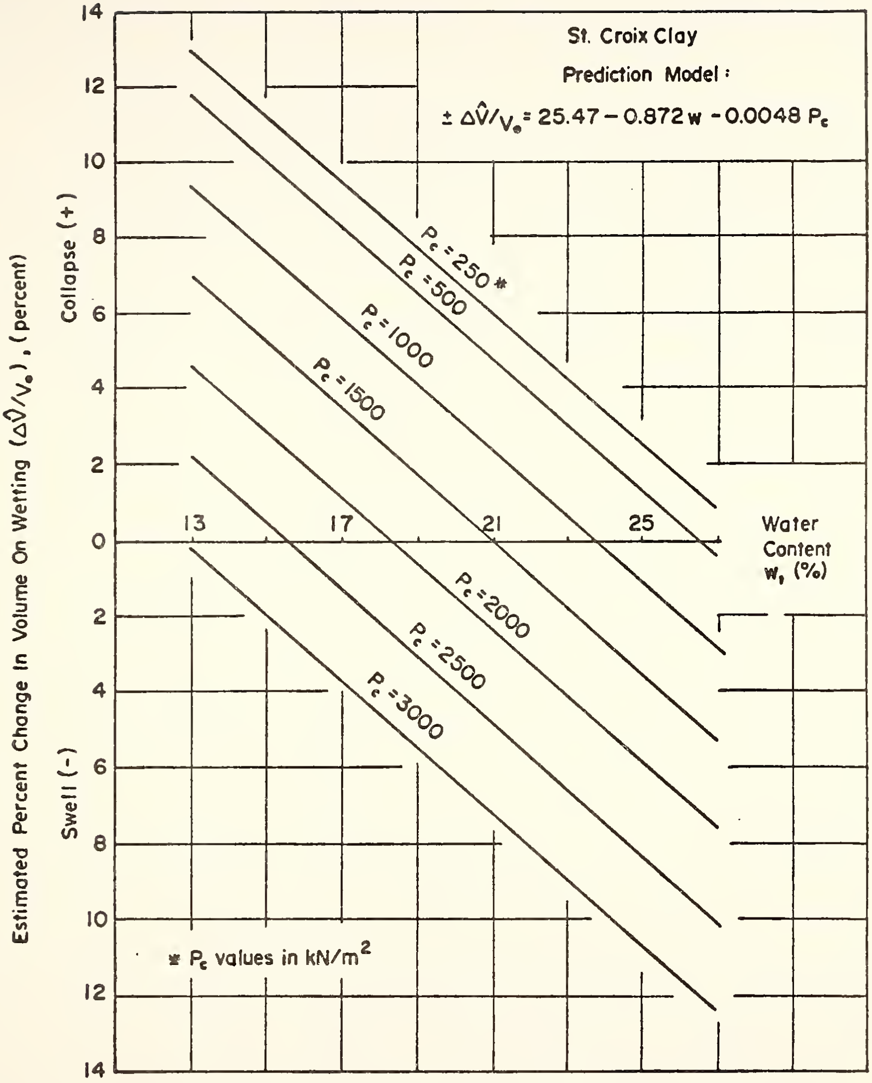

FIGURE 38 PREDICTION OF PERCENT VOLUME CHANGE ON WETTING

more toward swell (volume increase). Similar trends are established for increasing water content at a constant compaction pressure.

In connection with the previous discussion on the compactive prestress model, the effects of water content and compaction pressure on the percent volume change may be outlined as follows: (1) for a given compaction pressure, as the water content decreases, the pore water pressures become more negative, and there are many developed meniscii; on loading and wetting, there is more tendency toward volume decrease, and (2) for a given water content, as the compaction pressure increases, the soil skeleton rigidity increases; on loading and wetting, there is a softening affect, but the expansion of the double layer results in a volume increase. However, as before, it is believed that both must be considered jointly when examining this behavior.

The previous discussion concerning Figure 30 indicated that the relationship among initial void ratio (e_o), applied pressure (P_o), and percent volume change on wetting ($\Delta V/\Delta V_o$) was not well established due the influence of compactive prestress. Based on the fact that Equation (16) is expressed in terms of the same compaction variables as is Equation (15), this may suggest that $\hat{P}_s$ and $\Delta\hat{V}/\Delta V_o$ are somewhat related. Additionally, the fact that initial void ratio and confining pressure were not considered statistically significant, may also suggest that void ratio and confinement level have little effect on the volume change on wetting behavior of

compacted clays, due the influence of prestress and structure.

The relations shown in Figures 37 and 38 are not entirely applicable for the values of water content and compaction pressure plotted. Instead, each model is only applicable for its separate joint region of observations; that is, the region covered by both independent variables. (See Neter and Wasserman, 1974). Figure 39(a) shows this region for the compactive prestress model; Figure 39(b), for the one-dimensional volume change model. Each region was established by plotting the corresponding independent variables for each observation. Therefore, if either model is used, the respective independent variables must be computed, plotted, and fall within the limits of the cross-hatched region. If this restriction is not verified, then the computed estimated response value may be in error.

Consider how one may use these results in a design situation. Suppose an earthen compacted fill is to be constructed, and it is of concern that both the as-compacted and long term compressibilities be restricted to a small value. Earlier results indicated that the compressibility is relatively small in pressure regions below the prestress value. Therefore, one would select a prestress value equal to or greater than the applied pressure to be exerted by the overlying compacted material. Enter Figure 37 with this prestress value and obtain corresponding combination of water content and compaction pressure. These variables could then be plotted in Figure 38 to determine if the

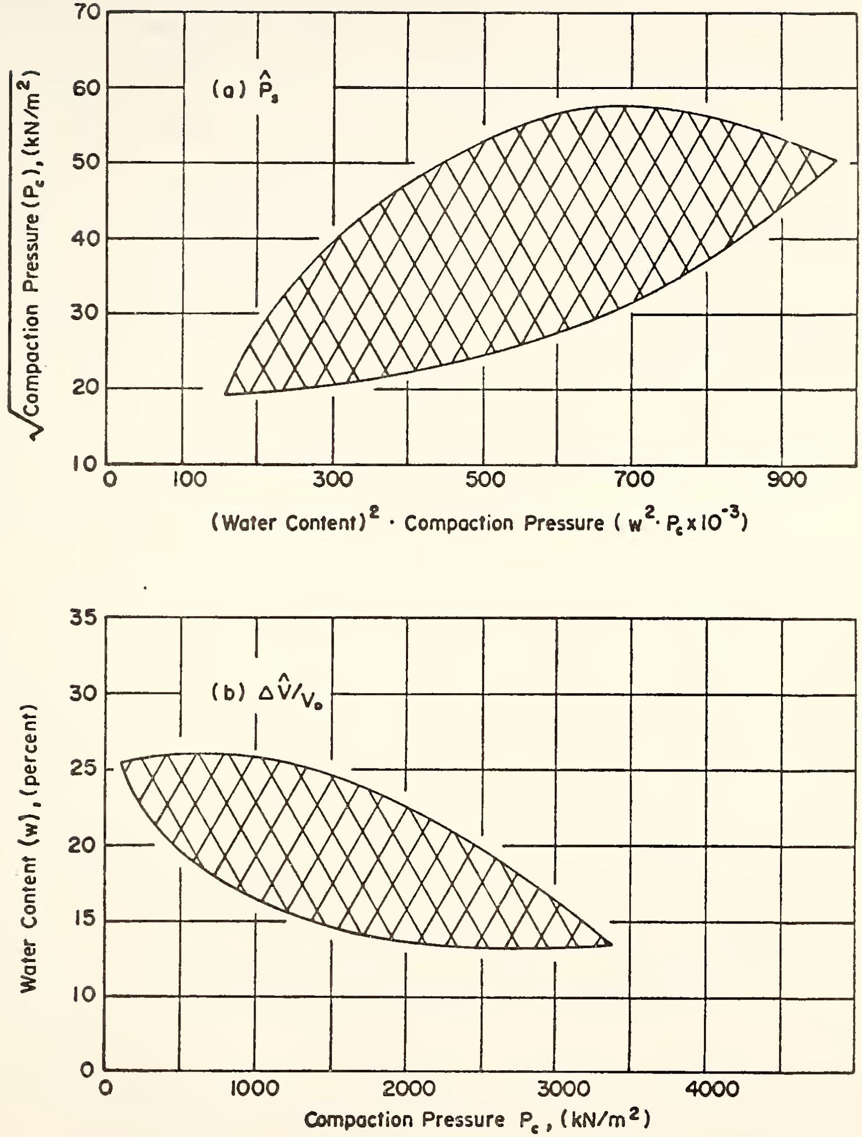

FIGURE 39 JOINT REGIONS OF OBSERVATIONS FOR PREDICTION MODELS

volume change on wetting meets the prescribed criterion.

It is recommended that the results presented in Figure 38 be used only to examine the qualitative influence of water content and compaction pressure on the response value. The in situ stress conditions in the field are difficult to determine and different from those established in the laboratory procedure (Leonards and Altschaeffl, 1971).

Other uses of these models exist. For example, it may be of interest to relate the compactive prestress value to the effective confining pressure, rather than the nominal compaction pressure, in order to determine a more accurate value of overconsolidation ratio (OCR).

Irrespective of the details, neither model can be used with confidence until the results presented herein are correlated with results for field-compacted samples of the same soil. Clearly, the variables controlling laboratory compacted behavior may be different than those controlling field compacted behavior (Price, 1978). If these correlations are accomplished, the designer would have a good handle on the in-service compressibility characteristics of the mass. This research is currently in progress.

CONCLUSIONS AND RECOMMENDATIONS

Conclusions

This report has examined the effect of laboratory kneading compaction on the as-compacted and soaked compressibility behavior of a single highly plastic compacted clay (St. Croix). An examination of the available literature provided an understanding of compacted clay behavior from a phenomenonological and engineering point of view. A detailed explanation of the experimental apparatus and procedures was presented to establish a suitable testing framework for field-compacted compressibility studies to follow for the same soil. The experimental and statistical results of this study lead to the following important conclusions:

(1) A large percentage of as-compacted compression occurs within the first minute of loading. The compression vs. time relations indicated similar fluid continuity conditions, i.e., continuous air voids, for dry and at optimum conditions.

(2) For an increasing molding water content and equivalent impact level, the as-compacted compressibility behavior was in agreement with the experimental results presented by Wilson (1952), Lambe (1958b), and Wahls et al., (1966). It is believed that this behavior

can be explained in view of the more recent evidence (Barden and Sides, 1970 and Hodek and Lovell, 1978a,b) concerning compacted clay macrostructure.

(3) Dry of optimum, the value of compactive prestress decreased with increasing molding water content and increased with increasing equivalent impact effort level. Wet of optimum, the value of compactive prestress was not influenced appreciably by varying the initial compaction variables.

(4) For the range of partial saturation considered, the ratio of compactive prestress to nominal compaction pressure was less than unity. This ratio tended to decrease with increasing initial degree of saturation.

(5) The back pressuring technique was an effective method for achieving full saturation of compacted specimens under a vertically applied load. The $\Delta u/\Delta\sigma$ build-up and dissipation curves indicated, that for dry and at optimum initial conditions, increasing compaction pressure decreases compacted clay skeleton compressibility.

(6) For the soaked condition, the Casagrande approximation for determining R_{100} was in agreement with the value obtained from pore pressure measurements for a load increment ratio of 0.5.

(7) The percent volume change on wetting could not be explained in terms of initial void ratio and the level of confinement on soaking. It is believed that this percent change is strongly influenced by the compactive prestress, although this was not proven by the experimentation.

(8) Soaked compressibility behavior may be summarized as follows:

   (a) For a given initial compaction condition, the soaked compressibility is greater than the as-compacted compressibility for the corresponding pressure ranges.

   (b) For a given compaction pressure and level of confinement on soaking, as the molding water content increases, the virgin compressibility, as measured by the compression index (C_c), decreases.

   (c) For a given degree of saturation, the virgin compressibility is little affected by increasing vertical confinement on saturation.

   (d) For a given degree of saturation and confinement level on soaking, as the compaction pressure increases, the virgin compressibility decreases.

(9) The best predictive models for compactive prestress and one-dimensional percent volume change on wetting were isolated using the SPSS procedures—SCATTERGRAM, STEPWISE, REGRESSION. The proposed

models were found to be statistically valid and accurate.

(a) For Compactive Prestress (P_s):

$$\hat{P}_s = -343.13 - 0.0020w^2 \cdot P_c + 48.91P_c^{1/2}$$

$$R^2 = 0.88$$

and (b) For 1-D Percent Volume Change on Wetting ($\Delta V/\Delta V_o$):

$$\hat{\Delta V}/\Delta V_o = 25.47 - 0.872w - 0.0048P_c \; ; \; R^2 = 0.86$$

where w = water content in percent and P_c = nominal compaction pressure in kN/m^2. Both equations allow one to predict or control the given response in terms of the important compaction variables, viz., water content and compaction pressure, for each respective joint region of observations.

Recommendations for Future Research

(1) The relative importance of field compaction variables should be examined in order to provide correlations between the laboratory and field compressibility characteristics for the as-compacted and soaked conditions.

(2) Laboratory studies concerning the effects of different modes of compaction on compactive prestress may prove useful for a variety of clays.

(3) The influence of pore size distribution on the pore air and pore water pressures established during compaction, as well as its effect on one-dimensional compressibility behavior, should be examined.

(4) The relationship between compactive prestress and the net or effective compaction energy causing densification should be determined for different modes of compaction.

(5) The effect of compactive prestress on volume change behavior on wetting and on the soaked and as-compacted shear strength behavior should be studied.

BIBLIOGRAPHY

BIBLIOGRAPHY

Abeyesekera, R.A. (1978), "Stress Deformation and Strength Characteristics of a Compacted Shale", Ph.D. Thesis, Purdue University, West Lafayette, Indiana, May, 420 pp. (Also Joint Highway Research Report No. 77-24).

Aitchison, G.D. (1956), "Some Preliminary Studies of Unsaturated Soils", Proceedings, Second Australia-New Zealand Conference on Soil Mechanics and Foundation Engineering, Christchurch, N.Z., January, pp. 173-191.

Aitchison, G.D. (1960), "Relationships of Moisture Stress and Effective Stress Functions in Unsaturated Soils", Proceedings, Conference on Pore Pressure and Suction in Soils, Butterworths, London, pp. 47-52.

Aitchison, G.D. (1965), Panel Discussion in Session 2, Proceedings, 6th International Conference on Soil Mechanics and Foundation Engineering, Montreal, Vol. III, pp. 318-321.

Aitchison, G.D. (1973), Part 2 of the General Report for Main Session 4, Proceedings, 8th International Conference on Soil Mechanics and Foundation Engineering, Moscow, Vol. III, pp. 161-190.

Aitchison, G.D. and Bishop, A.W. (1960), Separate Discussions to Session 1, Proceedings, Conference on Pore Pressure and Suction in Soils, Butterworths, London, pp. 63-68.

Bailey, M.J. (1976), "Shale Degradation and Other Parameters Related to the Construction of Compacted Embankments", MSCE Thesis, Purdue University, West Lafayette, Indiana, August, 230 pp. (Also Joint Highway Research Project Report No. 76-23).

Barden, L. (1965), "Consolidation of Compacted and Unsaturated Clays", Geotechnique, Vol. 15, No. 3, pp. 267-286.

Barden, L. (1974), "Consolidation of Clays Compacted Dry and Wet of Optimum Water Content", Geotechnique, Vol. 24, No. 4, pp. 605-625.

Barden, L., McGown, A., and Collins, A. (1973), "The Collapse Mechanism in Partly Saturated Soil", Engineering Geology, Vol. 7, pp. 49-60.

Barden, L. and Sides, G.R. (1970), "Engineering Behavior and Structure of Compacted Clay", Journal of the Soil Mechanics and Foundations Division, ASCE, Vol. 96, SM4, pp. 1171-1200.

Baver, L.D. (1956), Soil Physics, John Wiley & Sons, New York, p. 219.

Bhasin, R.N. (1975), "Pore Size Distribution of Compacted Soils After Critical Region Drying", Ph.D. Thesis, Purdue University, West Lafayette, Indiana, May, 222 pp. (Also Joint Highway Research Project Report No. 75-3).

Biot, M.A. (1941), "General Theory of Three-Dimensional Consolidation", Journal of Applied Physics, Vol. 12, pp. 155-164.

Bishop, A.W. (1959), "The Principle of Effective Stress", Teknisk Ukeblad, No. 39-106ARG, p. 859.

Bishop, A.W. (1960), "The Measurement of Pore Pressure in the Triaxial Test", Proceedings, Conference on Pore Pressure and Suction in Soils, Butterworths, London, pp. 38-46.

Bishop, A.W., Alpan, I., Blight, G.E., and Donald, I.B. (1960), "Factors Controlling the Strength of Partly Saturated Cohesive Soils", Research Conference on Shear Strength of Cohesive Soils, ASCE, Boulder, pp. 33-162.

Bishop, A.W. and Blight, G.E. (1963), "Some Aspects of Effective Stress in Saturated and Partly Saturated Soils", Geotechnique, Vol. 13, No. 3, pp. 177-197.

Bishop, A.W. and Donald, I.B. (1961), "The Experimental Study of Partly Saturated Soil in the Triaxial Apparatus", Proceedings, Fifth International Conference on Soil Mechanics and Foundation Engineering, Paris, Vol. I, pp. 13-21.

Black, D.K. and Lee, K.N. (1973), "Saturating Laboratory Samples by Back Pressure", Journal of the Soil Mechanics and Foundations Division, ASCE, Vol. 99, No. SM1, pp. 75-93.

Blight, G.E. (1963), "The Utilisation of Soil Suction in the Design of Earth Dam Embankments", Proceedings, Third Regional Conference for Africa on Soil Mechanics and Foundation Engineering, Vol. 1, pp. 141-144.

Briggs, L.J. (1897), "The Mechanics of Soil Moisture", Bulletin No. 10, U.S. Dept. of Agriculture, Division of Soils, Government Printing Office, Washington, D.C.

Buckingham, E. (1907), "Studies on the Movement of Soil Moisture", Bulletin No. 38, U.S. Dept. of Agriculture, Bureau of Soils, Government Printing Office, Washington, D.C.

Campbell, G.D. (1952), "The Compressibility Characteristics of a Bituminous Concrete Mix", A Report Submitted to Dr. G.A. Leonards in Fulfillment of a "Special Project" Course in Civil Engineering, Purdue University, West Lafayette, Indiana.

Carman, P.C. (1953), "Properties of Capillary-Held Liquids", Journal of Physical Chemistry, Vol. 57, pp. 56-64.

Crawford, C.B. (1964), "Interpretation of the Consolidation Test", Proceedings, Conference on Design of Foundations for Control of Settlement", ASCE, Evanston, Illinois, June, pp. 93-108.

Croney, D. (1952), "The Movement and Distribution of Water in Soils", Geotechnique, Vol. III, pp. 1-16.

Croney, D. and Coleman, J.D. (1953), "Soil Moisture Suction Properties and Their Bearing on the Moisture Distribution Soils", Proceedings, Third International Conference on Soil Mechanics and Foundation Engineering, Zurich, Vol. 1, pp. 13-18.

Croney, D. and Coleman, J.D. (1960), "Pore Pressure and Suction in Soils", Proceedings, Conference on Pore Pressure and Suction in Soils, Butterworths, London, pp. 31-37.

Croney, D., Coleman, J.D., and Black, W.P. (1958), "Movement and Distribution of Water in Soil in Relation to Highway Design and Performance", HRB Special Report 40, January, pp. 226-252.

Danielson, J. (1963), "Consolidation of Unsaturated Clay-Soils", Ph.D. Thesis, Colorado State University, Fort Collins, Colorado, 116 pp.

Draper, N.R. and Smith, H. (1966), Applied Regression Analysis, J. Wiley and Sons, New York, 407 pp.

Dunn, I.S. and Nielsen, J.P. (1959), "A Unified Consolidation Theory", Unpublished Report of the Advanced Soil Mechanics Laboratory, Dept. of Civil Engineering, Colorado State University, Fort Collins, Colorado.

Essigmann, M.F. (1976), "An Examination of the Variability Resulting from Soil Compaction", MSCE Thesis, Purdue University, West Lafayette, Indiana, August, 108 pp. (Also Joint Highway Research Project Report No. 76-28).

Fredlund, D.G. (1973), Discussion in Session 2, Proceedings, Third International Conference on Expansive Soils, Haifa, Israel, Vol. 2, p. 71.

Fredlund, D.G. and Morgenstern, N.R. (1977), "Stress State Variables for Unsaturated Soils", Journal of the Geotechnical Engineering Division, ASCE, Vol. 103, No. GT5, pp. 447-466.

Garcia-Bengochea, I. (1978), "The Relation Between Permeability and Pore Size Distribution of Compacted Clayey Silts", MSCE Thesis, Purdue University, West Lafayette, Indiana, May, 179 pp. (Also Joint Highway Research Project Report No. 78-4).

Gardner, W. (1920), "The Capillary Potential and Its Relation to Soil Moisture Contents", Soil Science, Vol. 10, pp. 103-126.

Gaudette, N.G., Jr. (1960), "Application of Kneading Compactor and Hveem Stabilometer to Bituminous Concrete Design in Indiana", MSCE Thesis, Purdue University, West Lafayette, Indiana, December, 238 pp. (Also Joint Highway Research Project Report No. 60-23).

Gibbs, H.J. and Coffey, C.T. (1963), "Measurement of Initial Negative Pore Pressure In Unsaturated Soil", Laboratory Report No. EM-665, Earth Research Program, Bureau of Reclamation, U.S. Dept. of Interior, Denver, Colorado.

Girault, P. (1960), "A Study on the Consolidation of Mexico City Clay", Ph.D. Thesis, Purdue University, West Lafayette, Indiana, June, 194 pp.

Hilf, J.W. (1956), "An Investigation of Pore-Water Pressure in Compacted Cohesive Soils", Technical Memorandum 654, U.S. Dept. of Interior, Bureau of Reclamation, Denver, Colorado, 109 pp.

Hodek, R.J. (1972), "Mechanism for the Compaction and Response of Kaolinite", Ph.D. Thesis, Purdue University, West Lafayette, Indiana, December, 269 pp. (Also Joint Highway Research Project Report No. 72-36).

Hodek, R.J. and Lovell, C.W. (1978a), "Soil Aggregates and Their Control Over Soil Compaction and Swelling", presented at January 15-19, 1979 meeting of TRB, to be published.

Hodek, R.J. and Lovell, C.W. (1978b), "A New Look at Compaction of Landfills", presented before AEG Conference, Hershey, Pennsylvania, October 18, 1979, to be published.

Jennings, J.E. (1960), "A Revised Effective Stress Law for Use in the Prediction of the Behaviour of Unsaturated Soils", Proceedings, Conference on Pore Pressure and Suction in Soils, Butterworths, London, pp. 26-30.

Jennings, J.E. and Burland, J.B. (1962), "Limitations of the Use of Effective Stress in Partly Saturated Soils", Geotechnique, Vol. 12, No. 2, pp. 125-144.

Keen, B.A. (1924), "On the Moisture Relationships in an Ideal Soil", Journal of Agricultural Science, Vol. 14, pp. 170-177.

Kelvin, L., W.T. (1871), "On the Equilibrium of Vapor at Curved Surface of Liquid", Philosophical Magazine, Vol. 42, No. 282, pp. 448-452.

Lambe, T.W. (1958a), "The Structure of Compacted Clay", Journal of the Soil Mechanics and Foundations Division, ASCE, Vol. 84, SM2, Paper No. 1654, pp. 1-34.

Lambe, T.W. (1958b), "The Engineering Behavior of Compacted Clay", Journal of the Soil Mechanics and Foundations Division, ASCE, Vol. 84, SM2, Paper No. 1655, pp. 1-35.

Lambe, T.W. (1960), "A Mechanistic Picture of the Shear Strength in Clay", Research Conference on Shear Strength of Cohesive Soils, ASCE, Boulder, pp. 555-580.

Lambe, T.W. (1961), "Residual Pore Pressure in Compacted Clay", Proceedings, Fifth International Conference on Soil Mechanics and Foundation Engineering, Paris, Vol. 1, pp. 207-212.

Langfelder, L.J., Chen, C.F., and Justice, J.A. (1968), "Air Permeability of Compacted Cohesive Soils", Journal of the Soil Mechanics and Foundations Division, ASCE, Vol. 94, SM4, pp. 981-1001.

Leonards, G.A. (1952), Discussion to "Effect of Compaction on Soil Properties", by S.D. Wilson, Proceedings, Conference on Soil Stabilization, M.I.T., June, pp. 159-161.

Leonards, G.A. (1975), "General Report on Partly Saturated Clays", Proceedings, Fifth Asian Regional Conference, Bangalore, India, in press.

Leonards, G.A. and Altschaeffl, A.G. (1971), Discussion, Journal of the Soil Mechanics and Foundations Division, ASCE, Vol. 97, No. SM1, pp. 269-271.

Leonards, G.A. and Girault, P. (1961), "A Study of the One-Dimensional Consolidation Test", Proceedings, Fifth International Conference on Soil Mechanics and Foundation Engineering, Paris, Vol. 1, pp. 213-218.

Lowe, J., III (1971), "New Concepts in Consolidation and Settlement Analysis", Terzaghi Lectures 1963-1972, ASCE, October, pp. 340-377.

Lowe, J., III and Johnson, T.C. (1960), "Use of Back Pressure to Increase Degree of Saturation of Triaxial Test Specimens", Research Conference on Shear Strength of Cohesive Soils, Boulder, pp. 819-836.

Lowe, J., III, Zaccheo, P.F., and Feldman, H.S. (1964), "Consolidation Testing With Back Pressure", Journal of the Soil Mechanics and Foundations Division, Vol. 90, SM5, pp. 69-86.

Matyas, E.L. and Radhakrishna, H.S. (1968), "Volume Change Characteristics of Partially Saturated Soils", Geotechnique, Vol. 18, pp. 432-448.

Mishu, L.P. (1963), "Collapse in One-Dimensional Compression of Compacted Clay Upon Wetting", MSCE Thesis, Purdue University, West Lafayette, Indiana, August, 105 pp.

Mitchell, J.K. (1976), Fundamentals of Soil Behavior, John Wiley and Sons, New York, pp. 186-196.

Muskat, M. (1946), The Flow of Homogeneous Fluids through Porous Media, 2nd Edition, J.W. Edwards, Ann Arbor, p. 764.

Neter, J. and Wasserman, W. (1974), Applied Linear Statistical Models, Richard D. Irwin, Homewood, Illinois, 842 pp.

Nie, N.H. et al. (1975), Statistical Package for the Social Sciences, 2nd edition, McGraw-Hill, New York, 675 pp.

Olson, R.E. (1963), "Effective Stress Theory of Soil Compaction", Journal of the Soil Mechanics and Foundations Division, ASCE, Vol. 89, SM2, pp. 27-45.

Olson, R.E. and Langfelder, L.J. (1965), "Pore Water Pressures In Unsaturated Soils", Journal of the Soil Mechanics and Foundations Division, ASCE, Vol. 91, SM4, pp. 127-150.

Plum, R.L. and Esrig, M.I. (1969), "Some Temperature Effects on Soil Compressibility and Pore Water Pressure", HRB Special Report 103, January, pp. 231-242.

Price, J.T. (1978), "Soil Compaction Specification Procedure for Desired Field Strength", MSCE Thesis, Purdue University, West Lafayette, Indiana, May, pp. 152.

Proctor, R.R. (1933), "Fundamental Principles of Soil Compaction", Engineering News-Record, Vol. 111, No. 9, August 31, pp. 245-248.

Reed, M.A. (1977), "Frost Heaving Rate of Silty Soils as a Function of Pore Size Distribution", MSCE Thesis, Purdue University, West Lafayette, Indiana, August, 116 pp. (Also Joint Highway Research Project Report No. 77-15).

Scott, J.C. (1977), "Examination of the Variability of the Soaked Strength of a Laboratory Compacted Clay", MSCE Thesis, Purdue University, West Lafayette, Indiana, May, 97 pp. (Also Joint Highway Research Project Report No. 77-8).

Schiffman, R.L., Chen, A. T-F, and Jordan, J.C. (1969), "An Analysis of Consolidation Theories", Journal of the Soil Mechanics and Foundations Division, ASCE, Vol. 95, SM1, pp. 285-312.

Schofield, R.K. (1935), "The pF of Water in Soil", Transactions, Third International Soil Congress, Vol. 2, pp. 37-48.

Schofield, R.K. and Da Costa, J.V. (1938), "The Measurement of the pF in Soil by Freezing Point", Journal of Agricultural Science, Vol. 28, No. 4, pp. 644-653.

Seed, H.B., Mitchell, J.B., and Chan, C.K. (1960), "The Strength of Compacted Cohesive Soils", Research Conference on Shear Strength of Cohesive Soils, ASCE, Boulder, pp. 877-964.

Skempton, A.W. (1954), "The Pore Pressure Coefficients A and B", Geotechnique, Vol. 4, No. 4, pp. 143-147.

Skempton, A.W. (1960), "Effective Stress in Soils, Concrete, and Rocks", Proceedings, Conference on Pore Pressure and Suction in Soils, Butterworths, London, pp. 4-16.

Sridharan, A. (1968), "Some Studies on the Strength of Partly Saturated Clays", Ph.D. Thesis, Purdue University, West Lafayette, Indiana, August, 179 pp.

Terzaghi, K. (1925), Erdbaumechanik, F. Deutecke, Vienna.

Terzaghi, K. (1936), "Shearing Resistance of Saturated Soils and the Angles Between the Planes of Shear", Proceedings, First International Conference on Soil Mechanics and Foundation Engineering, Cambridge, Vol. I, p. 54.

Teerawong, P. (1962), "One-Dimensional Consolidation of Unsaturated Clay", Ph.D. Thesis, Colorado State University, Fort Collins, Colorado, 107 pp.

Wahls, H.E., Fisher, C.P., and Langfelder, L.J. (1966), The Compaction of Soil and Rock for Highway Purposes, U.S. Dept. of Commerce, Bureau of Public Roads, FHWA-RD-73-8, 457 pp.

Wilson, S.D. (1952), "Effect of Compaction on Soil Properties", Proceedings, Conference on Soil Stabilization, M.I.T., June, pp. 148-158.

Wissa, A.E. (1969), "Pore Pressure Measurement in Saturated Stiff Soils", Journal of the Soil Mechanics and Foundations Division, ASCE, Vol. 95, SM4, pp. 1063-1073.

Woodsum, H.C. (1951), "The Compressibility of Two Compacted Clays", MSCE Thesis, Purdue University, West Lafayette, Indiana, June, 69 pp.

Yoshimi, Y. (1958), "One Dimensional Consolidation of Partially Saturated Soil", Ph.D. Thesis, Northwestern University, Evanston, Illinois, August, 149 pp.

Yoshimi, Y. and Osterberg, J.D. (1963), "Compression of Partially Saturated Cohesive Soils", Journal of the Soil Mechanics and Foundations Division, ASCE, Vol. 89, SM4, pp. 1-23.

APPENDICES

APPENDIX A

COMPACTION DATA

TABLE A1 MOISTURE·DENSITY DATA FOR THE THREE IMPACT COMPACTION LEVELS

Low Energy		Standard Proctor		Modified Proctor	
Water Content (%)	Dry Density γ_d (kN/m^3)	Water Content (%)	Dry Density γ_d (kN/m^3)	Water Content (%)	Dry Density γ_d (kN/m^3)
17.2	14.18	17.1	14.57	11.7	17.23
19.7	14.73	16.8	14.92	13.8	17.32
20.0	14.74	18.6	15.49	13.4	17.61
20.1	14.62	20.7	15.87	14.3	17.81
21.0	14.74	21.3	15.83	14.6	17.81
21.1	14.95	20.8	16.02	15.2	17.76
20.7	14.95	20.8	16.14	16.8	17.83
21.0	15.20	22.0	15.98	17.4	17.78
21.8	15.19	22.0	16.05	17.9	17.65
22.0	15.24	22.2	16.14	19.0	17.51
22.6	15.21	22.4	16.13	19.2	17.42
23.2	15.20	22.6	16.07	20.4	17.15
23.5	15.33	22.8	16.07	21.9	16.64
25.0	15.26	23.3	16.08	22.1	16.64
25.4	15.33	23.3	15.97	22.2	16.45
25.5	15.31	24.0	15.77	----	-----
27.9	14.91	24.2	15.72	----	-----
----	-----	24.9	15.48	----	-----
----	-----	25.7	15.15	----	-----
----	-----	27.3	14.86	----	-----

TABLE A2 DENSITY AND SATURATION DATA FOR MOLD AND OEDOMETER SAMPLES

Sample No.	Water Content (%)	Mold Sample		Oedometer Sample	
		Dry Density γ_d (kN/m^3)	Degree of Saturation S_r (%)	Dry Density γ_d (kN/m^3)	Degree of Saturation S_r (%)
LD1	20.60	14.00	60.0	13.97	59.8
SD8	19.38	15.13	66.5	14.62	61.8
LD3	20.51	14.78	66.9	14.27	62.2
LD2	20.60	14.61	65.6	14.85	65.3
SD4	18.95	15.17	65.5	15.26	66.4
SD9	19.59	15.54	73.2	15.06	66.6
MD2	13.96	17.67	70.5	17.65	70.2
SD10	19.37	15.62	71.6	15.65	71.9
LO1	23.26	14.86	76.8	15.74	80.1
SO3	21.37	15.70	79.9	15.76	80.6
LO3	24.27	15.58	89.1	14.91	80.7
SO11	21.65	15.59	79.6	15.72	81.1
SO8	21.71	15.58	79.7	15.78	82.0
MD1	14.67	18.11	79.4	18.31	82.1
SO9	21.21	15.99	82.7	15.99	82.7
MO2	15.71	17.82	81.3	18.10	85.1
MO1	16.20	18.04	86.8	17.97	85.9
MW5	19.57	17.35	94.0	16.86	87.2
MW1	19.59	17.39	94.7	16.99	87.9
MW3	19.74	19.35	94.8	16.87	88.1
SO16	22.68	16.17	90.1	15.97	88.2
SW3	25.71	15.38	91.6	15.13	88.3
LW3	26.98	15.05	91.6	14.82	88.4
SW7	24.87	15.60	91.5	15.38	88.7
SW2	25.38	15.49	92.0	15.24	88.7
SO12	22.32	16.24	90.5	16.15	89.2
LO2	23.85	15.76	90.0	15.77	89.6
SW4	25.05	15.56	91.7	15.42	89.8
SW6	24.72	15.67	92.1	15.64	91.5
SO13	22.67	16.17	90.9	16.25	91.9
SW8	24.71	15.62	92.0	15.68	92.1
LW2	27.94	14.74	90.5	14.88	92.5

APPENDIX B

COMPRESSIBILITY DATA

TABLE B1 AS-COMPACTED COMPRESSIBILITY TEST DATA

Applied Load (kN/m^2)	VOID RATIO					
	Sample Designation					
	LD1	LD2	LO1	LO2	LW2	LW3
0.0	0.9649	0.8838	0.8126	0.7451	0.8460	0.8544
9.80	0.9649	0.8838	0.8126	0.7451	0.8460	0.8544
15.20	0.9643	0.8821	0.8101	0.7439	0.8456	0.8525
22.65	0.9639	0.8806	0.8087	0.7420	0.8443	0.8497
34.03	0.9619	0.8782	0.8051	0.7387	0.8387	0.8419
49.52	0.9601	0.8765	0.7990	0.7334	0.8317	0.8293
76.49	0.9525	0.8707	0.7887	0.7256	0.8197	0.8119
114.54	0.9418	0.8628	0.7775	0.7161	0.8016	0.7912
171.52	0.9269	0.8496	0.7568	0.6998	0.7798	0.7668
257.33	0.9105	0.8313	0.7251	0.6789	0.7553	0.7395
386.10	0.8322	0.7860	0.6806	0.6539	0.7299	0.7176
579.39	0.7491	0.7155	0.6375	0.6301	0.7059	0.6905
859.16	------	0.6376	0.6072	0.6075	0.6698	0.6540
1289.61	------	0.5751	0.5790	0.5835	0.6242	0.6176
1954.24	------	0.5434	0.5487	------	------	------

TABLE B1 (Continued)

Applied Load (kN/m^2)	VOID RATIO						
	Sample Designation						
	MD1	MD2	MO1	MO2	MW1	MW3	MW5
0.0	0.5003	0.5565	0.5281	0.5168	0.6243	0.6277	0.6285
9.80	0.5003	0.5565	0.5281	0.5168	0.6243	0.6277	0.6285
15.20	0.5000	0.5560	0.5222	0.5163	0.6243	0.6277	0.6278
22.65	0.4997	0.5550	0.5213	0.5152	0.6243	0.6277	0.6258
34.03	0.4992	0.5534	0.5192	0.5140	0.6243	0.6256	0.6232
49.52	0.4986	0.5513	0.5169	0.5119	0.6223	0.6226	0.6175
76.49	0.4980	0.5491	0.5139	0.5090	0.6160	0.6167	0.6120
114.54	0.4965	0.5456	0.5104	0.5053	0.6106	0.6076	0.6025
171.52	0.4941	0.5410	0.5062	0.5016	0.6044	0.5971	0.5889
257.33	0.4901	0.5363	0.5010	0.4970	0.5977	0.5849	0.5720
386.10	0.4854	0.5311	0.4949	0.4922	0.5848	0.5629	0.5548
579.39	0.4795	0.5251	0.4889	0.4861	0.5754	------	0.5366
859.16	0.4725	0.5163	0.4813	0.4795	0.5589	------	0.5184
1289.61	0.4653	0.5082	0.4722	0.4712	------	------	0.4966
1954.24	0.4591	0.4970	0.4608	0.4608	------	------	0.4792
2931.50	0.4490	0.4760	0.4397	0.4427	------	------	------
4396.47	0.4383	0.4577	0.4118	0.4128	------	------	------

TABLE B1 (Continued)

Applied Load (kN/m^2)	VOID RATIO						
	Sample Designation						
	SD4	SD8	SD9	SD10	SO11	SO12	SO13
0.0	0.7990	0.8770	0.8238	0.7545	0.7473	0.7066	0.6905
9.80	0.7990	0.8770	0.8238	0.7545	0.7473	0.7066	0.6905
15.20	0.7986	0.8770	0.8238	0.7545	0.7473	0.7063	0.6905
22.65	0.7981	0.8768	0.8236	0.7543	0.7470	0.7061	0.6901
34.03	0.7975	0.8753	0.8215	0.7529	0.7467	0.7035	0.6897
49.52	0.7967	0.8725	0.8179	0.7510	0.7460	0.6982	0.6893
76.49	0.7905	0.8676	0.8115	0.7483	0.7453	0.6944	0.6892
114.54	0.7816	0.8587	0.7978	0.7439	0.7365	0.6823	0.6748
171.52	0.7745	0.8471	0.7810	0.7369	0.7233	0.6606	0.6573
257.33	0.7667	0.8312	0.7601	0.7269	0.7105	0.6428	0.6428
386.10	0.7521	0.8021	0.7347	0.7151	0.6877	0.6195	0.6211
579.39	0.7233	0.7460	0.6932	0.6965	0.6690	------	0.5928
859.16	0.6663	0.6601	0.6235	0.6645	------	------	------
1289.61	0.5967	0.5822	0.5504	0.6279	------	------	------
1954.24	0.5264	0.5244	0.4967	0.5615	------	------	------

TABLE B1 (Continued)

Applied Load (kN/m^2)	VOID RATIO						
	Sample Designation						
	SO16	SW2	SW3	SW4	SW6	SW7	SW8
0.0	0.7202	0.8014	0.8155	0.7810	0.7514	0.7854	0.7514
9.80	0.7202	0.8014	0.8155	0.7810	0.7514	0.7854	0.7514
15.20	0.7195	0.8006	0.8145	0.7792	0.7514	0.7848	0.7514
22.65	0.7188	0.7987	0.8090	0.7758	0.7514	0.7842	0.7510
34.03	0.7169	0.7968	0.7994	0.7727	0.7465	0.7825	0.7472
49.52	0.7128	0.7943	0.7932	0.7652	0.7405	0.7760	0.7413
76.49	0.7061	0.7910	0.7856	0.7521	0.7314	0.7671	0.7330
114.54	0.6957	0.7720	0.7694	0.7388	0.7240	0.7602	0.7204
171.52	0.6829	0.7465	0.7567	0.7219	0.7064	0.7398	0.7087
257.33	0.6660	0.7286	0.7291	0.7011	0.6924	0.7011	0.6906
386.10	0.6420	0.7040	0.7009	0.6727	0.6601	------	0.6741
579.39	0.6140	0.6834	0.6835	0.6526	------	------	------
859.16	0.5900	0.6563	0.6566	------	------	------	------
1289.61	0.5795	0.6314	0.6255	------	------	------	------
1954.24	------	0.6012	0.5970	------	------	------	------
2391.50	------	0.5805	0.5667	------	------	------	------

TABLE B1 (Continued)

Applied Load (kN/m^2)	Void Ratio S.D.* SO3	Applied Load (kN/m^2)	Void Ratio S.D. SO8	Applied Load (kN/m^2)	Void Ratio S.D. SO9	Applied Load (kN/m^2)	Void Ratio S.D. LO3	Void Ratio S.D. LD3
0.0	0.7423	0.0	0.7411	0.0	0.7180	0.0	0.8423	0.9240
9.80	0.7423	9.80	0.7411	9.80	0.7180	9.80	0.8423	0.9240
15.20	0.7419	15.20	0.7409	15.20	0.7177	15.20	0.8402	0.9230
22.65	0.7403	22.65	0.7400	22.65	0.7168	22.65	0.8382	0.9215
34.03	0.7376	34.03	0.7351	34.03	0.7142	34.03	0.8348	0.9182
49.52	0.7358	49.52	0.7302	49.52	0.7129	49.52	0.8292	0.9120
74.33	0.7316	74.34	0.7222	76.49	0.7103	76.49	0.8192	0.8995
108.36	0.7241	108.36	0.7154	114.54	0.7085	114.54	0.8040	0.8812
164.07	0.7164	164.07	0.7065	171.52	0.7061	171.52	0.7846	0.8609
247.72	0.7098	247.72	0.6911	257.33	0.6803	257.33	0.7633	0.8179
371.58	0.6955	371.58	0.6772	386.10	0.6554	386.10	0.7381	0.7279
554.19	0.6694	554.19	0.6492	579.39	0.6222	480.00	0.7144	0.6887
868.51	0.6200	839.08	0.6179	868.00	0.5877	------	------	------
1247.84	0.5859	1247.84	0.5865	1302.00	0.5598	------	------	------
1867.15	0.5682	1867.10	0.5594	1954.24	0.5417	------	------	------
-------	------	2795.97	0.5463	2931.50	0.5279	------	------	------

* S.D. refers to Sample Designation

TABLE B2 SOAKED COMPRESSIBILITY TEST DATA

Applied Load (kN/m^2)	VOID RATIO Sample Designation SWA	MWA	SDA	LOA	MOA
0.0	0.7532	0.5782	0.8738	0.8206	0.5188
9.80	0.7532	0.5782	0.8738	0.8206	0.5188
15.20	0.7521	0.5773	0.8729	0.8186	0.5185
22.65	0.7502	0.5759	0.8714	0.8131	0.5184
34.03	0.7469	0.5743	0.8684	0.8087	0.5179
49.52	0.7415	0.5716	0.8639	0.8012	0.5170
76.49	0.7337	0.5678	0.8574	0.7909	0.5152
114.54	0.7253	0.5623	0.8497	0.7781	0.5120
160.00	0.7182	0.5566	0.8420	0.7638	0.5078
160.00	0.7153	0.5896	0.7475	0.7625	0.5243
114.54	0.7232	0.6008	0.7542	0.7726	0.5320
76.49	0.7454	0.6346	0.7829	0.7950	0.5488
114.54	0.7432	0.6318	0.7795	0.7898	0.5474
171.52	0.7348	0.6217	0.7657	0.7761	0.5441
257.30	0.7226	0.6083	0.7441	0.7533	0.5376
386.10	0.7050	0.5888	0.7109	0.7228	0.5272
579.10	0.6748	0.5673	0.6670	0.6847	0.5135
868.72	0.6400	0.5456	0.6340	------	0.4986
1303.00	0.6049	0.5228	0.5926	------	0.4825
1954.60	------	------	0.5608	0.6048	0.4656
2931.90	------	------	------	------	0.4446

TABLE B2 (Continued)

Applied Load (kN/m^2)	VOID RATIO Sample Designation SDB	LDB	MDB	SWB	MOB
0.0	0.8143	1.1240	0.5568	0.7435	0.5633
9.80	0.8143	1.1240	0.5568	0.7435	0.5633
15.20	0.8132	1.118	0.5560	0.7424	0.5628
22.65	0.8115	1.109	0.5548	0.7401	0.5616
34.03	0.8096	1.100	0.5525	0.7367	0.5602
49.52	0.8069	1.084	0.5498	0.7308	0.5577
76.49	0.8027	1.061	0.5460	0.7222	0.5546
114.54	0.7959	1.031	0.5415	0.7113	0.5513
171.52	0.7878	0.974	0.5317	0.6970	0.5460
257.33	0.7741	0.8841	0.5311	0.6792	0.5417
320.00	0.7666	0.8337	0.5279	0.6683	0.5392
320.00	0.6718	0.6817	0.5770	0.6441	0.5743
171.52	0.6872	0.6998	0.6072	0.6572	0.5971
76.49	0.7491	0.7772	0.6381	0.6959	0.6584
114.54	0.7455	0.7709	0.6363	0.6929	0.6553
171.52	0.7312	0.7517	0.6321	0.6836	0.6466
257.33	0.7090	0.7266	0.6178	0.6684	0.6292
386.10	0.6799	0.6937	0.5984	0.6518	0.6078
579.15	0.6452	0.6547	0.5737	0.6296	0.5853
868.72	0.6042	0.6120	0.5476	0.5977	0.5589
1303.08	0.5647	0.5682	0.5207	0.5602	0.5285
1954.60	0.5301	------	------	------	------

TABLE B2 (Continued)

Applied Load (kN/m^2)	VOID RATIO Sample Designation SDC	 LDC	 LWC	 SOC	 LOC
0.0	0.8042	0.9240	0.8423	0.7427	0.8654
9.80	0.8042	0.9240	0.8423	0.7427	0.8654
15.20	0.8037	0.9230	0.8402	0.7411	0.8643
22.65	0.8023	0.9215	0.8382	0.7394	0.8630
34.03	0.8007	0.9182	0.8348	0.7359	0.8598
49.52	0.7989	0.9120	0.8292	0.7314	0.8537
76.49	0.7960	0.8995	0.8192	0.7237	0.8444
114.54	0.7914	0.8812	0.8040	0.7116	0.8323
171.52	0.7857	0.8609	0.7846	0.6971	0.8147
257.33	0.7766	0.8179	0.7633	0.6800	0.7844
386.10	0.7627	0.7279	0.7381	0.6601	0.7298
480.00	0.7526	0.6887	0.7144	0.6477	0.7020
480.00	0.6530	0.6359	0.6818	0.6303	0.6686
257.33	0.6652	0.6396	0.6835*	0.6390	0.6836
114.54	0.7041	0.6670	0.7002**	0.6639	0.7322
76.49	0.7425	0.7272	0.7307	0.6818	0.7747†
114.54	0.7404	0.7234	0.7281	0.6799	0.7728
171.52	0.7267	0.7118	0.7227	0.6750	0.7630
257.33	0.7041	0.6910	0.7108	0.6651	0.7357
386.10	0.6805	0.6675	0.6982	0.6513	0.7088
579.15	0.6505	0.6389	0.6789	0.6221	0.6784
868.72	0.6162	0.6046	0.6489	0.5985	0.6389
1303.08	0.5785	0.5649	0.6113	0.5640	0.5942
1954.63	------	------	------	------	0.5486

*Applied Load = 386.10 kN/m^2 ; **Applied Load = 171.52 kN/m^2 ;
†Applied Load = 91.96 kN/m^2

TABLE B2 (Continued)

Applied Load (kN/m^2)	Void Ratio S.D.* SOA	Applied Load (kN/m^2)	Void Ratio S.D.* SOB
0.0	0.7157	0.0	0.7111
9.80	0.7157	9.80	0.7111
15.20	0.7149	15.20	0.7103
22.65	0.7135	22.65	0.7095
34.03	0.7116	34.03	0.7080
49.52	0.7093	49.52	0.7061
76.49	0.7054	76.49	0.7033
114.54	0.7007	114.54	0.6969
160.00	0.6944	171.52	0.6883
160.00	0.6883	257.33	0.6779
200.00	0.6864	320.00	0.6716
250.00	0.6829	320.00	0.6658
312.50	0.6807	400.00	0.6641
390.60	0.6664	500.00	0.6551
488.28	0.6541	625.00	0.6428
312.50	0.6605	781.25	0.6261
160.00	0.6737	976.00	0.6099
240.00	0.6703	1220.70	0.5917
360.00	0.6691	1528.88	0.5728
540.00	0.6649	1907.34	0.5491
810.00	0.6589	-------	------
1215.00	0.6455	-------	------
1822.00	0.6279	-------	------

*S.D. refers to Sample Designation

APPENDIX C

SUPPLEMENTARY FIGURES

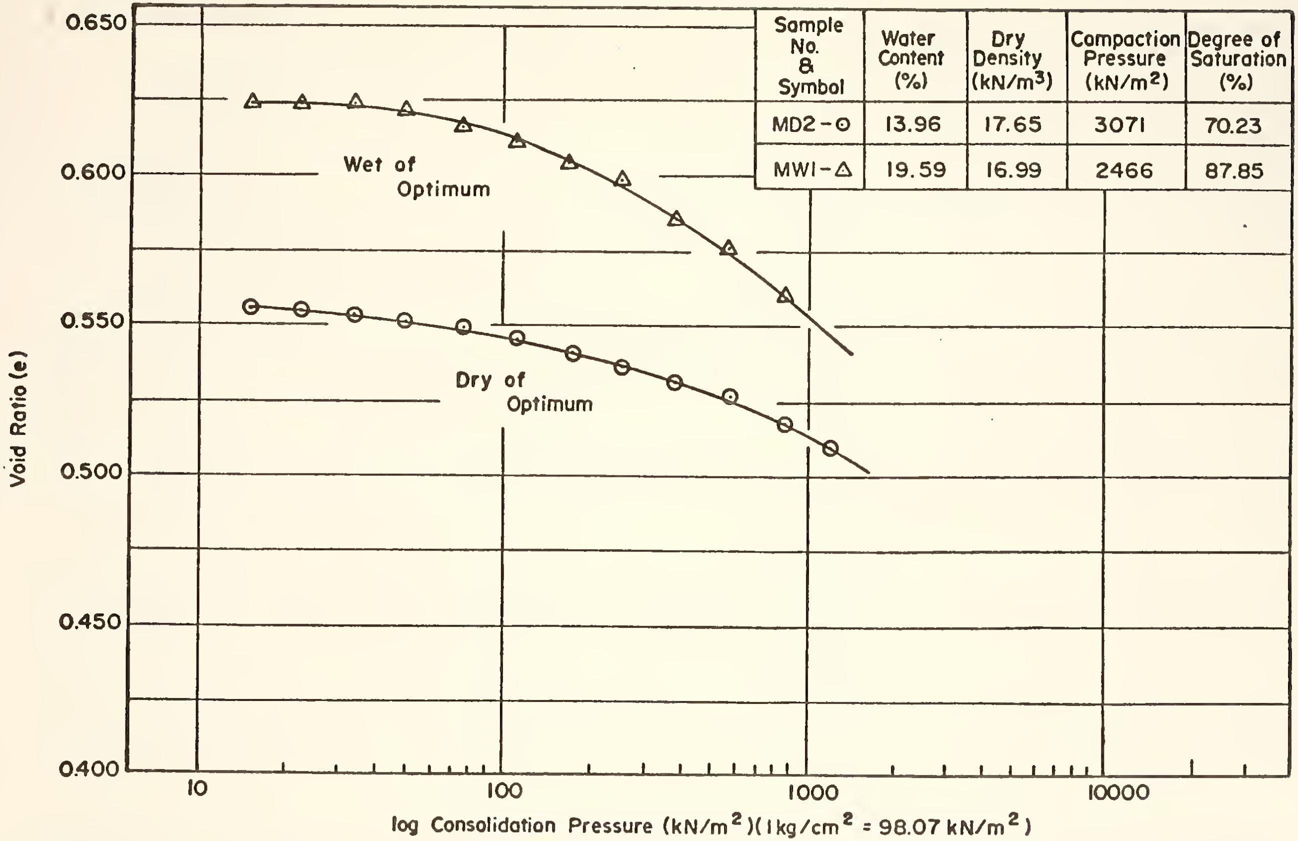

Sample No. & Symbol	Water Content (%)	Dry Density (kN/m^3)	Compaction Pressure (kN/m^2)	Degree of Saturation (%)
MD2 - ⊙	13.96	17.65	3071	70.23
MW1 - △	19.59	16.99	2466	87.85

FIGURE C1 EFFECT OF MOISTURE CONTENT ON COMPRESSIBILITY (MODIFIED PROCTOR)

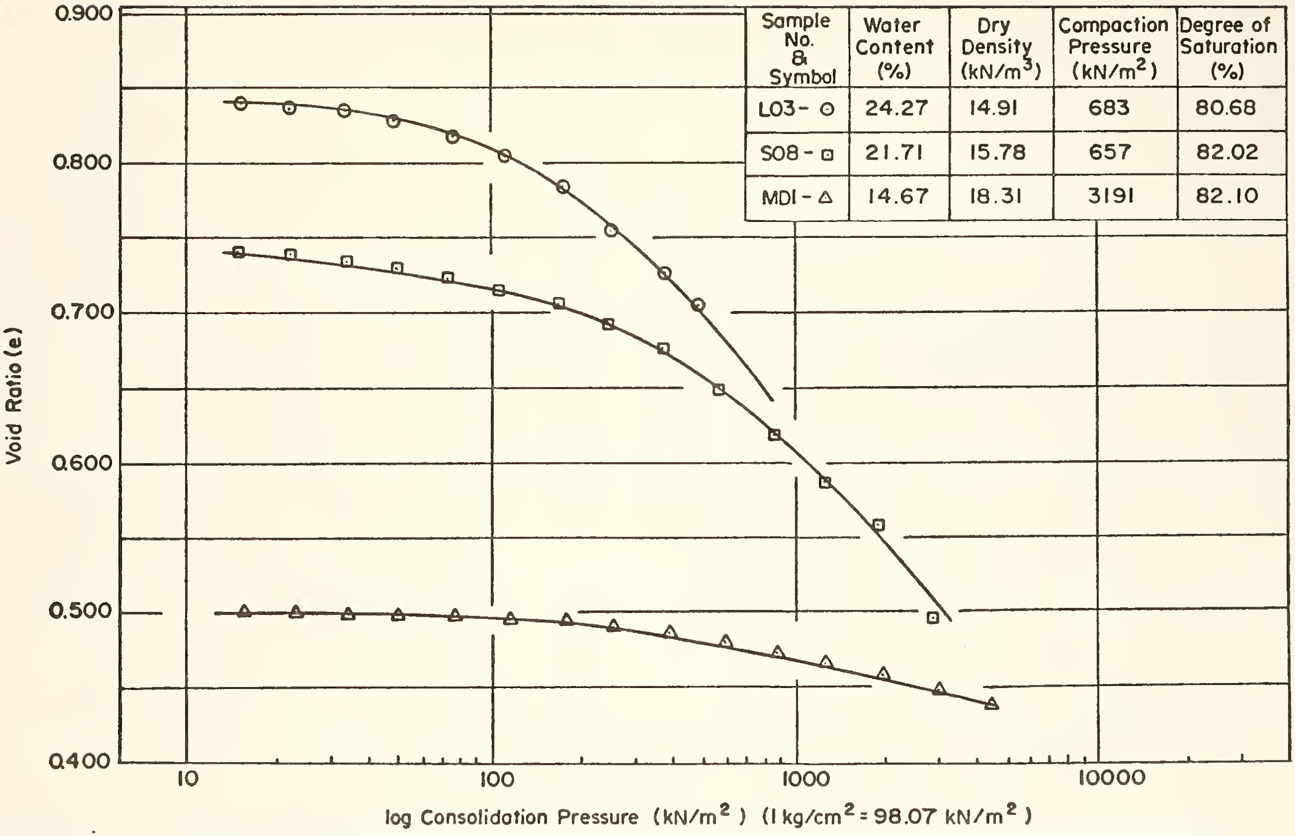

Sample No. & Symbol	Water Content (%)	Dry Density (kN/m³)	Compaction Pressure (kN/m²)	Degree of Saturation (%)
L03 - ⊙	24.27	14.91	683	80.68
S08 - ⊡	21.71	15.78	657	82.02
MDI - △	14.67	18.31	3191	82.10

FIGURE C2 EFFECT OF COMPACTIVE EFFORT ON COMPRESSIBILITY (NEAR OPTIMUM)

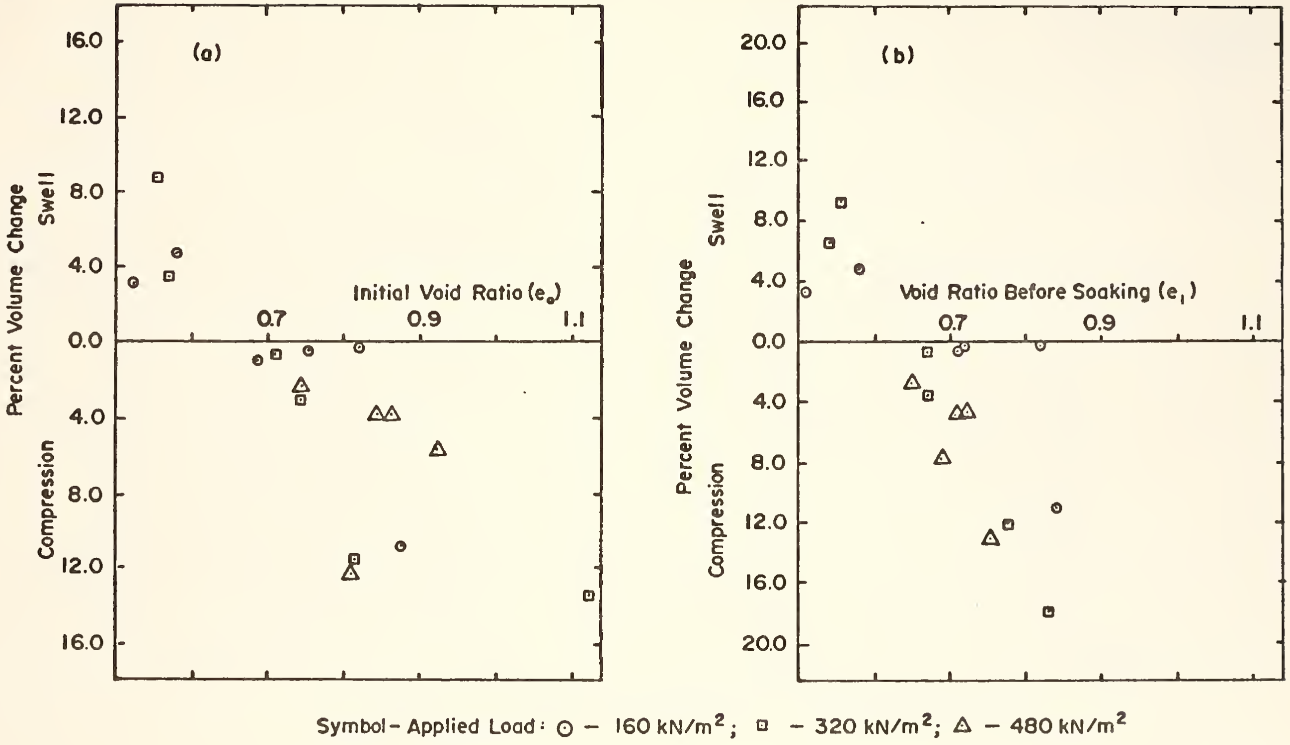

FIGURE C3 VOLUME CHANGE DURING SATURATION

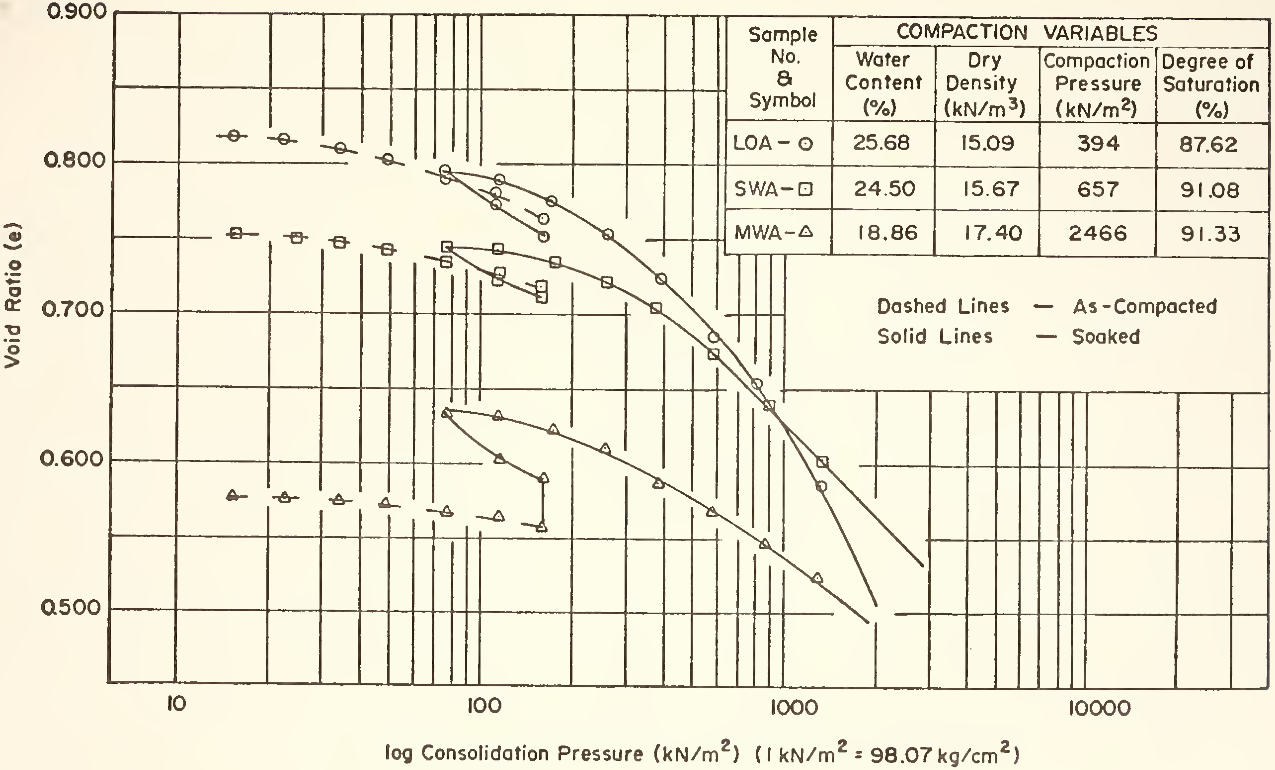

Sample No. & Symbol	COMPACTION VARIABLES			
	Water Content (%)	Dry Density (kN/m³)	Compaction Pressure (kN/m²)	Degree of Saturation (%)
LOA – ⊙	25.68	15.09	394	87.62
SWA – ⊡	24.50	15.67	657	91.08
MWA – △	18.86	17.40	2466	91.33

FIGURE C4 EFFECT OF COMPACTION PRESSURE ON SOAKED COMPRESSIBILITY BEHAVIOR (WET OF OPTIMUM)

APPENDIX D

LIST OF NEGATIVE NUMBERS FOR PHOTOGRAPHS

Figure No.	Negative No.
6	77634-12
8	77634-8
9	77634-15
10	77634-10
13	77634-14
14	77634-5
16	77634-2

COVER DESIGN BY ALDO GIORGINI